MINERALOGICAL MAGAZINE

JOURNAL OF THE MINERALOGICAL SOCIETY

Vol. 32 June 1961 No. 253

Tacharanite and other hydrated calcium silicates from Portree, Isle of Skye.

By Jessie M. Sweet, M.B.E., B.Sc., with analyses by D. I. Bothwell, B.Sc., and X-ray determinations by D. L. Williams.

Department of Mineralogy, British Museum (Natural History).

[Read 26 January 1961.]

Summary. The vesicles of an olivine-dolerite that occurs as a small outcrop near Portree in the Isle of Skye contain zeolites and some hydrated calcium silicates. These latter include tobermorite, xonotlite, gyrolite, and what is presumed to be a new member of the tobermorite group. An attempt is made to account for the sequence of crystallization of the minerals.

ABOUT half a mile north of Portree in the Isle of Skye on the Staffin road (A855) there is a small exposure of melanocratic olivine-dolerite with phenocrysts of olivine and ophitic augite. The rock is fine-grained and tough owing to the interlocking of the minute plagioclase feldspars. Other exposures in the immediate neighbourhood are of a highly vesicular olivine-basalt that has the normal inclusions of visible crystals of laumontite, mesolite, thomsonite, and analcime. Although there is no exposure showing the junction of the two rocks and the area does not yet appear to have been mapped, it would seem that this occurrence is an intrusion of a later date.

The minerals of the dolerite are of a different type from those of the surrounding rocks and all occur as fine-grained amygdales. These are also normally very tough like the parent rock. In 1959 a preliminary investigation yielded specimens of tobermorite, xonotlite, and gyrolite, with some mesolite. These first specimens have cores of tobermorite that are pale-pink and fine-grained with a rim of mesolite (B.M. 1959, 551–553) or of gyrolite also with a rim of mesolite (B.M. 1959, 555). Another specimen (B.M. 1959, 554) collected at this time needs a little more consideration. The core is a dense pinkish-white mineral surrounded by a thick glassy rim. The inner portion, with refractive index about

1·580, proved to be xonotlite (table I, anal. 1); a dehydration curve (fig. 1A) showed a loss of water beginning at 820° C., and complete at 1 050° C. The outer rim, uniaxial, negative, ω 1·548±0·003, was found to be gyrolite (table I, anal. 2); it is exceptionally hard (H. about 6)

TABLE I. Chemical analyses of hydrated calcium silicates from the Isle of Skye.

	1.	2.	3.	4.
SiO_2	50·1	50·0	41·8	46·17
Al_2O_3	—	3·5	5·6	4·26
Fe_2O_3	0·4	0·1	0·3	—
FeO	—	—	n.d.	0·15
MgO	—	trace	3·2	trace
CaO	46·2	32·3	33·6	35·15
Na_2O	—	0·8	0·6	0·56
K_2O	—	0·2	0·1	0·25
H_2O	3·4	13·1	*15·2	13·47
	100·1	100·0	100·4	100·01

1. Xonotlite, Portree, Isle of Skye. Analyst, D. I. Bothwell. (B.M. 1959, 554.)
2. Gyrolite, Portree, Isle of Skye. Analyst, D. I. Bothwell. (B.M. 1959, 554.)
3. Tacharanite, Portree, Isle of Skye. Analyst, D. I. Bothwell. (B.M. 1961, 163.)
4. Tobermorite, Loch Eynort, Isle of Skye. Analyst, D. I. Bothwell. (G. F. Claringbull and M. H. Hey, Min. Mag., 1952, vol. 29, p. 962.)

* Includes a little CO_2.

compared with normal gyrolite. The dehydration curve is shown in fig. 1B. It regains water lost at 110° C. on exposure to moist air, but no experiments were made to determine whether the water lost above this temperature is also zeolitic as the evidence of A. L. Mackay and H. F. W. Taylor suggests.[1] Both minerals are exceptionally difficult to break. Between the gyrolite and the rock is a thin layer of mesolite. Unfortunately this specimen was the only one of its kind found in either 1959 or 1960, but it does seem as if we have here a natural occurrence of the change-over from tobermorite to xonotlite described by H. F. W. Taylor.[2]

In June 1960 many more specimens were collected and proved rather bewildering in their variety. Some were hammered out of the dolerite; others were lying loose in the cutting, but all showed a chalky coating where exposed to weathering. This weathering had not penetrated far and the amygdales were all quite fresh inside. The minerals recognized are tobermorite, gyrolite, saponite, calcite, mesolite, thomsonite, and what appears to be a new member of the tobermorite group. The amygdales usually consist of two or more of the minerals. Typical examples

[1] A. L. Mackay and H. F. W. Taylor, Min. Mag., 1952, vol. 30, p. 84.
[2] H. F. W. Taylor, Min. Mag., 1959, vol. 32, p. 110.

are a nucleus of one mineral with a rim of another, often not easily discernible in the hand specimen, between it and the parent rock. Thus a core of tobermorite may have a rim of mesolite, gyrolite, or thomsonite. The tobermorite varies from fine-grained to distinctly fibrous material, with a slightly variable refractive index near 1·560, which though

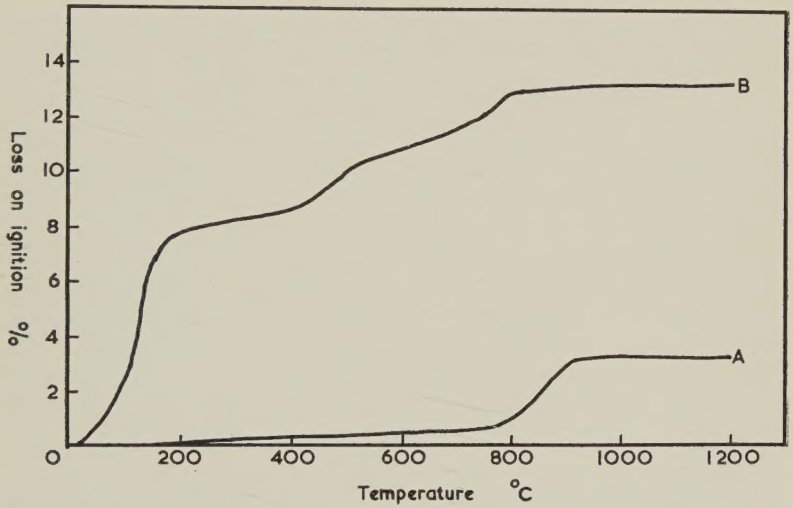

Fig. 1. A, Dehydration curve of xonotlite, Portree, Isle of Skye (B.M. 1959, 554). B, Dehydration curve of gyrolite, Portree, Isle of Skye (B.M. 1959, 554).

matted gives straight extinction. One specimen is penetrated by acicular crystals of yellow calcite (B.M. 1961, 158), while others show an additional mineral in either the core or the rim. Amygdales of gyrolite of varying hardness may be intergrown with mesolite or calcite with rims of thomsonite, mesolite, or tobermorite, or no rims at all. Other specimens consist of mixtures of the two zeolites and gyrolite with rims of gyrolite, tobermorite, or zeolite. One interesting specimen (B.M. 1961, 159) has a cream core resembling xonotlite but proved to be fine-grained calcite with a thick crust of gyrolite. Another specimen (B.M. 1961, 160) has a core of what appeared to be analcime (isotropic, refractive index *c.* 1·487), but an X-ray photograph showed it was a mixture of saponite and tobermorite; and yet another (B.M. 1961, 161) is a mixture of fibrous tobermorite, saponite, and probably cristobalite. This last mixture is white, soft, and earthy in appearance. The mesolite from this occurrence is rather unusual. It is normally finely fibrous and almost isotropic, but can, as is shown in a section from B.M. 1961, 162

(fig. 2), develop into paddle-shaped crystals in optical continuity, with medium birefringence, straight extinction, and positive elongation. It was at first thought that these might have been gonnardite, which has nearly the same optical properties, but X-ray photographs prove both to be mesolite.

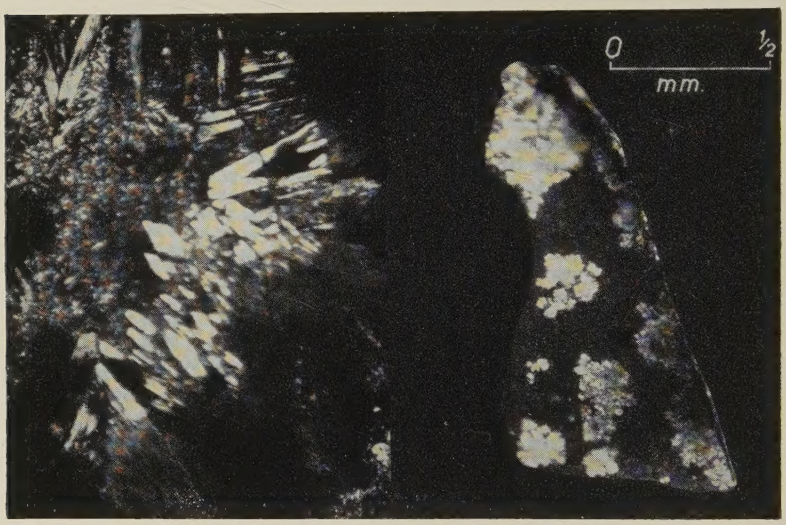

Fig. 2 (*left*). Acicular mesolite terminating in birefringent paddle-shaped crystals penetrating tobermorite, Portree, Isle of Skye. Crossed nicols, × 44 (B.M. 1961, 162).
Fig. 3 (*right*). Tacharanite, almost isotropic, with inclusions of birefringent gyrolite, fragment, Portree, Isle of Skye. Crossed nicols, × 50 (B.M. 1961, 163).

Two specimens deserve special mention. One of them (B.M. 1961, 163) consists of a core of tobermorite associated with a dense white mineral and surrounded by a rim of gyrolite and mesolite. This white mineral did not readily fall into line with any of those previously mentioned. Its refractive index was just less than 1·537 and it appeared to be cryptocrystalline but contained rosettes of another mineral with medium birefringence that proved to be gyrolite (fig. 3). Some of the 'isotropic' material was isolated and gave an X-ray pattern of a mineral in the tobermorite group but distinct from tobermorite or any other member of the group, natural or artificial. An attempt was then made to separate enough for analysis. This was very difficult as not only was the mineral exceedingly tough but it was also contaminated with gyrolite. With great patience Mr. D. L. Williams separated 29 mg. of the material on which all the subsequent work was done. A bulk density determination

gave D_4^{23} 2·36, but that of individual fragments varied. This was rather disturbing so some of the fragments were re-examined microscopically. They proved to be fibrous tobermorite with a refractive index just less than 1·560 mixed with some other substance. It was then suspected that the sample obtained was a mixture, but a repeat of the X-ray photograph on some of the original material newly detached confirmed its homogeneity (fig. 4 and table II).[1] Two tiny fragments left from the

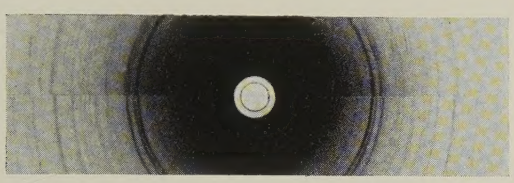

FIG. 4 (*upper*). X-ray photograph of tacharanite, Portree, Isle of Skye, 6 cm.-diam. camera (B.M. 1961, 163). (*lower*). X-ray photograph of type tobermorite, Tobermory, Isle of Mull, 6-cm. diam. camera (Heddle collection, Royal Scottish Museum, S.M.C. 435A1, X-ray No. 5418).

TABLE II. X-ray powder data for tacharanite from Portree, Isle of Skye (B.M. 1961, 163). Values from 6-cm. diam. camera, Cu-$K\alpha$ radiation.

d.	*I.*	*d.*	*I.*	*d.*	*I.*
12·7 Å.	**vvs**	**3·05 Å.**	**vs**	2·130 Å.	mw
8·40	m	2·98	vvw	2·080	vwb
7·10	vw	**2·89**	**s**	2·005	m
6·31	vvw	2·79	s	1·952	mw
5·66	mw	2·69	vvw	1·915	vw
5·16	ms	2·59	vvw	1·850	mw
4·16	vvw	2·495	vw	1·820	ms
3·75	w	2·440	m	1·738	mw
3·49	vw	2·375	vvw	1·675	m
3·37	m	2·295	vvw	1·641	m
3·16	vvw	2·185	vw	1·536	msb

first X-ray photograph and since stored in a gelatine capsule enclosed in a glass tube were then examined optically and found to be tobermorite with another mineral. X-rays confirmed that these fragments were in fact now a mixture of tobermorite and gyrolite. Therefore the new mineral on exposure to air obviously breaks down to tobermorite and gyrolite. Having realized this, the analysis was undertaken and gave the following result (table I, anal. 3), with the formula (Ca, Mg, Al) (Si, Al) $O_3.H_2O$.[2] The analysis of tobermorite from Sgúrr nam Boc, Loch

[1] Electron-diffraction work is being carried out by Dr. H. F. W. Taylor.

[2] After ignition the mineral was not gelatinized by concentrated HCl and it was necessary to fuse it with Na_2CO_3.

Eynort, Isle of Skye, is appended for comparison (table I, anal. 4). Dehydration was carried out to 1 050° C. on the sample and gave two distinct breaks in the curve at 350° C. and 650° C. (fig. 5). It is thought that this mineral is sufficiently distinctive to deserve a name of its own and that tacharanite (pronounced TĂ·KHERENAIT) from the Gaelic *tacharan* (a changeling) would be suitable, both from the nature of its behaviour and the wealth of folk-lore associated with the island in which it occurs.

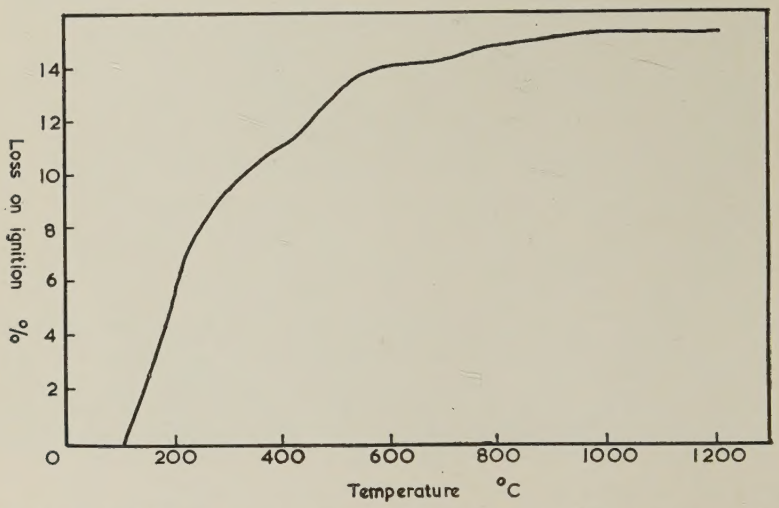

FIG. 5. Dehydration curve of tacharanite, Portree, Isle of Skye (B.M. 1961, 163).

A second specimen (B.M. 1961, 164) suspected of containing tacharanite was sectioned and showed a core of tobermorite surrounded by a zone of tacharanite enclosing radiating spherules of gyrolite and in its turn surrounded by mesolite. The impression is given that the gyrolite probably acts as centres of disintegration when the tacharanite is exposed to the atmosphere, and that tacharanite may be the parent mineral from which tobermorite, gyrolite, and xonotlite are formed.

In an attempt to find a clue to the history of the mineralization a few sections were cut of inclusions surrounded by the parent rock. In some cases there is a clear-cut junction between the amygdales and the rock; in others there has been quite an amount of disturbance. In fact in certain hand specimens there is a visible penetration of tobermorite and mesolite so as to surround some of the augite crystals (B.M. 1961, 165). It is supposed that the dolerite on cooling left vesicles that were later filled by a residual liquid containing calcium, magnesium, sodium,

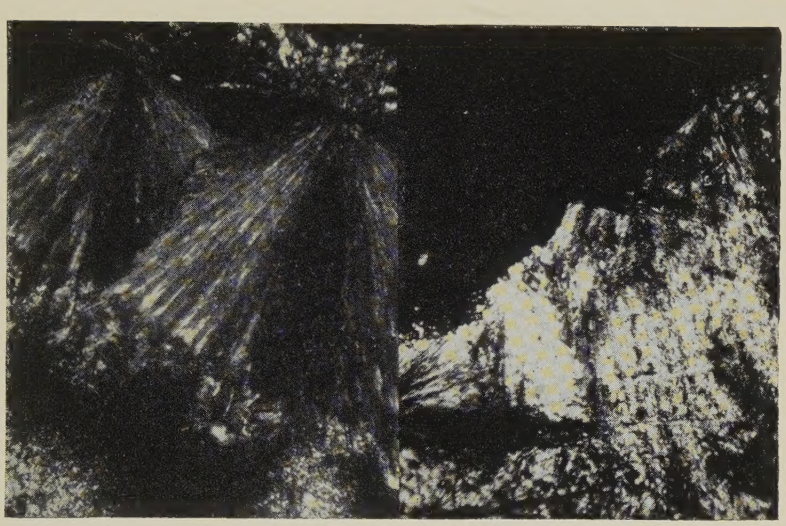

FIG. 6 (*left*). Radiating acicular mesolite with rosettes of gyrolite and almost isotropic tacharanite grading into tobermorite, Portree, Isle of Skye. Crossed nicols, × 44 (B.M. 1961, 164).

FIG. 7 (*right*). Fibrous tobermorite, probably pseudomorphous after mesolite. Portree, Isle of Skye. Crossed nicols, × 44 (B.M. 1961, 167).

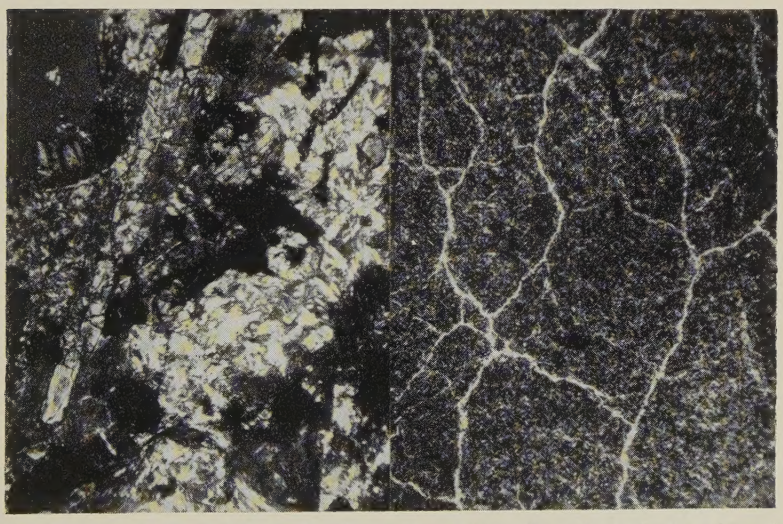

FIG. 8 (*left*). Olivine-dolerite showing a long prism of augite and alteration of feldspar crystals to tobermorite, Portree, Isle of Skye. Crossed nicols, × 44 (B.M. 1961, 167).

FIG. 9 (*right*). Tobermorite, showing shrinkage cracks filled in with isotropic material, Portree, Isle of Skye. Ordinary light, × 44 (B.M. 1961, 164).

aluminium, silica, carbon dioxide, and water—in fact all the constituents of the dolerite except iron, which has somehow disappeared. But this liquid has not simply filled all the vesicles giving the assemblage of zeolites and calcium silicates already noted. In fact there is some slight evidence that the zeolites were there first and the tobermorite appeared at a later stage. This is shown in one section where the fine grains of

TABLE III. The several associations of hydrated calcium silicates, zeolites, &c., observed at Portree, Isle of Skye.

Inner core.	Outer rim.
tobermorite	mesolite
,,	mesolite + gyrolite
,,	mesolite + calcite
,,	thomsonite
,,	thomsonite + calcite
,,	gyrolite
,, + gyrolite	mesolite
,, + gyrolite	thomsonite
,, + mesolite	mesolite
,, + calcite	mesolite
? pseudom. after mesolite	mesolite
gyrolite	mesolite
,,	thomsonite
,,	tobermorite
,, + mesolite	thomsonite + calcite
,, + calcite	mesolite
,,	no rim
xonotlite	gyrolite + mesolite
calcite	gyrolite
saponite	mesolite
,,	tobermorite
thomsonite	gyrolite
mesolite	mesolite + tobermorite
,, + thomsonite	mesolite
,, + gyrolite	gyrolite + calcite
,,	no rim

Also intimate intergrowths of thomsonite and mesolite in which either may predominate showing no definite zoning.

tobermorite are arranged in such a way that they seem to be replacing a mineral with radiating acicular structure such as the abundant mesolite (B.M. 1961, 167, fig. 7). In another section the tobermorite has invaded the parent rock and replaced some of the small feldspars (B.M.

1961, 167, fig. 8). In the section that shows the tacharanite the entire core is filled with fine-grained tobermorite revealing shrinkage cracks that have later been filled by an isotropic mineral with a lower refractive index than the tobermorite (B.M. 1961, 164, fig. 9). The tobermorite becomes increasingly fibrous as it reaches the zone containing the tacharanite and gyrolite. From these observations it seems clear that much more investigation is needed before a real idea of the history of the crystallization of these minerals can be formed. Table III shows the variation in association.[1]

Acknowledgements. I should like to thank Dr. M. H. Hey for all his advice and patience and also other members of the Department of Mineralogy for their help, including Miss E. E. Fejer for initial X-ray determinations, Mr. S. E. Ellis for petrological determinations, and Mr. T. D. Handslip for cutting the sections. I am also indebted to Dr. G. P. L. Walker for consultation on the mode of occurrence.

[1] The previous descriptions of Scottish tobermorite give very little information on the mode of occurrence—in fact Heddle only once mentions the parent rock as 'basic eruptive' in 'north-east Mull from Tobermory to Bloody Bay' (M. F. Heddle, Min. Mag., 1880, vol. 4, p. 119; The Mineralogy of Scotland, 1901, vol. 2, p. 83). Here the mineral is minutely granular and pale pink with a rim of mesolite and associated with xonotlite and gyrolite in neighbouring localities. His occurrence at Sgúrr nam Boc, Loch Eynort, Isle of Skye, shows material 'very arborescent and branching' with crystals that 'seem to obscure parallel to their length' (M. F. Heddle, Trans. Geol. Soc. Glasgow, 1892, vol. 9, p. 254).

The dehydration of brucite.

By M. C. Ball, A.R.I.C., and H. F. W. Taylor, D.Sc., Ph.D.

Department of Chemistry, University of Aberdeen, Scotland.

[Read 26 January 1961.]

Summary. This process has been reinvestigated, mainly with X-rays, using an FeO-containing, fibrous variety (nemalite), and also a nearly pure specimen. The results confirm that the transformation is oriented, the *c*- and *a*-directions of the brucite becoming the normals to (111) and ($1\bar{1}0$) in the periclase. There is an intermediate, spinel-like stage; the spinel *a*-axis is parallel to, and twice as long as, that of the periclase. This stage is especially prominent when nemalite is heated in air or nitrogen, but is shown also by the nearly pure material. The nemalite shows also a further intermediate stage under certain conditions. A new hypothesis is proposed for the dehydration mechanism, in which the number of oxygen atoms per unit volume is almost unchanged in those parts of the crystal that are converted into periclase. The process is essentially one of cation migration, and the occurrence of the spinel-like phase is readily explained. Similar mechanisms possibly apply to the dehydration of other lamellar hydroxides and oxy-hydroxides (e.g. gibbsite, kaolinite) and of certain carbonates and other oxy-salts.

MANY investigations on the dehydration of brucite ($Mg(OH)_2$) to periclase (MgO) have been reported. Among other approaches that have been followed are optics, X-ray crystallography, phase equilibria, thermodynamics and thermochemistry, chemical kinetics, and electron microscopy and diffraction. The earlier work was reviewed by Garrido (1951); among recent contributions may be mentioned those of Kennedy (1956), Roy and Roy (1957), Goodman (1958), Gregg and Razouk (1949), and Razouk and Mikhail (1959).

There are distinct indications of an intermediate stage in the process. Early signs of this were provided by optical studies (Rinne, 1891). Further evidence came from thermodynamic considerations (Roy and Roy, 1957) and from X-ray studies (Garrido, 1936*a*, 1951). Garrido showed that brucite crystals that had been dehydrated rapidly gave 'extra' X-ray reflections, which were not attributable to either brucite or periclase, though they could be indexed $\frac{1}{2}\frac{1}{2}\frac{1}{2}$ on the periclase axes. He concluded that they were produced by a form of MgO in which some of the cations were not in their normal positions. Not all of the more recent investigators, however, have agreed that a recognizable intermediate stage exists.

The aim of the present work was to find whether there is a distinct, intermediate stage that can be isolated, and if there is to determine at least some features of its crystal structure. It was hoped that such a study might throw new light on the mechanism of the dehydration process.

Material.

Two specimens of brucite were used:

The impure, fibrous variety (nemalite) from Asbestos, Quebec, Canada. This has been fully described (Berman, 1932; West, 1932, 1934; Garrido, 1936*b*; Donnay, 1945), and our own optical, X-ray, and analytical (table I) observations in general confirmed the earlier reports.

TABLE I. Chemical analyses.

	1.	2.	3.
SiO_2 . .	0·39	—	1·85
Fe_2O_3 . .	—	1·95	1·55
FeO . .	—	9·57	9·30
MnO . .	0·89	—	—
MgO . .	67·34	60·33	59·87
H_2O . .	31·52	28·60	27·90
	100·14	100·45	100·47

1. Brucite: Wood's mine, Texas, Pennsylvania, U.S.A. (Kurnakov and Chernykh, 1926).
2. Nemalite: Asbestos, Quebec, Canada (Berman, 1932).
3. Ditto, this investigation.

The fibres are pale green and sometimes many inches long, and are elongated parallel to *a*. The crystallites are well aligned in this direction but are rotated at random around it, even in thin fibres. Long-exposure X-ray rotation photographs showed the presence of intergrown chrysotile, with its *c*-axis perpendicular to the fibre direction, but gave no indication of any other phases in the fibres selected for the present work. It was assumed that the SiO_2 occurred as chrysotile, and (following Donnay, 1945) that the small Fe_2O_3 content could be attributed to magnetite and the deficiency in water to periclase, the last two being in amounts too small for detection with X-rays. It was thus calculated that the fibres contained 92% of brucite of composition $Mg_{0\cdot92}Fe_{0\cdot08}(OH)_2$ together with 4% of serpentine, 2% of magnetite, and 2% of periclase.

A nearly pure brucite from Wood's mine, Texas, Lancaster County, Pennsylvania, U.S.A. (B.M. 33222). This also has been fully described, most recently by Brindley and Ogilvie (1952). The crystals were colour-

less, hexagonal flakes with (0001) cleavage and though, as Brindley and Ogilvie showed, they are not true single crystals, they could be regarded as such for the present purpose. X-ray and optical study gave no indications of phases other than brucite. Chemical analysis (table I) shows the latter to have the approximate composition $Mg_{0\cdot99}Mn_{0\cdot01}(OH)_2$.

Experimental procedure.

Fibres of nemalite, and single crystals of the Pennsylvania brucite, were heated under various conditions causing partial or complete dehydration. The products were pseudomorphs, not significantly changed in external dimensions. They were studied mainly by single-crystal X-ray methods, using filtered cobalt radiation. Some of the heated nemalite fibres were crushed and powder patterns also obtained, using an 11·46-cm. diameter camera. The following heating conditions were used:

Rapid heating in air. The crystal or fibre was put in a platinum foil microboat, which was then placed on a ceramic surface in a furnace already at the selected temperature, which was probably reached by the crystal within 2 seconds.

Slow heating in air or nitrogen. The crystal or fibre, in a platinum boat, was placed in a cold tube furnace, the temperature of which was then raised at 30° C. per minute.

Rapid heating in air, nitrogen, or hydrogen. The crystal or fibre was placed in a platinum foil boat of V-shaped cross-section, which was contained in a vacuum desiccator filled with the desired gas. An electric current was passed through the boat from end to end, thereby heating the crystal or fibre to red heat in a few seconds. When nitrogen or hydrogen was used, the desiccator was evacuated and filled with the gas several times before the crystal was heated. The nitrogen used in these experiments was a commercial product containing 99·9% N_2. For some runs, it was further purified by passage over red-hot copper.

A specimen of $MgFe_2O_4$ was prepared for comparison work by reaction of laboratory grade MgO and Fe_2O_3 in appropriate proportions at 1 320° C. for 5 hours, followed by regrinding and reheating under the same conditions. Its X-ray powder pattern, obtained using an 11·46-cm. diameter camera, agreed substantially with that reported by Posnjak (1930). The cubic cell was found to have a 8·37$\pm$0·01 Å.

A quasi-static dehydration curve of nemalite (fig. 1) was obtained by heating a sample in a slow stream of 99·9% nitrogen at successively higher temperatures, each temperature being maintained until apparent

constant weight was attained. An unweighed sample was heated under identical conditions, and fibres were removed at each temperature for X-ray examination, the results of which are included in fig. 1.

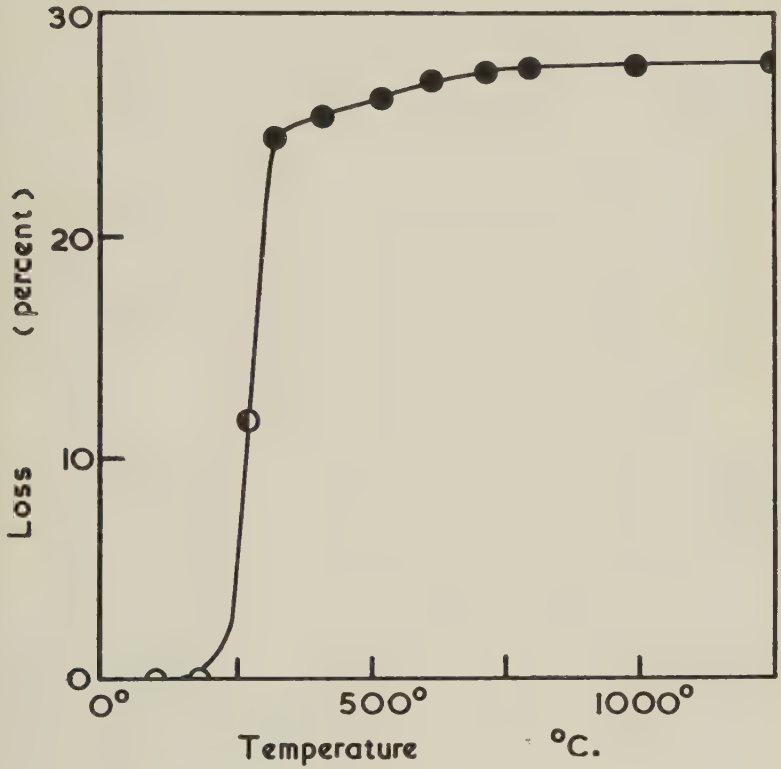

FIG. 1. Quasi-static dehydration curve for nemalite, showing results of X-ray examination of heated specimens. Phases detected: ○ brucite, ◐ brucite + MgO, ● MgO.

Results.

Phases detected in heated material. The X-ray patterns from heated crystals or fibres were found to depend on the heating rate and final temperature, and to a lesser extent on the period during which the latter was maintained. The reflections fell into the following five groups; all showed strongly preferred orientation: reflections of unchanged brucite (*B*); reflections of periclase (*P*); 'extra' reflections indexable on a spinel-type cell (*S*); additional 'extra' reflections not so indexable (*X*);

and reflections of metallic iron (Fe). Table II summarizes the types of reflections given by crystals or fibres heated under various conditions. Except with nemalite at 400° C., the time the final temperature was maintained was relatively unimportant. In general, the main effect of prolonging it was to give a sharper and clearer pattern in which weak reflections, including those of groups *S* and *X*, were more readily seen.

TABLE II. Groups of reflections detected in X-ray patterns of crystals or fibres heated under various conditions (summarized results). *B*, brucite; *P*, periclase; *S*, spinel-type extra reflections; *X*, further extra reflections; Fe, metallic iron.

Specimen and atmosphere.	Final temp. ° C.	Time final temp. was maintained.	Reflections detected in crystals after Slow heating.	Rapid heating.
Nemalite in air	400°	$\leqslant 1\frac{1}{2}$ hr.	*B*+weak *P*	*B*+weak *P*
	400°	$3\frac{1}{2}$–15 hr.	diffuse *P*	diffuse *P*
	500°	$3\frac{1}{2}$ min.–48 hr.	*P*	*P*+(sometimes) *S* & *X*
	600–700°	2–21 min.	*P*	*P*+weak *S*
	800–1 150°	2 min.–20 hr.	*P*+(sometimes) *S*	*P*+*S*
	1 350°	5 hr.	—	*P*+*S*
	c. 1 600°	1–5 min.	—	*P*
Nemalite in N_2	*c.* 800°	1–10 min.	*P*+weak *S*	*P*+*S*
Nemalite in H_2	*c.* 800°	1–10 min.	—	*P*+*S*+Fe
Pennsylvania brucite in air	400–750°	2–20 min.	*P*	*P*
	790–830°	2–60 min.	*P*	*P*+(sometimes) weak *S*
	800°	45 min.	—	*P*+stronger *S*

Crystallographic orientation of the periclase. The X-ray results for all samples where periclase was formed confirmed previous observations (Büssem and Köberich, 1932; West, 1932, 1934; Garrido, 1936*a*, 1951) on its orientation relative to that of the brucite. Fig. 2 shows the relationship; there are two principal orientations for the periclase; for both of them periclase (111) is perpendicular to brucite *c*, and periclase ($1\bar{1}0$) to brucite *a*. With the Pennsylvania brucite, one orientation always predominated over the other. This confirms Garrido's result (1951). The nemalite gave only fibre rotation patterns, in which the two orientations are indistinguishable.

The S- and X-reflections. The *S*- and *X*-reflections never occurred in the absence of *P*-reflections. They resembled these closely in diffuseness and angular spread, but were in general weaker. *S*-reflections were reproducibly developed and strongest in the patterns of nemalite fibres that had been heated rapidly in air or nitrogen to 800–1 150° C. (table II). With nemalite fibres that had been heated slowly or to other tempera-

tures, and with crystals of Pennsylvania brucite under any conditions, they were weaker, fewer, and less reproducibly produced.

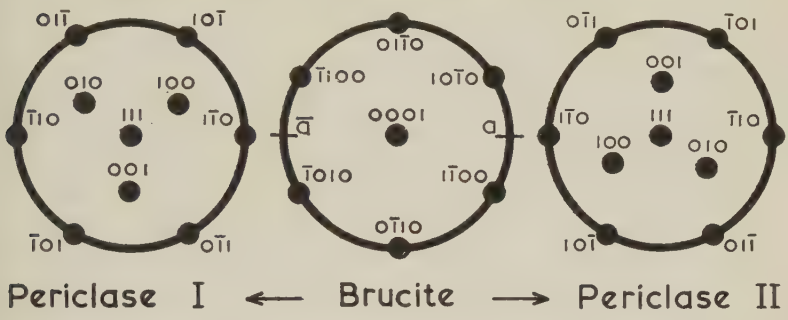

Fig. 2. Orientation relationships for the transformation of brucite into periclase, showing the brucite and the two orientations of the periclase in stereographic projection. Comparison of spacings: Brucite, c 4·75 Å., periclase d_{111} ($\frac{1}{2}\times$4·86) Å. Brucite, a 3·13 Å., periclase $d_{1\bar{1}0}$ 2·97 Å.

In the patterns from heated nemalite, some of the S-reflections occurred on the periclase layer lines, and others on additional layer lines corresponding to a doubling of the periclase repeat distance in the fibre direction. All could be indexed on a face-centred cubic lattice with its a-axis parallel to, and twice as long as, that of the periclase (i.e. a 8·42 Å.). This was also true of the S-reflections given by heated crystals of Pennsylvania brucite. This lattice is similar to that of a spinel and the relative intensities of the S-reflections given by heated nemalite were similar to those of the corresponding reflections of spinel itself ($MgAl_2O_4$). All of the P-reflections can necessarily also be indexed on the spinel-type lattice. The patterns as a whole, taking P- and S-reflections together, could thus be described as ones of periclase superimposed on ones of a spinel having an a-axis exactly twice that of the periclase. They might equally well be described as spinel-type patterns in which reflections with h, k, and l all even are anomalously strong.

West (1932, 1934) also noted the appearance of reflections attributable to a spinel in heated nemalite, and he concluded that $MgFe_2O_4$ had been formed through atmospheric oxidation of the FeO. The present work shows that this explanation is incorrect. Firstly, X-ray powder patterns showed a difference between the a-spacing of $MgFe_2O_4$ (8·37 Å.) and that of heated nemalite (8·42 Å.) several times greater than experimental error. Secondly, S-reflections were produced from nemalite on heating not only in air, but also in nitrogen or hydrogen. One sample,

which had been heated rapidly in nitrogen to red heat, and which gave strong *S*-reflections, was analysed for FeO. The result (12·91%) differed insignificantly from that found for the original material (12·88% referred to the dry weight). Another sample, which had been heated in hydrogen, gave *S*- and *P*-reflections as well as ones from metallic iron. It seems most unlikely that oxidation could have occurred under these circumstances. Thirdly, the *S*-reflections were also given, though they were fewer and weaker, by heated crystals of the Pennsylvania brucite, which is almost pure $Mg(OH)_2$.

Although *S*-reflections were given by heated specimens of both nemalite and Pennsylvania brucite, there were some differences in the relative intensities in the two cases. With the heated nemalite, the three strongest *S*-reflections were 220, 311, and 511 (or 333) indexed on spinel-type axes. In the other case they were 111, 220, and 311.

The fact that the *S*-reflections persist in heated nemalite up to at least 1 350° C. suggests, in view of the dehydration curve (fig. 1), that the phase yielding them can be anhydrous or nearly so. Specimens giving *S*-reflections that have been heated at lower temperatures appear still to contain some water. A nemalite fibre which had been heated rapidly to 800° C. so that it gave relatively strong *S*-reflections was weighed and ignited at 1 250° C. A loss of 1·9% occurred.

X-reflections were given irreproducibly by nemalite fibres heated rapidly to 500° C. They were very weak, and the only detectable ones appeared on additional layer lines corresponding to a quadrupling of the periclase repeat in the fibre direction. Such a quadrupling would be caused by a lattice that had a doubled *a*-axis, as in a spinel, but was primitive and not face-centred. However, the positions of the reflections on the layer lines did not agree with this hypothesis. Not enough *X*-reflections were present to allow a determination of the lattice giving rise to them. They can probably be attributed to some lattice related to that of periclase, but larger even than that of the spinel-like material.

The iron reflections. These were shown by a fibre of nemalite that had been heated to red heat in hydrogen; *P*- and *S*-reflections were also present. The iron reflections showed strong preferred orientation, comparable to that of the *S*- and *P*-reflections. The *a*-axis of the iron (body-centred cubic; *a* 2·86 Å.) was parallel to the fibre direction.

Discussion.

The present results confirm that distinct, intermediate stages in the formation of periclase can be recognized. These are most apparent with

nemalite, but are detectable also with the nearly pure $Mg(OH)_2$ from Pennsylvania.

Homogeneous and inhomogeneous dehydration mechanisms. The orientation relationship in the brucite periclase change is clearly determined primarily by a tendency for close-packed oxygen planes in the product to lie parallel to those in the starting material. Previous hypotheses, such as that of Goodman (1958), have been based on the assumption that the water is lost more or less uniformly from all parts of the crystal, i.e. that from every unit cell, containing one formula unit of $Mg(OH)_2$, one molecule of water is lost. The reaction has thus been visualized as a chemical condensation between the hydroxyl groups on the upper surface of each brucite layer and those on the lower surface of the next. Such a mechanism could be described as a homogeneous one.

A suitably elaborated homogeneous mechanism can explain the observed orientation relationship satisfactorily, but not the occurrence of a spinel-like intermediate stage. It is also difficult to see how one half of the oxygen ions could escape sideways, parallel to the plane of the layers, without completely disrupting the crystal structure. Tentatively, a different hypothesis can be considered in which the mechanism is assumed to be inhomogeneous. This implies that, in the brucite crystal, there develop donor and acceptor regions. The acceptor regions are the parts that are converted into periclase, which is produced, not by loss of hydroxyl ions, but by gain of cations and loss of protons. The donor regions are completely destroyed and become the pores that have been shown to exist in the pseudomorph (Goodman, 1958). Their cations migrate into the donor regions, and their hydroxyl ions provide all the oxygen for the water that is formed. These processes are represented diagramatically in fig. 3.

The spinel-like intermediate stage. The existence of such a stage follows reasonably from the assumption that the essential process is one of cation migration. If we consider an element of structure having four oxygen atoms per close-packed layer, there are, on the average, two cations per layer in brucite and four in periclase (fig. 4). The most obvious feature of the spinel structure is that it is an assemblage of close-packed oxygen ions with three cations per layer. In a general way, the formation of a spinel-like intermediate stage is readily explained as occurring naturally when the ratio of cations to oxygen passes through the value of 3:4.

In brucite the oxygen atoms are hexagonal close packed; in spinel and in periclase they are cubic close packed. It is therefore necessary

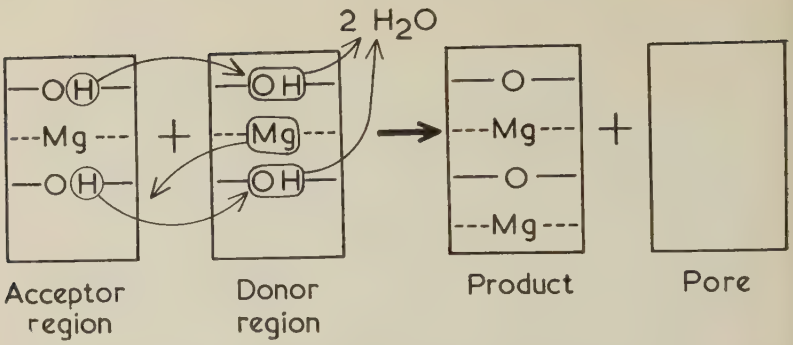

Fig. 3. Schematic representation of acceptor and donor regions, showing the migration of magnesium and hydrogen ions in opposite directions, and the expulsion of water from the donor regions.

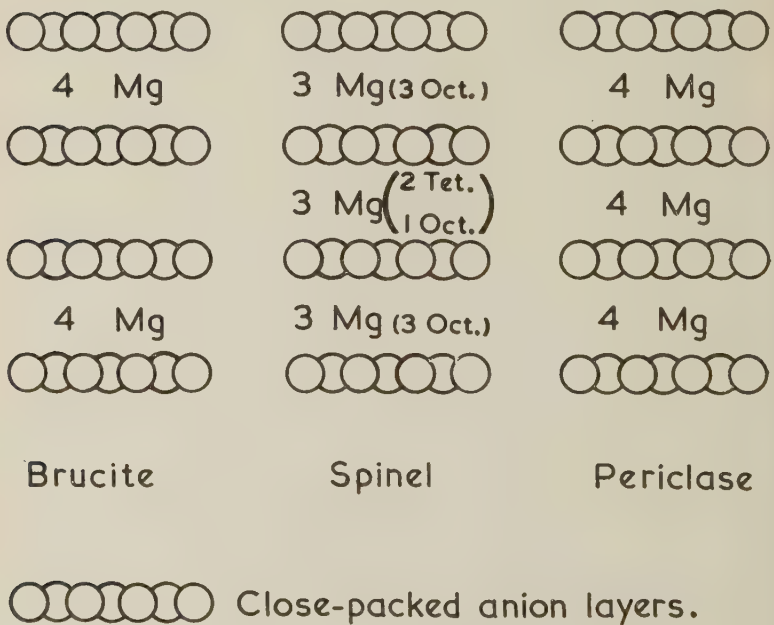

Fig. 4. Comparison of the structures of brucite, periclase, and the hypothetical spinel $Mg_3O_4H_2$. The numbers of magnesium ions in each case correspond to a unit of cross-section containing four O^2 or OH ions or both per close-packed layer.

to postulate that at some early stage in the transformation the oxygen layers slip over each other. Indirect evidence that such slip can occur is provided by the results of studies on the bending of MgO single crystals, which is known to involve movement of dislocations as in a metal (Mügge, 1919; May and Kronberg, 1960; Kelly and Williamson, 1960).

To balance the electrical charges, a true spinel intermediate stage would need to have the formula $Mg_3O_4H_2$. It may be supposed that the donor regions pass through this stage and that this is when the spinel-like structure begins to appear. However, the specimens in which *S*-reflections were actually observed were nearly or completely anhydrous and the structure therefore evidently retains spinel-like features after the cation: oxygen ratio has risen above the value of 3:4 characteristic of a true spinel. This can be explained by considering the different types of cation co-ordination, which can be tetrahedral or octahedral in the spinel (fig. 4). When more cations are added to the spinel structure, they must necessarily occupy vacant sites, which might also be either octahedral or tetrahedral. If it is assumed that the additional cations go entirely into octahedral sites, and that those already present in the spinel stay where they are, the result will be the periclase structure modified by the removal of one cation in eight to a tetrahedral site. This is assumed to be the situation approximated to in crystals giving *P*- and *S*-reflections; the two sets of reflections come from a single phase. Such crystals might equally well be described as ones of periclase containing a substantial proportion of Frenkel defects arranged in an ordered way. The present interpretation agrees with Garrido's view that some of the cations occupy anomalous positions in the intermediate material.

Transition to periclase: further considerations. The *X*-reflections apparently represent a more complex, though still ordered, arrangement of cations in tetrahedral sites with an equal number of octahedral vacancies. This structure is possibly derived from one formed before the cation:oxygen ratio is high enough to form a spinel.

The present results confirm Garrido's observation (1936*a*, 1951) that the periclase is formed in two principal orientations, one of which is better developed than the other. Garrido accounted for the latter fact by supposing that the cation–oxygen bonds were less disturbed in the formation of one of the two forms, but it seems that this cannot be correct, as the two are symmetrically related to the original brucite orientation (fig. 2). It appears more likely that, in any one crystal, transformation begins at more than one nucleus, and that at each

nucleus there is an equal probability of each orientation developing; the number of nuclei must be so small that unequal proportions of the two orientations usually arise. On the present hypothesis for the mechanism, the orientation produced depends on the direction in which oxygen sheets move relative to each other in the change from hexagonal to cubic close packing.

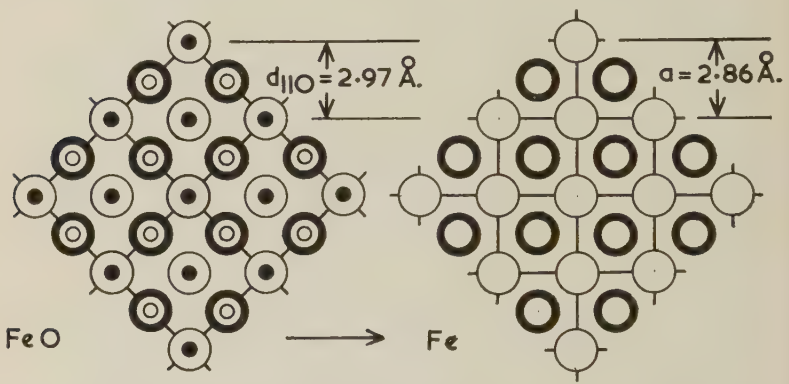

Fig. 5. The structures of FeO and metallic iron, drawn in the observed relative orientations; both structures are projected along a, which is 4·21 Å. long in FeO and 2·86 Å. in Fe. Large, open circles: Fe at height zero. Large, heavy circles: Fe at height $a/2$. Small, full circles: Oxygen at height zero. Small, open circles: Oxygen at height $a/2$.

The fact that the S- and X-reflections are given chiefly by crystals that have been heated rapidly can perhaps be explained by assuming that, under these conditions, a large proportion of the cations are migrating simultaneously. Movement of the cations probably becomes more difficult after all or most of the protons have been lost, and there will be a good chance that a cation in a tetrahedral site will not manage to escape from it before this has happened. Subsequent migration, in anhydrous material, is then very slow below about 1 600° C. With slowly heated crystals, the number of cations migrating simultaneously must be smaller, and there is a greater chance of the stable, periclase structure being formed before all the water has been lost. The persistence of the intermediate structures is stronger with nemalite than with the Pennsylvania brucite. This can possibly be attributed to the presence of the silicon, which by its ready adoption of fourfold co-ordination in some way stabilizes the spinel-like structure. Magnesium is not often found in tetrahedral co-ordination, though a well-established example is to be found in melilite (Warren, 1930; Smith, 1953).

The iron reflections. The occurrence of preferred orientation in these reflections can be attributed to a similarity between the positions of the iron atoms in the metal and those of the cations in periclase. If these cations were all Fe^{2+}, reduction to the metal could be effected by removal of the oxide ions followed by a small contraction in the lattice dimensions parallel to the fibre direction and a larger one perpendicular to it (fig. 5). The process can perhaps be visualized as involving cation migrations so as to cause segregation of regions of pure FeO in the oxide, followed by a migration of oxygen, possibly in atomic rather than ionic form, to combine with hydrogen on the surface of the crystallite.

Comparison with the decompositions of other minerals. Brucite is related structurally to a number of other lamellar hydroxides and oxy-hydroxides, such as gibbsite, kaolinite, and various compounds of iron, and one might expect similar mechanisms to apply to the dehydration reactions of all these substances. It is thus possible that the extensive published data relating to the dehydration processes of these other minerals may be better explained by inhomogeneous mechanisms than by the homogeneous ones that have generally been proposed. The same thing may be true of the decompositions of certain oxy-salts, such as chalybite ($FeCO_3$). Bernal, Dasgupta, and Mackay (1959) noted the occurrence of an oriented decarbonation in this case and drew attention to the difficulty of reconciling this with the fact that two-thirds of the oxygen is lost. This difficulty disappears if an inhomogeneous mechanism is accepted.

Acknowledgements. This research formed part of a programme supported by the Johns-Manville Corporation, whom we thank for generous financial support, and also for the nemalite specimen. We thank the British Museum (Natural History) for the specimen of brucite from Pennsylvania.

References.

Berman (H.), 1932. Amer. Min., vol. 17, p. 313.
Bernal (J. D.), Dasgupta (D. R.), and Mackay (A. L.), 1959. Clay Minerals Bull., vol. 4, p. 15.
Brindley (G. W.) and Ogilvie (G. J.), 1952. Acta Cryst., vol. 5, p. 412.
Büssem (W.) and Köberich (F.), 1932. Zeits. physikal. Chem., ser. B, vol. 17, p. 310.
Donnay (J. D. H.), 1945. Univ. Toronto Studies, Geol. Ser., No. 49, p. 5.
Garrido (J.), 1936*a*. Compt. Rend. Acad. Sci. Paris, vol. 203, p. 94.
—— 1936*b*. An. Soc. Españ. Fís. Quím., vol. 34, p. 853.
—— 1951. Ion. Rev. Españ. Quím. Aplic., vol. 11, pp. 206, 220, 453.
Goodman (J. F.), 1958. Proc. Roy. Soc., ser. A, vol. 247, p. 346.
Gregg (S. J.) and Razouk (R. I.), 1949. Journ. Chem. Soc., Suppl. vol., p. S 36.

Kelly (A.) and Williamson (G. K.), 1960. 5th Internat. Congr. Cryst., Abstracts of Communications, p. 33.

Kennedy (G. C.), 1956. Amer. Journ. Sci., vol. 254, p. 567.

[Kurnakov (N. S.) and Chernykh (V. V.)] Курнаков (Н. С.) и Черных (В. В.), 1926. [Зап. Росс. Мин. Общ. (Mém. Soc. Russe Min.), vol. 55, p. 74 (English with Russian summary)]; abstr. in Neues Jahrb. Min., 1927, Abt. A, vol. 1, p. 313.

May (J. E.) and Kronberg (M. L.), 1960. Journ. Amer. Ceram. Soc., vol. 43, p. 525.

Mügge (O.), 1919. Nachr. Gesell. Wiss. Göttingen, Math.-Phys. Kl., p. 47.

Posnjak (E.), 1930. Amer. Journ. Sci., ser. 5, vol. 19, p. 67.

Razouk (R. I.) and Mikhail (R. Sh.), 1959. Egypt. Journ. Chem., vol. 2, p. 207.

Rinne (F.), 1891. Zeits. deutsch. geol. Ges., vol. 43, p. 231.

Roy (D. M.) and Roy (R.), 1957. Amer. Journ. Sci., vol. 255, p. 573.

Smith (J. V.), 1953. Amer. Min., vol. 38, p. 643.

Warren (B. E.), 1930. Zeits. Krist., vol. 74, p. 131.

West (C. D.), 1932. Amer. Min., vol. 17, p. 316.

—— 1934. Ibid., vol. 19, p. 281.

Contribution to the study of ore minerals in some igneous rocks from Assynt.

By E. F. Stumpfl, Dr. rer. nat.

University College, London, W.C. 1.

[Taken as read 26 January 1961.]

Summary. The parageneses of opaque minerals in three Assynt rocks are described. A biotite-diorite dyke-rock of Lewisian age is characterized by a primary igneous assemblage of Fe–Ti oxides, pyrrhotine, and pentlandite. Effects of metamorphism are recognized, particularly in the oxidation of ilmenite in a Lewisian epidiorite dyke-rock. Cromaltite contains a primary assemblage of oxide minerals together with a later hydrothermal sulphide assemblage. Evidence from the opaque minerals cannot be reconciled with a theory of limestone assimilation. The correlation of the distribution of Co, Ni, and Cu in the rocks with the opaque minerals present is considered.

THE following account is presented as a supplement to the existing descriptions of a few selected and well-known rock-types in the Assynt district. It has been customary to discuss the opaque minerals as 'accessory ore minerals', although in the rocks selected they amount to an appreciable proportion of the minerals present. Study of the opaque minerals in the rocks selected has provided some interesting data regarding petrogenesis.

Three rock-types have proved of particular interest: epidiorite from Allt a Mhuilinn; biotite-diorite as described by Teall (1907) from Loch Bad nam Ban, Lochinver; and cromaltite from Ledmore, Assynt. The first two rocks occur as dykes in the Lewisian. The epidiorite is older than the biotite-diorite, and has been subject to metamorphism.

The *epidiorite* has been metamorphosed to a considerable extent. Originally a dolerite, the ferromagnesian constituents in the rock have been altered almost completely into hornblende. The main constituents are now hornblende associated with plagioclase.

The ore paragenesis has been affected by the alterations in an impressive way.

A typical feature of the primary ore content of the epidiorite is the scarcity of ilmenite exsolution lamellae in the magnetite. The magnetite grains are martitized, mainly in an irregular way. The alteration

into hematite proceeds from the rim of the grains and from cracks, and only rarely follows the more usual {111} directions (fig. 9). At high magnification ($\times$ 500) a fine pattern of unmixing lamellae is seen to be arranged parallel to {100}. This feature possibly corresponds to what Ramdohr (1953) describes as original ulvöspinel dissolved out of magnetite. The presence of ulvöspinel would indicate an excess of FeO in the original magnetite.

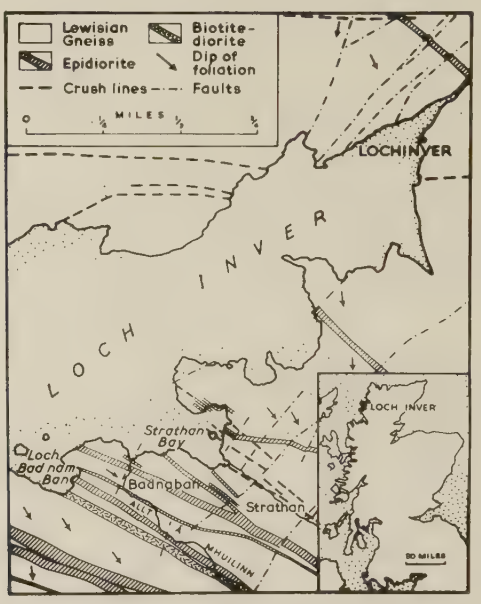

Fig. 1: Geological sketch-map of the dykes on the south shore of Lochinver (after Macgregor and Phemister).

Ilmenite follows magnetite in quantity and frequently is associated with the latter. To a large extent ilmenite has been affected by the alteration which has taken the form of oxidation according to the following reaction:

$$2\,FeTiO_3 + O \rightarrow Fe_2O_3 + 2\,TiO_2.$$

The products of this reaction are fine-grained, mostly symplektic intergrowths of rutile and hematite as illustrated in fig. 9. The grain size of the intergrowth may vary considerably and irregularly within a single grain. It is doubtful in such cases whether the variable coarseness of the

rutile–hematite intergrowths can be simply correlated with the temperature of formation. Ramdohr (1940) has emphasized that alteration of this type is frequently a product of metamorphism.

Occasionally the optical orientation of the ilmenite has been taken over by the intergrowth so that all the hematite in a single altered grain shows simultaneous extinction. In grains that are made up of both ilmenite and magnetite, the much lower resistance of the former to decomposition is clearly demonstrated. The magnetite that has survived alteration forms thin lamellae parallel to {0001} in certain ilmenites ('magnetoilmenites'), as illustrated by fig. 10. These lamellae are products of early unmixing, which took place in ilmenites containing both Fe_2O_3 and FeO in excess.

Amongst sulphide minerals only pyrite need be mentioned, occurring in irregular aggregates. In addition very minute grains of pyrite are frequently accumulated along grain boundaries. The latter especially seem to represent a very late formation, possibly due to hydrothermal activity. The comparison of biotite-diorite and epidiorite shows the extent to which alteration affects not only the transparent, but also the opaque minerals.

Biotite-diorite. This rock belongs to a system of dykes that have a NW.–SE. trend and cut Lewisian orthogneisses on the south shore of Lochinver. The emplacement of the biotite-diorite took place during Lewisian times. In hand-specimen the diorite is dark green to black, with many specks of sulphide ore visible macroscopically. In thin sections (fig. 2) the rock is made up of olivine, augite, and biotite, enclosed by plagioclase. The composition of the plagioclase was determined as An_{40}. The texture is distinctly poikilitic. The olivine frequently shows corona structure. All stages of alteration of the augite into hornblende can be observed. If this process proceeds to completion, hornblende and plagioclase remain the main constituents of the rock.

The main features of ore paragenesis are apparent at low magnification. The basic character of the rock is underlined by the occurrence of titanomagnetite, which is the dominant ore mineral and occurs occasionally as euhedral crystals, but mostly in typical skeletal forms filling interstices between the silicate minerals. It has obviously been formed after the crystallization of most silicates. The common distribution of titanomagnetite in this position within the crystallization sequence of coarse-grained igneous rocks has been stressed by Ramdohr (1940). The sizes of the titanomagnetite grains range mostly between 0·1 and

0·4 mm., but in some cases reach 1 mm. The comparatively high Ti-content in the titanomagnetite has to a certain extent been unmixed as ilmenite lamellae. These lamellae occur partly in the well-known arrangement transecting the whole grain in a pattern parallel to {111} of the magnetite (fig. 3). In some instances the ilmenite forms broad,

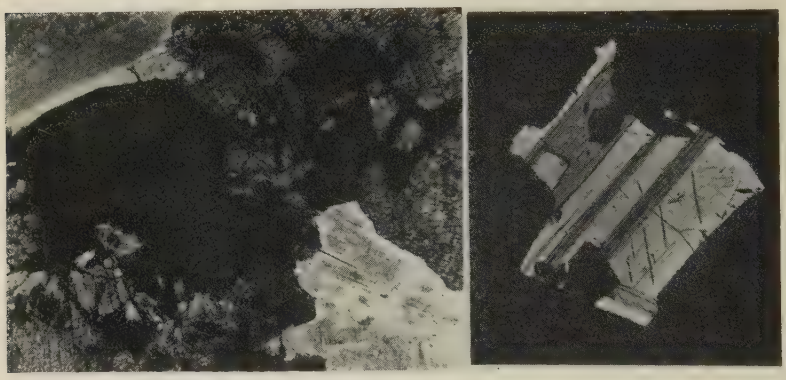

FIGS. 2 and 3: FIG. 2 (*left*). Biotite-diorite, Loch Bad nam Ban. Olivine, augite, biotite, iron ore, plagioclase. ×20. FIG. 3 (*right*). Biotite-diorite, Loch Bad nam Ban. Magnetite (light grey) with unmixing lamellae of ilmenite (medium to dark grey, reflection pleochroism) (111) and small exsolution bodies of spinel || (100). Oil immersion, reflected light. ×250.

patchy lamellae with rounded boundaries. This type of unmixing is rather rare and its genetical significance is not yet fully understood.

Patterns of spinel (mainly hercynite) exsolution are to be observed in many magnetites (fig. 3). A noteworthy feature of some grains of titanomagnetite is a distinct anomalous anisotropy under crossed nicols. In plain polarized light the reflectivity is normal. According to Ramdohr (1960), who was the first to observe this feature, it is due to formation of 'abnormal mixed crystals'.

Magnetite of later origin also occurs in rims around olivine. Hornblende has formed from olivine and contains magnetite in very fine-grained symplektic intergrowths (fig. 4). The structure of this intergrowth is often obscured in thin-section because of its extremely fine nature. The magnetite thus formed may in many cases continue into surrounding biotite.

Friedrich (1955) has described similar symplektic intergrowths from a gabbro-diorite in the Melibocus area, Odenwald, Germany. They have to be explained as synantetic rims in the sense of Sederholm (1916),

not as eutectic, unmixing, or replacement structures. Similar intergrowths of magnetite with augite have been observed also.

Ilmenite is closely associated with magnetite and forms typical lamellae of varying widths parallel to {111} of the magnetite. Very small, partly rounded grains of spinel are frequently concentrated along

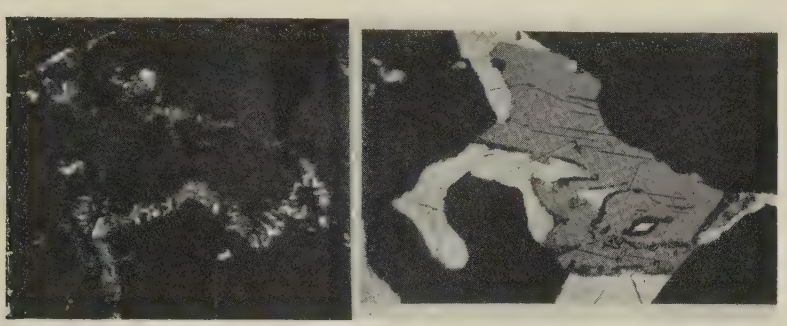

FIGS. 4 and 5: FIG. 4 (*left*). Biotite-diorite, Loch Bad nam Ban. Magnetite (white) forms graphic intergrowths with hornblende around olivine (dark grey). Reflected light, oil immersion. ×160. FIG. 5 (*right*). Biotite-diorite, Loch Bad nam Ban. Ilmenite (medium grey) forms graphic intergrowth with silicates (dark grey); magnetite (light grey) in irregular patches. Reflected light, oil immersion. ×140.

bigger ilmenite lamellae. In smaller amounts, ilmenite occurs as independent grains or irregularly intergrown with magnetite. Subordinate amounts of ilmenite participate in the formation of oxide–silicate symplektites.

A rare, but interesting, feature is graphic intergrowths of ilmenite and silicate minerals, ilmenite constituting the host mineral (fig. 5). Newhouse (1936) records a similar observation from a diabase near Bechtoldsville, Pennsylvania.

The single grains of ilmenite seem to have formed shortly before the magnetite, as shown, for instance, in fig. 5. Similar age relations have been observed by Ramdohr (1940) in a great variety of coarse-grained igneous rocks. This statement does not, of course, apply to the unmixing lamellae of ilmenite. The general evidence that both ore minerals form after the main silicate crystallization is not affected by this observation.

Ilmenites that show unmixing of hematite parallel to {0001} are present in small amounts. The exsolution takes place in thin lamellae. In many coarse-grained igneous rocks this type is much more common.

Pyrrhotine is, after magnetite and ilmenite, the most widespread ore mineral. It mostly occurs in more or less rounded grains (globules) of up to 0·02 mm. diameter. Big grains, which contain other sulphides as well, may reach 1 mm. diameter. The appearance of pyrrhotine is distinctly different from that of the oxide ores. These globules represent

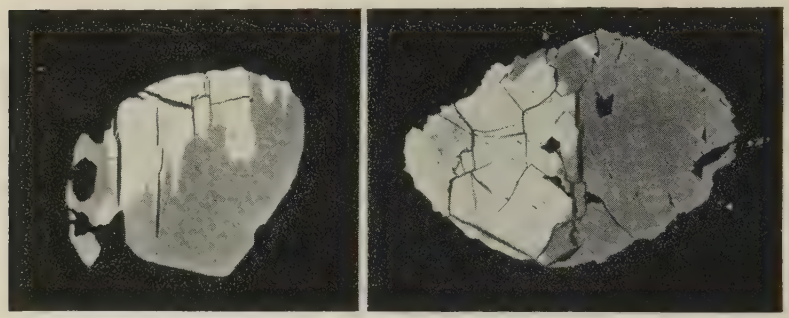

Figs. 6 and 7: Fig. 6 (*left*). Biotite-diorite, Loch Bad nam Ban. Pyrrhotine (medium grey) and typical 'flame-like' bodies of pentlandite, which prefer basal directions of the pyrrhotine. Reflected light, oil immersion. ×230. Fig. 7 (*right*). Biotite-diorite, Loch Bad nam Ban. Pyrrhotine (medium grey), pentlandite (white, excellent cleavage) ‖ (111), and chalcopyrite (light grey, soft). Reflected light, oil immersion. ×160.

original immiscible droplets of sulphide liquid as described by Newhouse (1936).

Pentlandite occurs as typical 'flames' (fig. 6) in many pyrrhotines, or associated with pyrrhotine as relatively large grains with pronounced cleavage. A typical assemblage is illustrated in fig. 7.

Finally, chalcopyrite should be mentioned, which frequently is to be seen together with pyrrhotine–pentlandite intergrowths. Chalcopyrite is quantitatively insignificant.

The participation of both pyrrhotine and pentlandite in the formation of sulphide–silicate intergrowths, as shown in fig. 8, is most unusual. This type of pyrrhotine occurrence is not mentioned in the excellent account by Newhouse (1936), nor is the graphic intergrowth of pyrrhotine and pentlandite with silicates recorded by Ramdohr (1945) in his comprehensive survey of 'myrmekite'.

Cromaltite is a melanite pyroxenite of unusual character, which occurs as a small dyke in ledmorite (= melanite-malignite) near Bad na h'Achlaise, Ledmore, Assynt. Both the cromaltite and ledmorite are genetically related to the post-Cambrian Loch Borolan Alkaline Com-

plex and were described by Shand (1930, 1939). Cromaltite occupies an important place in petrological literature because of controversy regarding limestone syntexis in relation to the origin of alkali rocks. In hand-specimen the rock is dark green, coarse-grained and cut by many carbonate veins. Pyroxene, melanite, and biotite are the main consti-

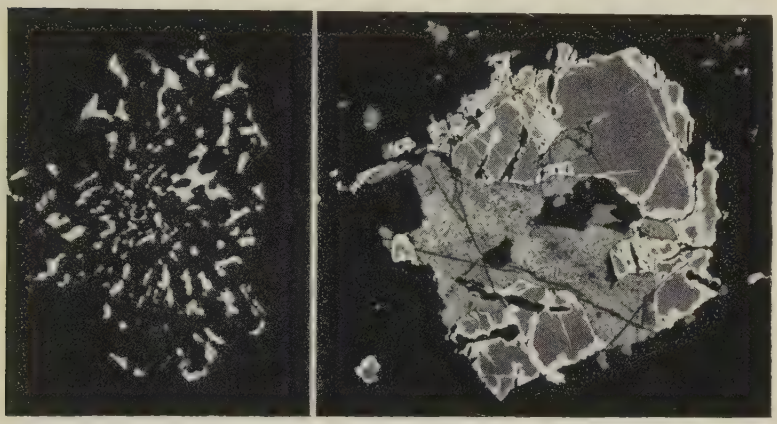

FIGS. 8 and 9: FIG. 8 (*left*). Biotite-diorite, Loch Bad nam Ban. Pyrrhotine (light grey) and pentlandite (white) in graphic intergrowth with silicate mineral. Reflected light, oil immersion. ×160. FIG. 9 (*right*). Epidiorite, Allt a Mhuilinn. Magnetite (medium grey) changed into hematite along cracks and grain boundaries; ilmenite has been decomposed to form a fine-grained graphic intergrowth of rutile and hematite. Reflected light, oil immersion. ×160.

tuents, intergrown with one another and accompanied by ore and apatite as accessory minerals. Fig. 11 shows a typical section of cromaltite. An unusually high content of lime reported in old analyses is mainly to be related to the carbonates, which replace the silicates.

Typical features of the ore paragenesis are the dominance of ilmenite-poor titanomagnetite, the widespread occurrence of pyrite and chalcopyrite, and the small amounts of bornite, covelline, and linnaeite.

Magnetite occurs in two generations: big grains with a diameter of about 1 mm., and smaller individuals of 0·1–0·5 mm. diameter. The latter are frequently completely decomposed to form leucoxene. The bigger magnetites are distinctly rounded and suggest the possibility of magmatic corrosion, and hence of the relatively early formation of magnetite. Exsolution of spinel (hercynite) is widespread, parallel to {111} in typical patterns. Intense cataclasis that has affected the rock

as a whole has resulted in fracturing many of the magnetite grains, thus providing channels for martitization.

Rutile is a further decomposition product of magnetite and often surrounds the latter in rings of well-developed crystals, as well as in irregular zones. This feature shows clearly in both thin and polished sections.

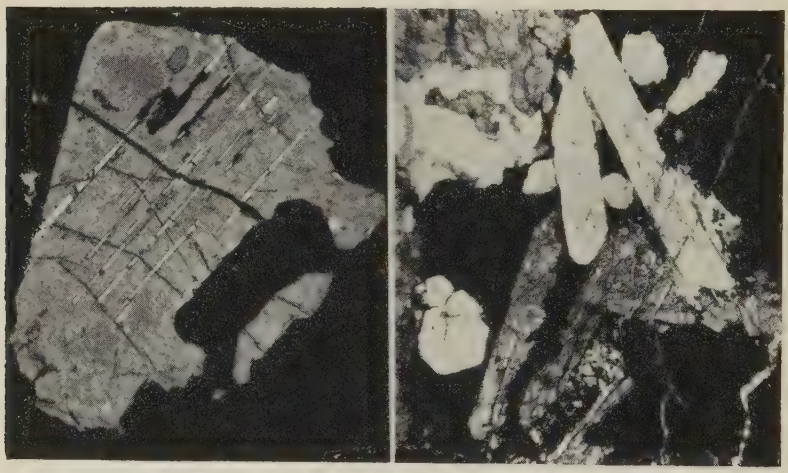

Figs. 10 and 11: Fig. 10 (*left*). Epidiorite, Allt a Mhuilinn. Ilmenite with (partly oxidized) unmixing lamellae of magnetite (0001) ('magnetoilmenite'). The ilmenite is, to a considerable extent, changed into a graphic intergrowth of rutile and hematite. Reflected light, oil immersion. ×160. Fig. 11 (*right*). Cromaltite, Bad na h'Achlaise. Typical section, melanite, augite, apatite, magnetite. ×30.

The amount of sulphides present is considerable. Pyrite sometimes replaces magnetite, but mostly it forms big crystals, which are frequently replaced in turn by chalcopyrite along fractures (fig. 12). To a small extent, chalcopyrite is also present as small grains amongst the silicates. The ore minerals have obviously recrystallized relatively easily after the deformation of the rock. This process is illustrated, for instance, by chalcopyrite grains that are composed of numerous small, intensely twin-lamellated crystals of different optical orientation.

Bornite is associated with chalcopyrite when the latter occurs in pyrite grains as well as inclusions in magnetite. It has formed at about the same time as chalcopyrite.

Small amounts of linnaeite join chalcopyrite in the replacement of pyrite. Its light-grey colour with violet tint in oil immersion and its

isotropy are distinctive features. Phemister (1931) has shown that calcium and iron carbonates replace the silicates, and thus the original interpretation of Shand (1910) suggesting the assimilation of limestone by the cromaltite must be discounted. The views of Phemister are supported by ore-microscopic evidence. The oxide minerals, mainly represented by titanomagnetite, are typical constituents of the original

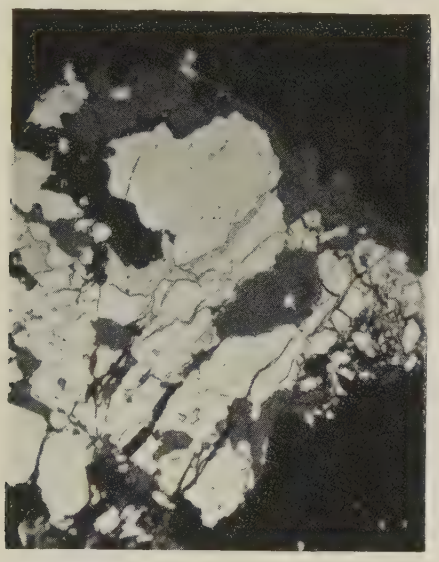

Fig. 12: Cromaltite, Bad na h'Achlaise. Magnetite (dark grey) is replaced by pyrite (white), which in turn is replaced by chalcopyrite (light grey). Reflected light, oil immersion. ×100.

ultrabasic rocks. The sulphides have been introduced later, most probably simultaneously with the carbonates. There are, of course, slight differences in age as far as the sulphides are concerned. Pyrite is the oldest, followed by chalcopyrite, bornite, and linnaeite. Thus the occurrence of linnaeite, which so far has not been recorded from igneous rocks, can be explained as a product of late hydrothermal activity. Finally, covelline may be mentioned, since it occurs very occasionally as an alteration product of chalcopyrite.

Distribution of Co, Ni, *and* Cu.

Co, Ni, and Cu were determined using a Hilger large quartz spectrograph (E 742) and following the variable internal standard method with

background correction recommended by Mitchell (1948). The Diabase W 1 was used as an external standard taken to contain 51 p.p.m. Co, 82 p.p.m. Ni, and 110 p.p.m. Cu (Ahrens and Fleischer, 1960). The results are shown in table I. The high Ni content of the biotite-diorite has to be ascribed to the considerable amount of pentlandite associated with pyrrhotine.

Table I. Distribution of Co, Ni, and Cu (in p.p.m.) in some Assynt rocks.

	Co	Ni	Cu
Epidiorite . .	57	27	206
Biotite-diorite . .	106	267	130
Cromaltite . .	54	9	420

The high value for Cu (420 p.p.m.) in cromaltite is obviously caused by the presence of chalcopyrite and bornite. No copper sulphides have been detected in polished sections of epidiorite. Nevertheless, the rock contains a considerable amount (206 p.p.m.) of Cu. Most probably, the original sulphides have been decomposed by slight weathering with retention of the copper. A similar case has been discussed by Wager, Vincent, and Smales (1957). The values for Co do not show any relation to the observed content of ore minerals in the rocks concerned.

Acknowledgements. I wish to thank Dr. J. R. Butler, of the Imperial College of Science and Technology, who kindly arranged for me to work in the Geochemical Laboratory of the above-mentioned institution, for his help and advice.

References.

Ahrens (L. H.) and Fleischer (M.), 1960. Report on Trace Constituents in Granite G-1 and Diabase W-1. U.S. Geol. Surv. Bull. 1113.

Friedrich (G.), 1955, Heidelb. Beitr. Min. Petr., vol. 5, p. 65.

Johannsen (A.), 1958. A descriptive petrography of the igneous rocks. Chicago (University of Chicago Press).

Macgregor (M.) and Phemister (J.), 1958. Geological Excursion Guide to the Assynt District. Edinburgh and London (Oliver & Boyd).

Mitchell (R. L.), 1948. Commonwealth Bureau of Soils, Technical Communication No. 44.

Newhouse (W. H.), 1936. Bull. Geol. Soc. America, vol. 47, p. 1.

Phemister (J.), 1931. Geol. Survey Gt. Britain, Summary of Progress, p. 58.

Ramdohr (P.), 1940. Abh. Preuss. Akad. Wiss., nat.-math. Kl., No. 2.

—— 1945. Neues Jahrb. Min., Beil-Bd. 79A, p. 161.

—— 1953. Econ. Geol. (Chicago), vol. 48, p. 677.

—— 1960. Die Erzmineralien und ihre Verwachsungen. Berlin (Akademie-Verlag).

Sederholm (J. J.), 1916. Bull. Comm. Géol. Finlande, No. 48.

Shand (S. J.), 1910. Trans. Edin. Geol. Soc., vol. 9, part 3, p. 202.
—— 1939. Journ. Geol., vol. 17, p. 408.
Teall (J. J.), 1907. Mem. Geol. Survey Gt. Britain, p. 99.
Vincent (E. A.) and Phillips (R.), 1954. Geochimica Acta, vol. 6, p. 1.
Wager (L. R.), Vincent (E. A.), and Smales (A. A.), 1957. Econ. Geol. (Chicago), vol. 52, p. 855.

Solid-solution relationships in some titaniferous iron oxide ores of basic igneous rocks.

By J. B. Wright, M.A., B.Sc., F.G.S.

Dept. of Geology and Mineralogy, University of Oxford.[1]

[Taken as read 23 March 1961.]

Summary. Calculations are presented, based on modal and chemical analyses of titaniferous iron ore minerals from two localities (Skaergaard and Schmoo Lake). They show that Fe:Ti ratios are constant for granular aggregates of ilmenite and titaniferous magnetite formed at any one stage in the cooling history of the containing rock body. From this and other evidence it is concluded that the aggregates are the result of exsolution from original high-temperature cubic solid solutions. For the Skaergaard rocks, the problem of separately crystallized ilmenite, distinct from the granular aggregates, is also discussed.

TITANIFEROUS iron ores in basic igneous rocks generally consist of ilmenite grains in close association with titaniferous magnetite containing exsolved lamellae of ilmenite or ulvöspinel or both (together with small amounts of aluminous spinels, with which this study is not concerned). The ulvöspinel intergrowth in titaniferous magnetite is always very fine, while ilmenite is exsolved as masses of widely varying size, from large lamellae and irregular blebs down to intergrowths as fine as those of ulvöspinel. The ilmenite grains in the assemblages are often idiomorphic towards the titaniferous magnetite (fig. 1), and can occasionally be seen passing into the larger blebs and lamellae of ilmenite in the latter (fig. 3*a*). The granular aggregates of ilmenite and titaniferous magnetite as a whole, however, are nearly always interstitial to the surrounding silicates.

The origin of the granular aggregates has been attributed by previous workers either to exsolution (Edwards, 1938; Evrard, 1949; Vincent and Phillips, 1954) or to contemporaneous crystallization (Buddington *et al.*, 1955; Heier, 1956). Quantitative data presented here, derived from modal and chemical analysis, suggest that an origin by exsolution processes is perhaps the more likely.

[1] Present address: Geological Survey of Kenya, P.O. Box 30009, Nairobi.

The materials used in this investigation were eleven representative samples from the Skaergaard layered intrusion, east Greenland, and six random samples from the Schmoo Lake titaniferous iron ore, Quebec.

The Skaergaard samples.

Vincent (1960) has described in detail the titaniferous iron oxide ores and their intergrowths in rocks of the Skaergaard intrusion. The ores first appear in significant amount as a primary precipitate phase, rather high in the Lower Olivine Gabbros. At and above this level they are always much more concentrated in melanocratic than in average bands, sometimes forming over half the rock by volume.

The samples used were from adjacent average and melanocratic bands and from transgressive ore-rich veins in the layered Skaergaard intrusion, east Greenland (heights, in metres, refer to level in the layered intrusion):

E.G. 5052	830 m.	Average band	Lower Olivine Gabbros
E.G. 5051		Melanocratic band	
E.G. 2307	850 m.	Average band	
E.G. 2308		Melanocratic band	
E.G. 4353	1 150 m.	Less melanocratic band	Middle Gabbros
E.G. 4359		More melanocratic band	
E.G. 2574	1 730 m.	Average band	Hortonolite Ferrogabbros
E.G. 2580		Average band	
E.G. 2569		Melanocratic band	
E.G. 4458A	805 m.	Transgressive ore-rich veins	Lower Olivine Gabbros
E.G. 4355	1 150 m.		Middle Gabbros

Distinct from the granular aggregates of titaniferous magnetite and ilmenite, these Skaergaard rocks also contain separate ilmenite crystals, usually entirely surrounded by silicates. Such ilmenite typically occurs as elongate subhedral crystals—often in short chain-like aggregates—contrasting with the irregular but usually roughly equant form of the ilmenite grains associated with titaniferous magnetite; and it is largely confined to average bands in which the ores are not a major constituent (table I). Phillips (Vincent and Phillips, 1954) also distinguished this ilmenite and regarded it as a separately crystallized component of the ores—a conclusion supported by the present study.

Textural features typical of Skaergaard titaniferous iron oxides are illustrated in fig. 1.

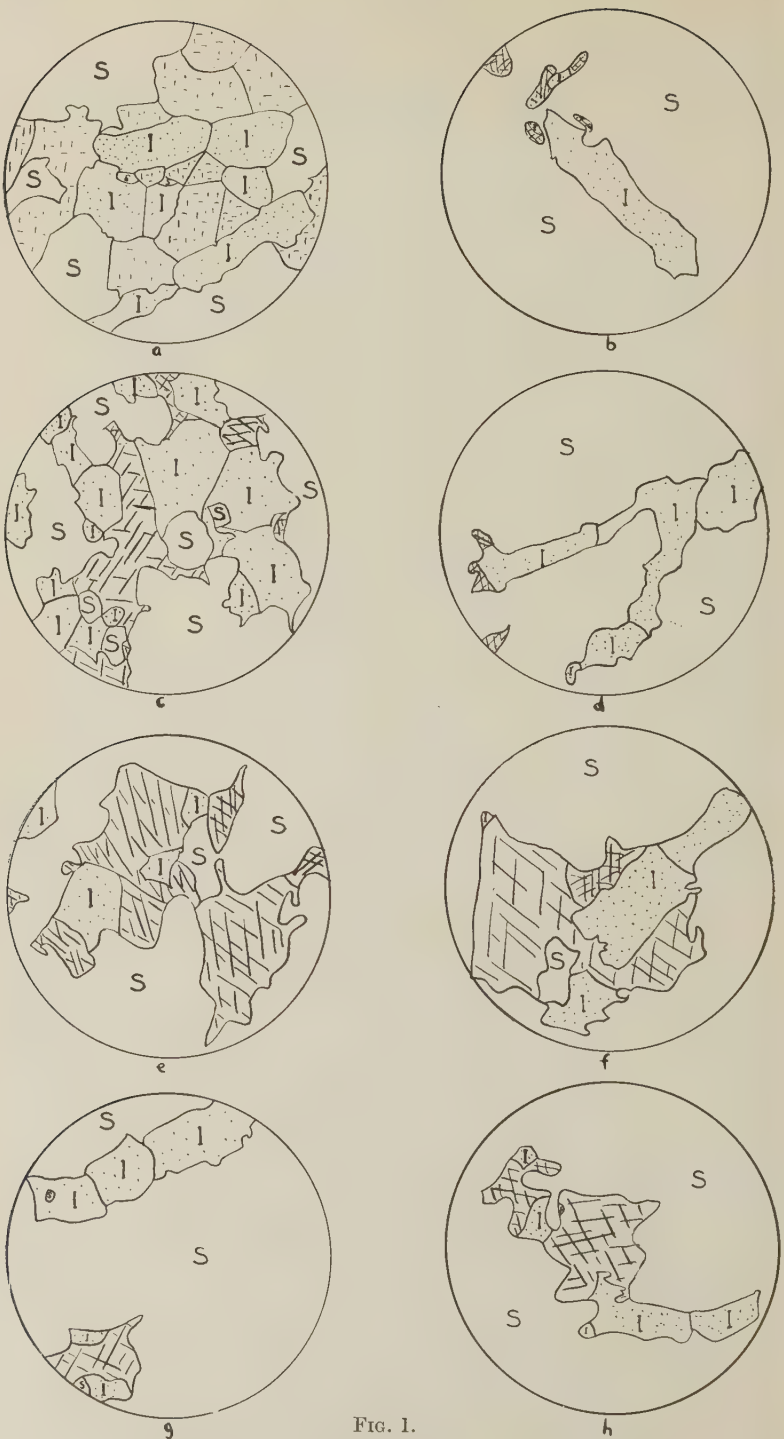

FIG. 1.

Modal analysis. Modal measurements were made in reflected light on polished sections, using a Swift automatic point counter; the three ore components counted were: titaniferous magnetite; ilmenite associated with titaniferous magnetite as grains, and exsolved from it as blebs and lamellae sufficiently large to be removed after crushing to 200 mesh size (cf. fig. 3*b*) during separation for chemical analysis; and separately crystallized ilmenite, in elongate crystals, typically surrounded by silicates, but sometimes connected to the granular aggregates of titaniferous magnetite and ilmenite (fig. 1*b*, *f*, *h*).

The modal determinations consisted of two mutually perpendicular traverses across a polished section, each usually of 1 400 or more counts. In table I the figures for each specimen are the averages of at least two such determinations.

From the figures in tables I and II it may be concluded that in general the ore minerals of average bands contain relatively more granular ilmenite in association with titaniferous magnetite than those of melanocratic bands (table I). Furthermore, the titaniferous magnetites of ores in the average bands are generally more oxidized than those in melanocratic bands (table II), and the titanium in them is usually exsolved as ilmenite; whereas ulvöspinel is commoner in the more reduced melanocratic bands (cf. Vincent and Phillips, 1954; Vincent, 1960). This relationship does not always hold, for in the Middle Gabbro

---

Fig. 1. (*a*) E.G. 2308. Granular association of ilmenite and ulvöspinel-rich magnetite; both minerals are better-formed than at higher levels in the intrusion, but the association as a whole is interstitial to the surrounding silicates.

(*b*) E.G. 2307. Elongate discrete ilmenite crystal in optical continuity with the ilmenite of the small interstitial ilmenite-titaniferous-magnetite association at its upper end.

(*c*) E.G. 4359. Association of ilmenite and ilmenite-rich magnetite; ilmenite is idiomorphic towards magnetite, but the whole is markedly interstitial towards the silicates.

(*d*) E.G. 4353. Aggregate of elongate discrete ilmenite grains, associated at extreme left with a little titaniferous magnetite.

(*e*) E.G. 2569. Interstitial association of ilmenite and titaniferous magnetite, the ilmenite showing a rather irregular habit towards the magnetite.

(*f*) E.G. 2574. An elongate ilmenite crystal forms part of an interstitial titaniferous-magnetite-ilmenite association. The outer portion would be modally counted as discrete ilmenite.

(*g*) E.G. 2574. Another aggregate of discrete ilmenite crystals, quite well-formed.

(*h*) E.G. 2580. Another example of discrete ilmenite attached to an interstitial association of titaniferous magnetite and ilmenite.

Magnification throughout approx. ×17. S, silicates; I, ilmenite (stippled); ornamented, titaniferous magnetite with lamellae of ulvöspinel and/or ilmenite.

TABLE I. Volume % iron ore minerals (balance is silicates).

Sample.	Titaniferous magnetite.	Ilmenite with titanif. mag.	Separately crystallized ilmenite.
E.G. 5052	5·0	5·9	3·6
5051	27·3	24·2	0·7
2307	7·1	3·7	3·7
2308	32·4	11·2	0·8
4353	5·2	8·0	9·8
4359	13·3	19·9	4·1
2574	3·8	2·6	4·3
2580	3·2	2·5	3·2
2569	20·8	6·0	0·2
4458A	79·2	13·3	—
4355	67·4	16·8	—

TABLE II. Partial analyses of titaniferous magnetites and ilmenites from the Skaergaard intrusion (weight %). Figures in parentheses are estimated from analyses of Skaergaard ilmenites (published by Vincent and Phillips, 1954) at levels in the intrusion similar to those from which the samples under discussion were taken, bearing in mind that the ilmenite in average bands is likely to be slightly more oxidized than that in melanocratic bands.

	Titaniferous magnetite.			Ilmenite.		
	FeO	Fe_2O_3	TiO_2	FeO	Fe_2O_3	TiO_2
E.G. 5052	39·6	41·2	13·2	(40·0)	(4·5)	(51·0)
5051	42·2	34·4	17·4	(40·5)	(4·0)	(51·0)
2307	40·4*	38·8*	15·4*	(40·0)	(4·5)	(51·0)
2308	46·3‡	28·6‡	19·3‡	40·3*	3·9*	51·2*
4353	39·8†	36·8†	15·6†	(40·5)	(5·5)	(50·0)
4359	34·1†	40·7†	18·6†	(40·0)	(6·0)	(50·0)
2574	33·9*	44·7*	17·2*	(41·5)	(4·0)	(51·5)
2580	32·1	46·3	12·8	(41·5)	(4·0)	(51·5)
2569	41·8‡	31·4‡	22·5‡	42·7*	2·6*	52·0*
4458A	42·8	33·2	18·3	(40·0)	(5·0)	(51·0)
4355	40·1†	36·9†	16·6†	(40·0)	(5·0)	(51·0)

* From Vincent and Phillips, 1954, slightly amended values.
† From Vincent *et al.*, 1957.
‡ Mean of two analyses.

pair, E.G. 4353 and 4359 (probably slightly unusual layered-series rocks), not only are the relative modal amounts of titaniferous magnetite and associated granular ilmenite nearly the same (table I), but E.G. 4353, with less ore, carries a more reduced titaniferous magnetite than E.G. 4359, which is richer in ore (table II).

Using the data listed in tables I and II and specific gravity values of 5·0 as a roughly calculated average for titaniferous magnetite, and 4·7 for ilmenite, weight ratios of Fe:Ti have been calculated for the following three ore components: titaniferous magnetites alone; granular aggregates of titaniferous magnetite and ilmenite; and total titaniferous iron oxides, comprising the granular aggregates together with the separately crystallized ilmenite.

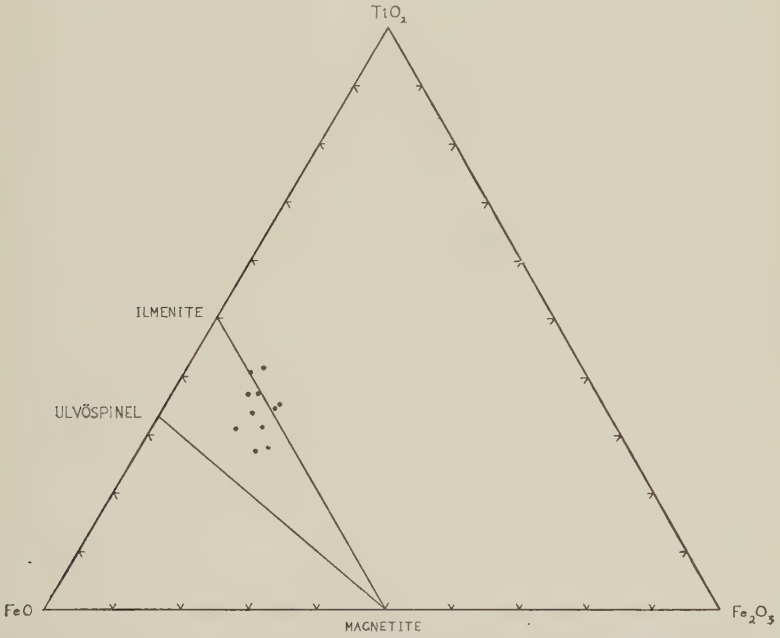

FIG. 2. Calculated molecular compositions of the granular ilmenite–titaniferous-magnetite associations, to illustrate their approximate position within the $FeO–Fe_2O_3–TiO_2$ system.

The ratios are listed in table III and in fig. 2 are shown the calculated mol. % compositions of the granular aggregates in the $FeO–Fe_2O_3–TiO_2$ ternary system.

From table III it is clear that, at a given level in the normal layered series rocks, the weight ratios of Fe:Ti in the titaniferous iron ores of adjacent average and melanocratic bands are much closer for the granular aggregates of titaniferous magnetite and ilmenite than for titaniferous magnetites alone, or for the total ores. Figures in table III

TABLE III. Weight ratios Fe:Ti for titaniferous iron ores in the Skaergaard rocks.

Sample.	Titaniferous magnetite. Fe:Ti	Diff.	Granular aggregates of titanif. magn. and ilmenite. Fe:Ti	Diff.	Total titaniferous ores (includes separately crystallized ilmenite). Fe:Ti	Diff.
E.G. 5052 Average band	7·54	2·07	2·34	*0·04*	1·94	0·40
5051 Melanocratic band	5·47		2·38		2·34	
2307 Average band	6·37	1·54	3·12	*0·01*	2·34	0·70
2308 Melanocratic band	4·83		3·11		3·04	
4353 Less melanocratic band	6·04	1·13	2·04	*0·08*	1·61	0·24
4359 More melanocratic band	4·91		1·96		1·85	
2574 Average band	5·60	3·42	2·62	*0·29*	1·87	1·01
2580 Average band	7·45		2·71		1·95	
2569 Melanocratic band	4·03		2·91		2·88	
4458A, 4355 Transgressive veins	5·14, 5·70	0·56	3·95, 3·85	*0·10*	No separately crystallized ilmenite	

show that the total titaniferous iron oxides of average bands have the lowest Fe:Ti ratios of all; this is due to the relatively large amounts of separately crystallized ilmenite in them (table I).

It has already been observed that in average bands the titaniferous magnetite is usually more oxidized than in the melanocratic bands. Vincent (Vincent and Phillips, 1954) considered this to be mainly due to differing amounts of interprecipitate liquid relative to ores, in adjacent average and melanocratic bands. The partial dissociation of water at high temperatures in such liquids is generally considered to govern the oxidation-reduction equilibria in crystallizing magmas. There may be other factors involved to account for such anomalous relationships as are observed in E.G. 4353 and 4359, mentioned above; but they need not be considered here.

Assuming that they crystallized as separate entities from the magma, titaniferous magnetites occurring in adjacent bands at a given level of the intrusion would have crystallized from the magma at the same time and therefore under the same conditions. They might therefore be expected to have the same Fe:Ti ratios, irrespective of differing oxidation states resulting from subsequent influence of the interprecipitate liquid. But, as was noted by Vincent and Phillips (1954), the composition of titaniferous magnetites from adjacent bands is very variable, and this is reflected in their greatly differing Fe:Ti ratios (table III). In

fact, it is the granular aggregates of titaniferous magnetite and ilmenite that have closely similar Fe:Ti ratios in adjacent bands. It is therefore concluded that *granular aggregates of titaniferous magnetite and ilmenite are the product of exsolution from high temperature solid solutions, which originally separated from the magma as a single crystalline phase.*

The proposed solid solutions may most simply be regarded as members of the cubic binary magnetite–ulvöspinel series (Vincent *et al.*, 1957), in which oxidation of ulvöspinel would result in formation and exsolution of rhombohedral ilmenite. In support of this view may be cited some heating experiments, which have shown that magnetite–ilmenite intergrowths can only be homogenized by reducing the ilmenite to ulvöspinel (Wright, 1959). Other heating experiments, however (Vincent *et al.*, 1957), have indicated that a cubic polymorph of ilmenite, γ-$FeTiO_3$, may well form part of the high-temperature solid solutions, together with magnetite and ulvöspinel. In this case, exsolution of ilmenite would result from simple symmetry inversion as well as by oxidation of ulvöspinel. On this hypothesis, the exsolution processes are rather more complex than those involving merely oxidation of ulvöspinel, but, as they have already been adequately discussed by Nicholls (1955) and Vincent *et al.* (1957), they do not require further comment here. Vincent (1960) has, however, made some pertinent comments on the relative merits of the two hypotheses.

Exsolution from the solid solutions is considered to have commenced with separation of the relatively large idiomorphic ilmenite grains in the aggregates. As the temperature fell, and diffusion processes became more sluggish, ilmenite would cease to exsolve as grains, remaining in the titaniferous magnetite as blebs and ultimately lamellae. Exsolution of ulvöspinel would not commence until about 600° C. or lower, according to present knowledge of the solvus form in the Fe_3O_4–Fe_2TiO_4 binary system (Vincent *et al.*, 1957). Clearly, more ilmenite would have been exsolved in those bands (usually more melanocratic) where interprecipitate liquids were more abundant relative to ore minerals and could oxidize more of the ulvöspinel component in the solid solutions.

The textures illustrated in fig. 1, showing the frequently idiomorphic habit of ilmenite grains towards titaniferous magnetite, are consistent with an origin by exsolution. The interstitial habit of the aggregates as a whole towards silicate minerals, however, indicates that there was some subsequent addition of material from the interprecipitate liquid.

The separately crystallized ilmenite is thought to have separated from the magma after the granular aggregates, because it is mainly confined

to the average bands (table I). If it had crystallized before the aggregates, it would chiefly be found in the melanocratic bands, and the Fe:Ti ratios would then have been abnormally low for the total ores of those bands. If, on the other hand, it had crystallized at the same time as the granular aggregates, it would be distributed between adjacent bands in much the same proportions, and the Fe:Ti ratios for the total ore assemblages of those bands would not differ as strikingly as they do (table III, third column).

It has been suggested that the ilmenite accumulated in average bands because it is less dense than magnetite: but ilmenite can be only slightly less dense than magnetite containing as much TiO_2 as these solid solutions presumably did when they first crystallized. Furthermore, both minerals are much denser than the olivine and pyroxene, which mainly accumulate in melanocratic bands: so that contemporaneous crystallization of magnetite-rich solid solutions and separate ilmenite would result in the latter being also mainly confined to the melanocratic bands.

Below about 800 m. in the Skaergaard intrusion, titaniferous iron oxide ores constitute only around 1% of the rocks. Therefore, during early separation of magnesian olivines and pyroxenes, which form most of the lower part of the layered pile, the magma must have become enriched in both Fe and Ti. Titaniferous iron ores would only start to separate in quantity when, broadly speaking, the amount of iron and titanium in the magma had increased sufficiently (cf. Vincent, 1960). But if the magmatic Fe:Ti ratio were not low enough at this stage, conditions in the magmatic environment might well tend to favour formation of cubic magnetite-rich solid solutions, with Fe:Ti ratios of between about 2 and 3 to 1, rather than ilmenite, in which Fe:Ti is only about 1·2 to 1. When these solid solutions crystallized, the entry of relatively larger amounts of iron than titanium into them might well lower the magmatic Fe:Ti ratio sufficiently to permit separation of ilmenite. In this way, a crop of magnetite-rich crystals would separate and accumulate in a melanocratic band, to be followed by ilmenite, which would perforce settle in the overlying adjacent average band. Hence the apparent anomaly of much lower overall Fe:Ti ratios in the total titaniferous ore mineral assemblages of average bands (table III, third column). The main drawback to this simple picture lies in its implication that crystallization of iron oxide ores was periodic rather than continuous, although closely related to the rhythmic pattern of convective circulation in the Skaergaard magma, which was responsible for the layered structure of the intrusion (Wager and Deer, 1939).

The transgressive ore-rich veins. The similarity of Fe:Ti ratios in the two samples from these veins (E.G. 4458A and 4355), both for the titaniferous magnetite components and the overall ore assemblages, is very striking (table III). It may be complete coincidence that two narrow veins 300 m. apart in the layered series should be in almost the same state of oxidation; but they are both transgressive and devoid of separately crystallized ilmenite, and are considered to be somewhat late-stage segregations in the intrusion (L. R. Wager, personal communication), so that these points of resemblance may have genetic significance.

The Schmoo Lake samples.

The six random samples from the Schmoo Lake ore body[1] were also modally analysed, but the modes must be regarded as approximate only: the ore textures are very much coarser than those in the Skaergaard rocks, and representative sections could not be obtained with the size of polished mounts available. There is no separately crystallized ilmenite in these rocks, for which the modes are:

	C.S.L. nos.					
	1	2	3	4	5	6
Titaniferous magnetite . . .	85·5	96·0	82·0	80·5	56·4	82·2
Ilmenite with titaniferous magnetite .	11·9	2·0	11·9	9·8	22·0	13·5

The relative amounts of titaniferous magnetite and ilmenite within the ore body are very variable, as is the composition of titaniferous magnetite. However, overall ore analyses of the samples are available, the relevant parts of which are reproduced in table IV, and show a remarkably constant Fe:Ti ratio for the six samples, although it is rather higher than those for the Skaergaard ores.

Textural features of two Schmoo Lake samples are shown in fig. 3, and these, together with the figures in table IV, indicate that the ilmenite and titaniferous magnetite in the ore body are probably genetically related, by exsolution from original solid solutions, in the same way as the components of similar aggregates in the Skaergaard rocks. As there is no discrete ilmenite, all the titanium in the Schmoo Lake ores was used in the formation of the solid solutions, which table IV shows to have Fe:Ti ratios higher than any in the Skaergaard.

[1] A titaniferous iron ore segregate in Precambrian anorthosites at Lac la Blache, Saguenay County, Quebec. The samples, C.S.L. nos. 1 to 6, were kindly provided by Dr. J. P. Girault.

TABLE IV. Chemical analyses of Schmoo Lake titaniferous magnetite and overall ore analyses, with Fe:Ti ratios.

C.S.L. no.	Titaniferous magnetite. FeO	Fe_2O_3	TiO_2	Fe:Ti	Overall ore analysis. Fe	TiO_2	Fe:Ti
1 . .	34·7	37·4	20·5	4·32	48·43	21·86	3·69
2 . .	45·0*	25·8*	21·9*	4·06	48·36	21·35	3·78
3 . .	43·4*	29·3*	21·3*	4·24	48·25	21·78	3·69
4 . .	34·6	40·7	17·7	5·22	48·12	21·44	3·74
5 . .	33·8*	51·7*	9·4*	11·17	46·93	20·12	3·89
6 . .	42·7	31·4	19·1	4·80	48·19	20·70	3·88
Max. diff. in Fe:Ti ratio			7·11				0·20

* From Vincent *et al.*, 1957, table I.

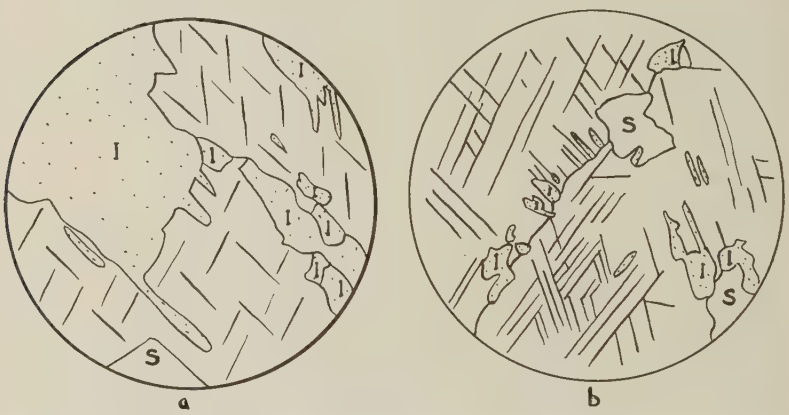

FIG. 3. (*a*) C.S.L. no. 5. Lamellae project into titaniferous magnetite from ilmenite grains, which are idiomorphic towards it.

(*b*) C.S.L. no. 4. Ilmenite blebs pass into long lamellae in titaniferous magnetite. The blebs and broader lamellae are large enough to be removed during separation for analysis (p. 781).

Magnification approx. ×20. S, silicate; I, ilmenite (stippled); ornamented, titaniferous magnetite with lamellae of ilmenite.

Conclusions.

Features of titaniferous iron oxide ores described and discussed here point to an origin by exsolution for granular aggregates of titaniferous magnetite and ilmenite, rather than by simultaneous crystallization. On the latter hypothesis it would be necessary to postulate two generations of ilmenite crystallized direct from the Skaergaard magma, the first preceding the titaniferous magnetite with which it is associated

(because of its frequently idiomorphic habit towards the latter), the second forming the separately crystallized ilmenite. But it is more difficult to explain how separate crystallization, even if simultaneous, followed by clustering of titaniferous magnetite and ilmenite grains into aggregates, can account for consistently similar Fe:Ti ratios in the aggregates of adjacent bands—one would expect them to be as variable as those of the other ore components.

In rocks lacking separately crystallized ilmenite it is possible that granular aggregates of ilmenite and titaniferous magnetite would always have Fe:Ti ratios greater than 3—as in the transgressive veins of the Skaergaard, and the Schmoo Lake ores. Values of around 3 or less for this ratio would then be the expression of sufficient titanium in the original magma to permit separate primary crystallization of ilmenite—as in the normal layered Skaergaard rocks. These figures are further supported by calculations based on approximate data for titaniferous ores separated from two Cuillin gabbros. There is no separate ilmenite, and Fe:Ti is around 4·3:1 for the granular aggregates of titaniferous magnetite and ilmenite.

Further work with titaniferous ores of other basic rocks is necessary before the conclusions arrived at above can be confirmed. In ores where there is no separate ilmenite component, as in the Schmoo Lake samples, overall analyses of separated ore minerals can be made, obviating the errors inherent in calculations based on chemical and modal analyses. Such calculations become necessary, however, once a separate ilmenite phase is present, although they need not take the form of those used here.

Acknowledgements. Grateful thanks are due to Dr. E. A. Vincent, Dr. G. M. Brown, and Prof. L. R. Wager for reading the manuscript and making corrections and many helpful suggestions.

References.

Buddington (A. F.), Fahey (J.), and Vlisidis (A.), 1955. Amer. Journ. Sci., vol. 253, p. 497.

Edwards (A. B.), 1938. Proc. Australian Inst. Min. Met., vol. 110, p. 39.

Evrard (P.), 1949. Econ. Geol., Chicago, vol. 44, p. 210.

Heier (K.), 1956. Amer. Journ. Sci., vol. 254, p. 505.

Nicholls (G. D.), 1955. Phil. Mag., suppl. vol. 4, p. 113.

Vincent (E. A.), 1960. Neues Jahrb. Min., Abh., vol. 94, p. 993.

—— and Phillips (R.), 1954. Geochimica Acta, vol. 6, p. 1.

—— Wright (J. B.), Chevallier (R.), and Mathieu (S.), 1957. Min. Mag., vol. 31, p. 624.

Wager (L. R.) and Deer (W. A.), 1939. Medd. Grønland, vol. 105, p. 1.

Wright (J. B.), 1957. Unpublished B.Sc. thesis, Oxford University.

—— 1959. Min. Mag., vol. 32, p. 32.

The use of petrographic methods for the identification of non-metallic inclusions in steel.

(With Plates XIII to XVI.)

By C. G. Nicholson, A.Met., F.I.M., F.G.S.

The Brown-Firth Research Laboratories, Sheffield 4.

[Taken as read 23 March 1961.]

Summary. It is shown that petrographic methods, using the microscope and micro-refractometer, can be a valuable aid in the identification of non-metallic inclusions in steel, even when their size is only a small fraction of a millimetre. Special ways of preparing the samples are given, and some of the methods used in examination are indicated. Natural chromite, corundum, merwinite, mullite, quartz, rhodonite, spinels, and zircon are taken as examples of the minerals found.

EVERY commercial steelmaking process yields a product that falls short of 100% purity. Though the skill of the steelmaker inevitably plays a large part in the control of quality, the nature of the impurities and, to a certain extent, the quantity present are related to the steelmaking process and to the type of steel that is being made.

Some writers on non-metallic inclusions have applied the term 'slag' to all solid impurities present in the ingot, but it is more usual to retain this word for the native inclusions resulting from reactions taking place in the molten metal, following additions to the melt. This entrapped slag represents a very small proportion of the total produced, the greater part rising to the surface and being separated from the metal. Native slag particles, together with foreign matter due in the main to chemical or physical attack on the refractories, constitute the non-metallic inclusion content of the steel.

It may appear from this that all non-metallic inclusions are artificial minerals, existing separately or in combination. This is not so. A number of natural minerals, for example quartz, zircon, and native chromite, are occasionally introduced into steel as a result of refractory failures. Even the minerals of slags, though artificial in origin, often have natural equivalents from which they may differ slightly in their optical con-

stants. Examples of such minerals are rhodonite and the iron olivine, fayalite. Mullite, though not a common mineral in nature, is of frequent occurrence as a reaction product in the foreign matter found in steels.

Previous work.

The examination of non-metallic inclusions has given rise to a considerable literature. The *Bibliography of Non-Metallic Inclusions in Iron and Steel*, published in 1935 by the Mining and Metallurgical Advisory Boards, Pittsburgh, Pennsylvania, contained over two thousand references. Though for the purposes of this bibliography the definition of a non-metallic inclusion embraced a much broader field than that included in the present paper, it is obviously impossible in a limited space to do justice to the large amount of research that has been done in this sphere. It must therefore suffice to refer to a small number of works that are readily accessible, and to rely on their bibliographies for further information.

From among the more important publications reference must first be made to the early classic by Benedicks and Löfquist (1930), which covers over three hundred pages. The series of five papers by Portevin and Castro, which appeared in the *Journal of the Iron and Steel Institute* between 1935 and 1937, is particularly noteworthy for its two hundred and thirty-five excellent photo-micrographs, taken with different types of incident illumination. Among more modern works may be mentioned the paper by Rait and Pinder (1946), entitled *The Origin and Constitution of Certain Non-Metallic Inclusions in Steel*, which combines the use of chemical, metallographic, and X-ray methods.

In view of the limited use that has been made of transmitted light in the identification of inclusions, particularly in this country, it is interesting to note that, as long ago as 1931, Hartmann employed an extraction method, followed by the mixing of the residue with Canada balsam, to make possible the use of a transmitted light petrological microscope for distinguishing between inclusions originating from the slag and from the refractory lining of the furnace; while in 1936 Yakshevich used a universal stage for the determination of the mineralogical constitution of some non-metallic inclusions in steel.

On the contrary, papers dealing with the mineralogical constitution of furnace slags are usually illustrated with photo-micrographs taken by transmitted light. Such is the case in Agrell's *Mineralogical Observations on Some Basic Open-Hearth Slags*, which appeared in 1945. The pioneer

paper by Whiteley and Hallimond (1919) on *The Acid Open Hearth and Slag* includes paired illustrations of samples as seen by transmitted and incident light—a practice that has much to commend it.

Methods used in the present investigation.

In the investigations described in the present paper, transmitted light petrographic methods have been mainly used, preceded by an examination in incident light—the metallographer's principal tool. Incident light should here be taken as including not merely incident illumination by coated glass plate or prism, but also dark ground illumination and the use of polarized light. Specialized methods of ore microscopy, calling for additional equipment and, in general, suited to larger objects than are available in many non-metallic inclusions, have not been used in the present investigation.

Where possible and advantageous, the normal microscopical examinations have been supplemented by refractive index measurements by the Becke method, in conjunction with the Leitz-Jelley micro-refractometer. The help of X-rays has been sought only rarely, and then mainly to support or contradict conclusions previously reached by petrographic analysis. The results considered in this paper may therefore be fairly taken as indicating what can be done in this sphere by anyone who has at his disposal a high-grade petrological microscope, well equipped for observations by incident and transmitted light, and possessing facilities for the taking of photo-micrographs, and either a comprehensive set of refractive index liquids or some form of micro-refractometer.

All of the transmitted light work has been done on chemically extracted inclusions.

Preparation of the specimens. The method of preparation of metallographic specimens for examination under the microscope by incident light is well known, though it may vary in detail from one laboratory to another. The surface to be examined is first carefully ground on a fine wheel until flat, the specimen being kept cool by frequently dipping it into cold water. The specimen is then polished on a graded series of emery papers attached to revolving tables, usually finishing on a '000' paper. The final polishing is done on lubricated rotating cloth-covered laps charged with 6μ and 1μ diamond pastes, though with the 6μ grade the uncoated surface of a disc of photographic paper is often preferred to cloth. In special cases a 0·25μ diamond lap is also used. The diamond

paste gives sharp outlines to any inclusions that may be present and avoids the building up of polishing medium round the harder particles and the dragging out of softer ones: it yields a clear polish ideally suited for observations of morphology, so far as this can be seen in section. Unfortunately it robs the inclusions of one of their characteristic features—differential hardness effects. Because of this it is often desirable to finish the sample with a light hand polish on a moistened Selvyt cloth, charged with γ-alumina, to produce a small amount of relief.

The method employed in this investigation in the preparation of thin sections through the extracted non-metallic inclusions was essentially that in general use for petrological specimens, modified by special precautions necessitated by the very small size of many of the samples. To facilitate the handling of inclusions, which may measure a small fraction of a millimetre in diameter, the method of mounting over a flake of muscovite recommended by Holmes (1921) for the preparation of slices through oolite-grains and organisms was adopted. Unless the inclusion was exceptionally large, 600 mesh carborundum only was used to rub a flat on it. This process was controlled by repeated observation with a low-power stereo-binocular microscope, viewing through the back of the slide with incident light being generally the more useful. A suitable flat having been prepared, cuts were made within the margin of the mica plate and the surrounding balsam was cut away. If this is done with transmitted light under a stereo-binocular microscope fitted with partially crossed polars, a satisfactory contrast can be arranged between the balsam and the mica; the limits of the latter may otherwise be difficult to see through the roughened upper surface of the mount. The mica was then cleaved and the tiny inclusion was lifted on its mount and stuck face downwards on a thin glass slide coated with Lakeside 70 plastic, prior to the rubbing down of the second side. Lakeside 70 was used instead of Canada balsam at this stage to reduce the risk of disintegration of delicate inclusions during capping.

In certain cases inclusions can with advantage be mounted without sectioning. This method is probably most suitable for those extracted from slabs, hot-rolled sheets and expanded tubes, in which inclusions consisting of glass spheres in the ingot have usually become deformed during hot work, finishing as approximations to triaxial ellipsoids. In such inclusions the length of the intermediate axis may be several times that of the shortest one. During mounting in hot balsam setting takes place with the shortest axis of the ellipsoid vertical, the resulting slide being a useful substitute for a parallel-sided slice.

Examination of the specimens. The methods used in examination are well known to mineralogists. They include observations of the degree of transparency, shape (including the crystallographic forms present), colour, cleavage, twinning, refractive index relative to the surrounding medium and, where possible, an accurate determination of at least the mean value. With the aid of polarised light it is determined whether the given mineral is isotropic or anisotropic, and, if it should prove to be anisotropic, the order of the birefringence; the maximum value of its extinction angle, which may be zero; whether it is uniaxial or biaxial, and whether its optical character is positive or negative. The determination of the optic axial angle of a biaxial mineral, or at least the value of 2E, may be well worth while, especially where it is impracticable to obtain a reliable figure for the mean refractive index. Even an approximate value, estimated from an examination of the curvatures of the isogyres, is better than none. The fact that this constant is influenced by solid solution concentrations makes it less reliable as an aid to identification in certain cases, but its determination may make it possible to place a mineral in its approximate position in a solid solution series. All of these optical properties, and the ways in which they are determined, have been dealt with in detail by Johannsen (1918), Hartshorne and Stuart (1960), and others, though some authors omit reference to the less commonly used methods. Determinative tables, based on various optical properties, are available in a number of textbooks, for example Larsen and Berman (1934), Winchell (1931) and, for slag and ceramic minerals, Rigby (1948), who also gives a list of references to photographs and a useful bibliography.

Examples from the present investigation. A residue that was extracted from a high chromium steel slab affords a good illustration of the triaxial ellipsoidal type of inclusion to which reference was made in the preceding paragraph.

A preliminary incident light survey of inclusions *in situ* in a polished section of this steel, followed by their examination in the rinsing water after extraction (pl. XIII A), indicated that they could be conveniently classified under three main heads, though mixed types were of frequent occurrence. The three primary types were: inclusions rich in lath-like crystals (pl. XIII B); inclusions rich in spinels (pl. XIII C); and glassy inclusions showing only surface globules (pl. XIII D).

Detailed examination of a number of inclusions of type 1 suggested, from the shape and optical properties of their characteristic phase, that they consisted of a merwinite-bearing slag. Thus the lath-like crystals

were found to be slightly shuttle-shaped, their birefringence was low, and their maximum extinction angle was approximately 36°. Additional evidence that these lath-like crystals were merwinite was provided by a conoscopic examination of the specially selected example illustrated in pl. XIII E. This gave a biaxial positive interference figure, showing the

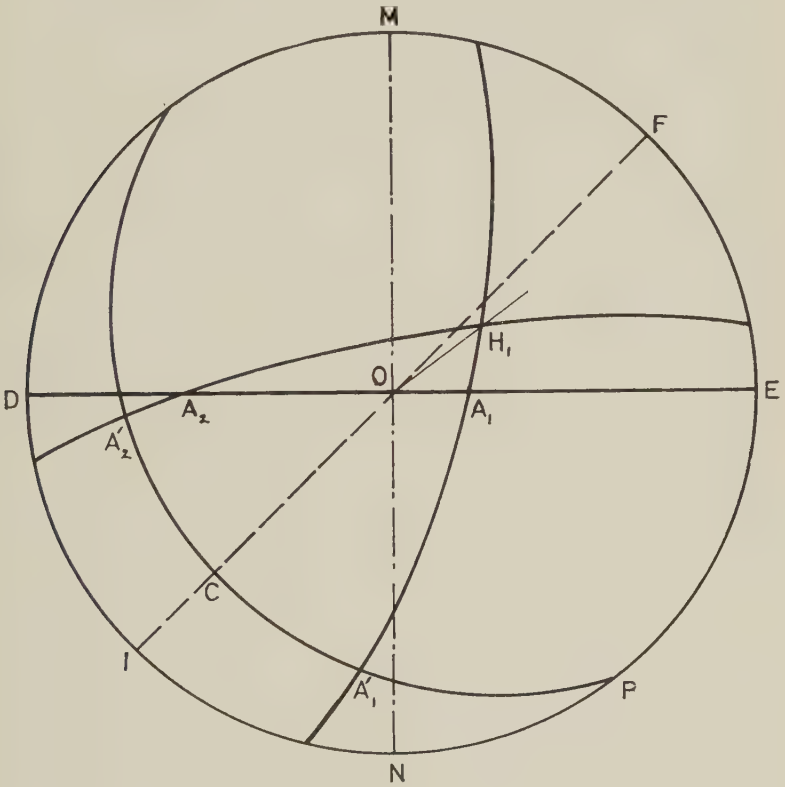

FIG. 1.

point of emergence of one optic axis. A determination of the optic axial angle was made by Wright's modification of Becke's method, for use when the point of emergence of only one optic axis appears in the field (Wright, 1911). Readings were taken on the isogyre, when straight and curved, with a modified Becke-Klein eye-piece, fitted with a calibrated coordinate micrometer scale, and plotting of the derived points was done over a 20 cm. Postel or angle meridian net. Since the optic axial angle was being checked for that of merwinite and direct measurement

of the mean refractive index was not possible in this case, the value obtained by Phemister (1942) for merwinite in blast furnace slag, namely $\beta = 1{\cdot}714$, was used. The final construction was as in fig. 1. The value found for the optic axial angle was $2V = 70° \pm 2°$, being the distance between A_1 and A_2 as read over the Postel net. This value is in close agreement with that found by Phemister (1942), namely $69° \pm 2°$.

Chromium-bearing spinels, probably agreeing most nearly in composition with picotite, are an important feature of these inclusions, and type 2 consists of these golden brown crystals in a glassy matrix (pl. XIII c). They rarely show a regular octahedral form, frequently being distorted to give elongated crystals with or without a dodecahedral face developed parallel to the flattened surface of the inclusion. When twinned they sometimes show complex geniculations (pl. XIII f).

Type 3 consists merely of a glass with globular sulphides in the surface (pl. XIII d). These show light grey under vertical illumination and are readily attacked by dilute sulphuric acid. Their identity was further confirmed by the orange ring test of Whiteley (Berglund: translated by Dearden, 1931). They were missing from inclusions extracted in hot hydrochloric acid, but retained when the iodine extraction method was used.

The use of exothermic compounds[1] to facilitate feeding during casting has sometimes led to the formation of foreign inclusions of considerable complexity. Since a wide departure from equilibrium conditions exists in these inclusions, the presence of incompatible phases is to be expected.

Small pieces of exothermic head, which may become entrapped near the top of an ingot, normally show an irregular, though somewhat softened, outline due to their origin as solid fragments; while original quartz, only partly changed to cristobalite and set in a porous and partially opaque ground mass, is a prominent feature, surrounded by phases mostly formed or modified by the exothermic reaction (pl. XIV a).

Of much greater variability and mineralogical interest are those in-

[1] Exothermic compounds, as used in the steel industry, consist of mixtures which react exothermally when strongly heated. They are made either as a powder, or as a refractory head—a reservoir, open top and bottom, with which a modified exothermic powder is incorporated during the process of manufacture. Though their precise composition varies with the maker, exothermic powders may be regarded as consisting of four intimately associated parts: a fuel (aluminium), an oxidizing agent (such as mill scale), a flux (such as calcite), and a refractory powder (often consisting largely of quartz sand). The object of using exothermic compounds is to retain a supply of liquid metal for a sufficient length of time to 'feed' or fill up potential contraction cavities, which would otherwise form in the main body of the solidifying casting or ingot.

clusions introduced by the incorrect use of exothermic powders. Since these are not designed to retain a fixed shape, much more evidence of fusion is to be expected. As is the case with fragments of exothermic head, original quartz from the sand in the mixture may be present, but perhaps the most characteristic phase in these inclusions is, in the author's experience, a pink corundum often heavily corroded or associated with the product of a peritectic reaction. Though it crystallizes in six-sided tablets, these are most often seen in section as pleochroic laths, giving straight extinction and showing maximum absorption when their length lies parallel to the plane of vibration of the lower nicol. These laths commonly show rhombohedral faces and twinning is not infrequent. Most attempts to obtain an interference figure in the obviously tabular crystals failed, partly because of this thinness, but also because they are rarely found free from obstruction. Clearly defined uniaxial negative interference figures, badly 'off centre', were given by a few of the laths that, by reason of their greater thickness, as measured in a direction perpendicular to the plane of the section, stood a better chance of spanning the depth of the slide. A fragment of one of these inclusions was crushed and a refractive index determination made by the immersion method, in conjunction with the Becke test. Though many of the fragments were still surrounded by the ground mass, a few edges were free and a value of approximately 1·767 was obtained (pl. XIV B). Sometimes the corundum laths have heavily corroded surfaces (pl. XIV C), but under favourable conditions these crystals may show very regular outlines, with a thin coating due to an arrested peritectic reaction. If this reaction, the product of which is apparently $CaO.6Al_2O_3$ (Filonenko, 1949, 1950), is enabled to continue by extremely slow cooling or reactivated by reheating to the peritectic temperature, the core gradually disappears and the thickened coating, sometimes lengthened by the addition of curved awns, may appear in section as a tube or simply as two parallel straight lines (pl. XIV E and F). These features are often seen more clearly by either vertical or dark field illumination in a solid polished specimen than by transmitted light in a thin section.

In striking contrast with the clearly defined crystals of corundum formed on cooling from the high temperatures of an exothermic reaction, are those found in inclusions produced when an alumina mould paint is washed by a limy slag. Irregular and spherical inclusions of this kind, as extracted from a casting and *in situ*, are shown in pl. XV A and B respectively. In those of irregular shape the proportion of mould paint

is very high, corundum being present as the original crushed fragments, though with their outlines considerably rounded. Their identity was confirmed by the observation of their characteristically low birefringence and by conoscopic examination, which showed them to be a uniaxial negative mineral. Though some of the globular inclusions consisted largely of slag or a slaggy reaction product, most were of intermediate types; one example, in which much original corundum still remains, is illustrated in pl. XV E and F.

Though mullite may be introduced into the microstructure of an inclusion as a result of peritectic reaction, this mineral occurs more usually, and often in considerable quantity, as a direct crystallization. Thus when a refractory of the fireclay type suffers a slag attack mullite becomes a prominent feature. A fragment of such a refractory, existing as a foreign inclusion in steel, was extracted and sectioned. It is shown between crossed nicols in pl. XVI A. Much mullite is present together with a cracked and partially absorbed grain of quartz. The optic axial angle, determined on the almost square cross-section of a similar sample of mullite, was found to be $43° \pm 2°$, a value agreeing with that given by Rigby (1948), namely 45°, but considerably higher than that given by Larsen and Berman (1934), namely 20° approx.

Rhodonite is frequently found in certain acid open hearth slags. It is the major constituent in the thin section of the slag inclusion shown in pl. XVI B. The dark phase present is an opaque spinel.

Reference has already been made to quartz, chromite, and zircon as examples of minerals of natural origin, which have found their way into steel by way of refractories. The quartz usually shows heavy cracking, due, at any rate in part, to passing through the α–β change. This sometimes happens several times, in alternate directions, during a series of heat treatments. Reaction borders are common. Conversion to a high temperature modification is not as common as might be expected. Chromite, showing a marked octahedral cleavage, is occasionally found as a cause of long, broken streaks on the surface of a cold rolled sheet (pl. XVI C, D, and E). An example of zircon with quartz, in a spherical inclusion found in a steel casting, is illustrated by Clark and Houseman (1959).

Conclusions.

It has been shown how some of the transmitted light methods of petrographic research can be a valuable aid to the identification of non-metallic inclusions chemically extracted from steel. There will be the

greatest gain when these methods supplement, not replace, those already in operation: but even when used alone they can provide valuable information some of which, such as the indication of the relationship between the phases present, is directly obtainable in no other way. Brief reference has been made to the origin of some of the inclusions described. To consider further the conclusions that should be drawn when a given mineral association is found to be present would be out of place in this context.

Acknowledgements. The author wishes to acknowledge his indebtedness to his colleagues R. Pemberton and J. W. Shillito respectively for the chemical extraction of the inclusions and for the making of the modified Becke-Klein eye-piece. His grateful thanks are also due to Professor A. Stuart, who supplied the standard muscovite used in the determination of the Mallard constant of the equipment, and to Mr. H. W. Kirkby, Director of Research, for permission to publish this paper.

References

Agrell (S. O.), 1945. Journ. Iron & Steel Inst., London, vol. 152, no. 2, p. 19.

Benedicks (C.) and Löfquist (H.), 1930. Non-Metallic Inclusions in Iron and Steel. (Chapman & Hall, London.)

Berglund (T.), translated by Dearden (W. H.), 1931. Metallographers' Handbook of Etching, p. 121. (Pitman & Sons, Ltd., London.)

Clark (P. W.) and Houseman (D. H.), 1959. British Foundryman, Oct. 1959, p. 445.

Hartmann (F.), 1931. Arch. Eisenhütt., vol. 4, p. 601.

Hartshorne (N. H.) and Stuart (A.), 1960. Crystals and the Polarising Microscope. (Ed. Arnold (Publishers) Ltd., London.)

Holmes (A.), 1921. Petrographic Methods and Calculations. (Thos. Murby & Co., London, pp. 245–246.)

Johannsen (A.), 1918. Manual of Petrographic Methods. (McGraw-Hill Book Co. Inc., New York and London.)

Larsen (E. S.) and Berman (H.), 1934. The Microscopic Determination of the Non-Opaque Minerals. U.S. Geol. Surv. Bull. no. 848.

Phemister (J.), 1942. Min. Mag., vol. 26, p. 225.

Portevin (A. M.) and Castro (R.), 1935–7. Journ. Iron & Steel Inst., London, vol. 142, no. 2, p. 237; vol. 143, no. 2, p. 213; vol. 144, no. 1, p. 223.

Rait (J. R.) and Pinder (H. W.), 1946. Ibid., vol. 154, no. 2, p. 371.

Rigby (G. R.), 1948. The Thin Section Mineralogy of Ceramic Materials. (Brit. Refract. Research Assoc.)

Whiteley (J. H.) and Hallimond (A. F.), 1919. Journ. Iron & Steel Inst., vol. 99, no. 1, p. 199.

Winchell (A. N.), 1931. The Microscopic Characters of Artificial Solid Substances or Artificial Minerals. (John Wiley & Sons Inc., New York, & Chapman & Hall, London.)

Wright (F. E.), 1911. The Methods of Petrographic-Microscopic Research. Carnegie Inst. Washington, Publ. 158.

[Yakshevich (F. A.)] Якшевич (Ф. А.), 1936. [Заводская Лаборатория (Factory Lab.), vol. 5, p. 41]; abstr. in Brit. Chem. Abstr., ser. B, 1937, p. 351, and in Chem. Abstr., 1936, vol. 30, p. 4448.

Explanation of Plates XIII to XVI.

Plate XIII

A. Residue extracted from a high chromium steel slab, photographed in water. Transmitted light, × 150 diams.

B. Type 1 inclusion *in situ*. Incident light, × 150 diams.

C. Type 2 inclusion *in situ*. Incident light, × 375 diams.

D. Type 3 inclusion *in situ*. Incident light, × 750 diams.

E. Extracted inclusion of merwinite-bearing slag. Transmitted light, × 750 diams.

F. Extracted inclusion containing chromium-bearing spinels (picotite?), some of which show complex twinning, × 750 diams.

Plate XIV

A. Fragment of an exothermic head, entrapped near the top of a high-speed ingot. Photographed *in situ* by incident light, with partially crossed nicols in order to show the residual quartz grains. × 30 diams.

B. Fragment of an inclusion introduced by the incorrect use of an exothermic powder, immersed in a solution of refractive index 1·767. Note the optical merging of the lath with the fluid, as indicated by the arrow. Transmitted light, × 600 diams.

C. Inclusion introduced by the incorrect use of an exothermic powder. The heavily corroded plates consist of pink pleochroic corundum. The matrix is a glass throughout which small crystals of a spinel are scattered. The larger white patches are metal. Incident light, × 120 diams.

D. A thin section through the inclusion illustrated in C. Transmitted plane polarised light, × 120 diams.

E. An inclusion of similar origin, but from a different casting. Here the sharply defined corundum crystals are coated with a layer of $CaO.6Al_2O_3$, which preserves the regular outline while the peritectic reaction exhausts the core through rifts, which form at points farthest from the centre of the crystal. Incident light, × 300 diams.

F. A more advanced stage in the peritectic reaction. Two $CaO.6Al_2O_3$ shells, which are partially emptied, are approaching the appearance of hollow tubes seen in section. Others, still unperforated, remain with their content intact. Incident light, × 300 diams.

Plate XV

A. A cluster of inclusions, some irregular in shape while others are spheres, extracted from near the surface of a casting, made in a mould treated with an alumina paint. Incident light, × 60 diams.

B. Section cut perpendicular to the surface of the casting, showing a mixed cluster of inclusions. Incident light, × 30 diams.

C. Thin section of one of the irregular shaped inclusions, which consists essentially of alumina mould paint. Transmitted light, × 60 diams.

D. Part of the same inclusion showing the sub-angular shapes adopted by the particles of corundum. Transmitted light, × 300 diams.

E. Section through one of the spherical inclusions. Transmitted light, × 60 diams.

F. Part of the same inclusion, in which the corundum grains are bonded by a reaction product due to slag attack. Transmitted light, × 300 diams.

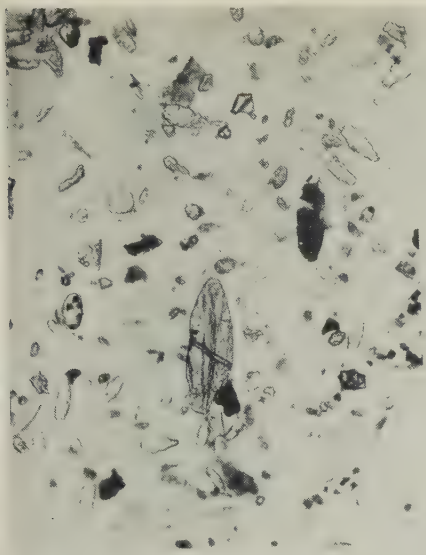

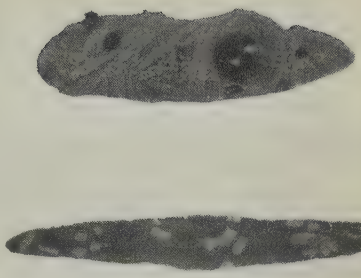

B

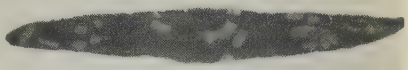

C

D

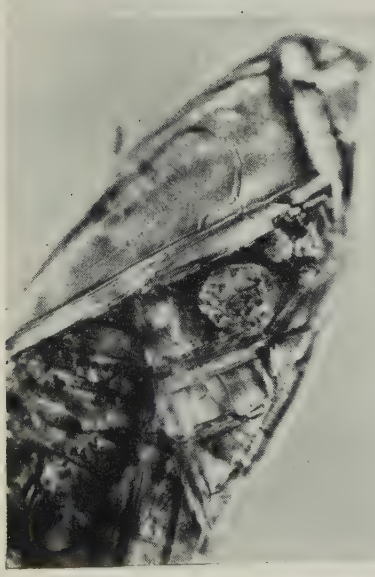

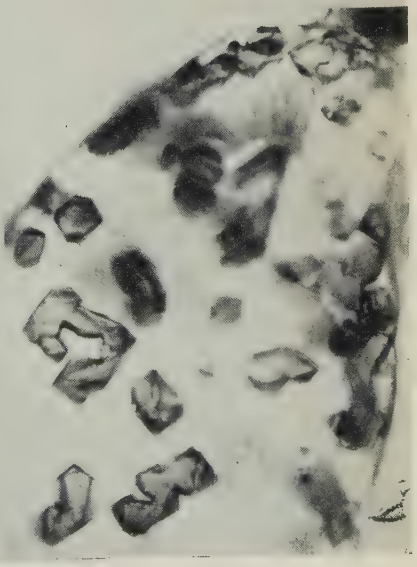

F

C. G. Nicholson: Identification of inclusions in steel

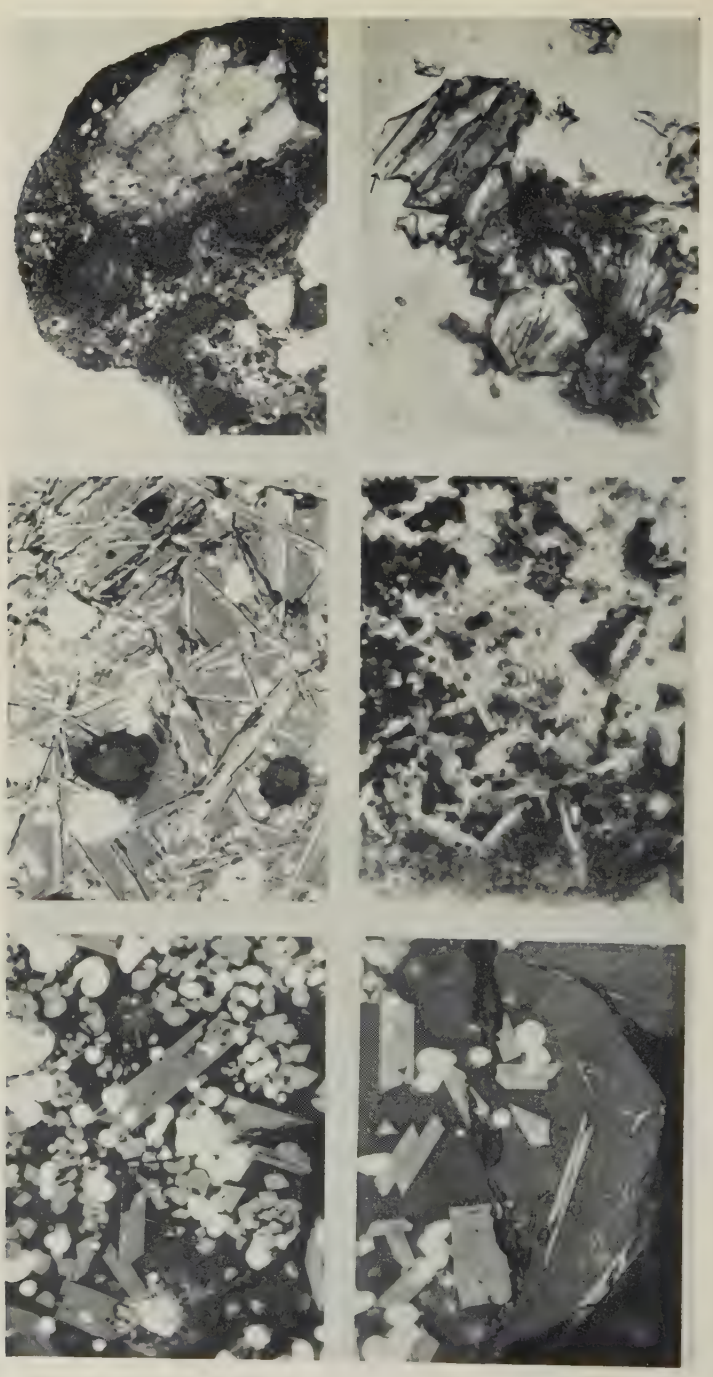

C. G. Nicholson: Identification of inclusions in steel

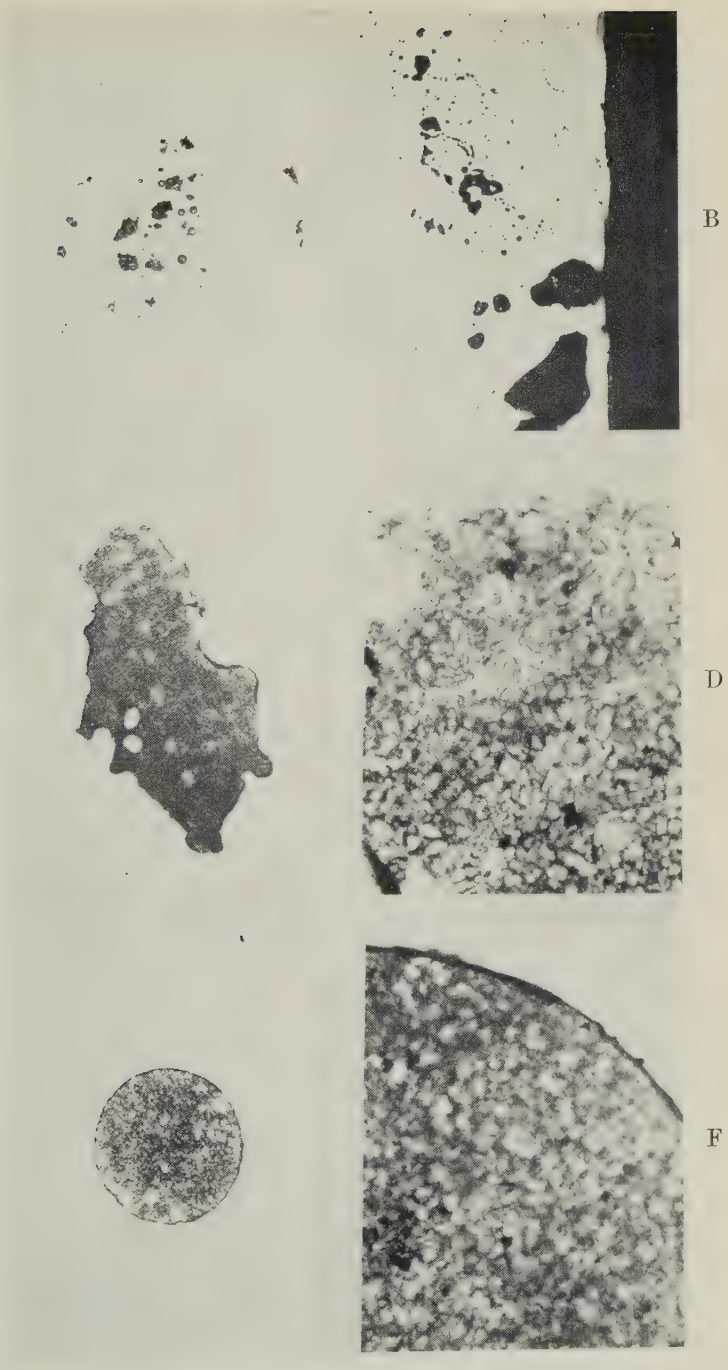

C. G. Nicholson: Identification of inclusions in steel

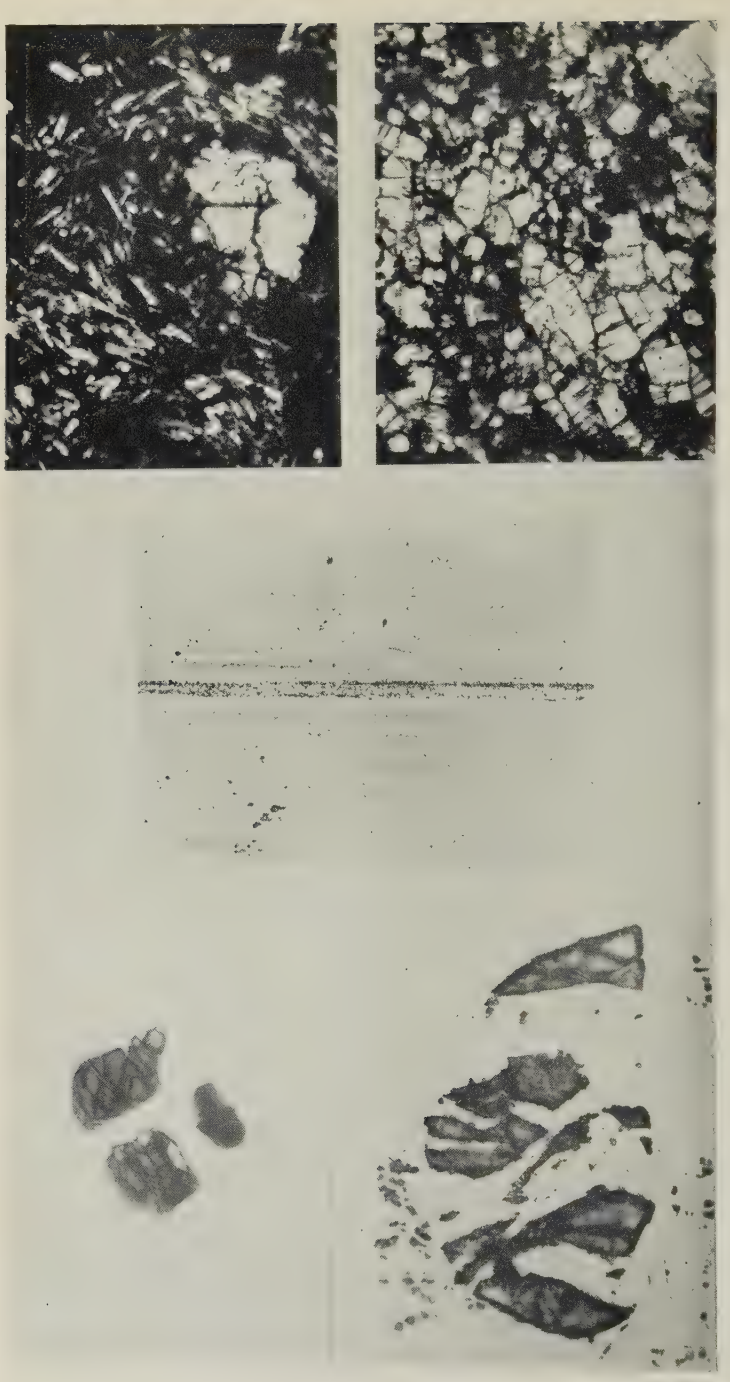

C. G. NICHOLSON: IDENTIFICATION OF INCLUSIONS IN STEEL

PLATE XVI

A. Quartz and mullite in a foreign inclusion introduced as a result of slag attack on a fire-clay type of refractory. The quartz, which is heavily cracked and corroded, is surrounded by a zone of glass. Beyond this relatively clear space, a dense crystallization of mullite is seen. Transmitted light with crossed nicols, × 120 diams.

B. Rhodonite, associated with an opaque spinel, in a slag inclusion extracted from a billet of acid open-hearth steel. Transmitted light, × 120 diams.

C. Streak on the surface of a pressing made from a cold rolled sheet of an 18/8 type of stainless steel. Incident light, × 6 diams.

D. Three fragments of chromite of refractory origin, extracted from the streak shown in C. Note the clearly defined octahedral cleavage. Photographed in water by incident light, with a 4 mm. water immersion objective, × 300 diams.

E. Fragments of refractory chromite as seen in a streak similar to that illustrated in C, after a light surface polish. This print has been rotated through 90° relative to the streak. Octahedral cleavage is again present. Incident light, × 300 diams.

Addendum. Booker *et al.* (1960) carried out a comprehensive examination of aluminous inclusions in iron, employing a replica extraction method previously used by two of the authors. Examination was by incident light, transmitted polarized light, electron microscopy, and X-ray diffraction.

Additional references:

BOOKER (G. R.) *et al.*, 1960. Journ. Iron Steel Inst., London, vol. 196, p. 294.

[FILONENKO (N. E.)] Филоненко (Н. Е.), 1949. Доклады Акад. Наук СССР [Compt. Rend. Acad. Sci. URSS], vol. 64, p. 529.

[—— and LAVROV (I. V.)]—и Лавров (И. В.), 1950. Журн. Прикл. Хим. [Journ. Appl. Chem.], vol. 23, p. 1040.

Methods for the chemical analysis of meteorites. I. Siderites.

By A. A. Moss, B.Sc., Ph.D., F.S.A., M. H. Hey, M.A., D.Sc., and D. I. Bothwell, B.Sc.

Department of Mineralogy, British Museum.

[Read 23 January 1958.]

Summary. Simple chemical procedures (colorimetric and gravimetric) for the determination of Co, Cr, Cu, Ga, Ni, P, and S in an iron meteorite or in the separated metallic phase of a pallasite are described; the minimum size of sample is discussed. A procedure for the quantitative removal of the metallic, sulphide, and phosphide phases from a stone or siderolite is described, and is applicable to the quantitative isolation of silicate and oxide inclusions from siderites (other than some very high in nickel).

ONE of the major difficulties in meteoritic studies is the variable quality of the chemical data. Work on the rocks G1 and W1 has shown that even when well-tried standard methods are available there is an uncomfortably wide spread in the results obtained by different analysts or even by the same analyst at different dates.[1] The meteoriticist is in a far worse position than the petrologist, for not only are there few standard, commonly accepted techniques, but the shortage of material and the gross inhomogeneity of many meteorites are apt to make it difficult to obtain a representative sample and the analytical problems are much more serious. Wahl[2] and others have shown that the figures for alkalis and alumina in stones are commonly gravely in error, and it is doubtful if any but the most modern figures for cobalt or copper in irons are satisfactory.

[1] H. W. Fairbairn *et al.*, U.S. Geol. Surv. Bull. no. 980, 1951; H. W. Fairbairn and J. F. Schairer, Amer. Min., 1952, vol. 37, p. 744 [M.A. **12**–33]; H. W. Fairbairn, Geochimica Acta, 1953, vol. 4, p. 143 [M.A. **12**–264]; A. A. Smales, D. Mapper, and A. J. Wood, Analyst, 1957, vol. 82, p. 75 [M.A. **13**–250]; S. S. Goldich and E. H. Oslund, Bull. Geol. Soc. Amer., 1956, vol. 67, p. 811 [M.A. **13**–467]; A. A. Smales, Geochimica Acta, 1955, vol. 8, p. 300 [M.A. **14**–43]; J. P. Riley, Anal. Chim. Acta, 1958, vol. 19, p. 413 [M.A. **14**–87]; R. C. Chirnside, Journ. Soc. Glass Technol., 1959, vol. 43, p. 5 T [M.A. **14**–383]; J. P. Riley and H. P. Williams, Mikrochim. Acta, 1959, p. 804 [M.A. **14**–455].

[2] W. Wahl, Geochimica Acta, 1950, vol. 1, p. 28 [M.A. **11**–261]; W. Wahl and H. B. Wiik, ibid., p. 123 [M.A. **11**–437].

At their meeting at Mexico in 1956 the Permanent Commission on Meteorites of the International Geological Congress recognized the development of reliable methods for the chemical analysis of meteorites as an urgent need, and over the past four years we have sought to meet this need; the present paper will, it is hoped, be the first of several on analytical techniques particularly adapted to work on various classes of meteorites. Recent developments in physical and other specialized methods of analysis, particularly radioactivation and X-ray fluorescence and microanalyser methods, radioactive tracer techniques, and mass spectrography, provide invaluable methods for a very wide range of trace elements; but there are many laboratories where these techniques are not available, and our experience has shown that many trace elements can readily be determined by colorimetric and other methods that call for little or no special equipment beyond that available in any laboratory practising rock analysis. Little modification has been necessary to adapt many of the colorimetric methods used by E. B. Sandell and his fellow workers[1] to meteorite analysis, and these methods have in general proved outstandingly reliable.

Meteorites are in general far from uniform in composition even within a moderate-sized mass: the combination of white aubrite and black enstatite chondrite in Cumberland Falls is unique, but Wahl[2] has shown that many other stony meteorites are breccias, often on a fairly large scale, containing fragments of two or more different types; non-uniformity in irons is less spectacular, apart from the gradations from a pallasite to a pure siderite in some specimens of Brenham, but the distribution of inclusions is often far from uniform, and it is by no means certain that differences between two or more analyses of the same fall[3] are always due to analytical error.

In polymict brecciated stones we should expect the composition of many of the constituent minerals to vary from fragment to fragment, but variation has also been demonstrated in apparently monomict stones, for instance in the feldspar of Juvinas.[4] A detailed study of the chemistry (including trace elements) and physical properties of the

[1] E. B. Sandell, Colorimetric Determination of Traces of Metals, 3rd edn, New York and London, 1959.

[2] W. Wahl, Geochimica Acta, 1952, vol. 2, p. 91 [M.A. 11–526].

[3] See, for example, the entries in G. T. Prior, Catalogue of Meteorites, 2nd edn, London, 1953, under Cape York, Otumpa, Mount Joy, Glorieta Mountain, Prambanan, Cratheús, and Rodeo. On the other hand, the widely differing analyses for the different masses of Babb's Mill and of Staunton may indicate distinct falls.

[4] P. M. Game, Min. Mag., 1957, vol. 31, p. 656.

several distinct phases in a range of stony meteorites and, if possible, in the distinct fragments of a polymict brecciated stone may be expected to yield interesting results, and it is hoped to undertake such a study as soon as the necessary techniques have been perfected.

In the present article we consider a method for the determination of Co, Cr, Cu, Ga, Ge, Ni, P, and S in a siderite or in the separated metallic phase of a pallasite, and a method for the removal of the metallic, phosphide, and sulphide phases from a stone or a siderolite, or for the quantitative isolation of the silicate and oxide phases from a siderite.

Visible inclusions of troilite are often large and very irregularly distributed; and in some meteorites (e.g. La Primitiva) there are large drop-like inclusions of schreibersite, while others contain coarse lamellae of schreibersite. It seems preferable to avoid, as far as possible, all macroscopic inclusions; but where the inclusions are of small or moderate size and regularly distributed, then a sample large enough to ensure that they will be correctly represented must be taken (compare below). If the inclusions are coarse and can be avoided, and if a bulk composition is desired, a separate analysis of the inclusions and an areal analysis of as extensive a cut surface or surfaces as possible will be the most satisfactory procedure. But there seems little point in computing the bulk composition of a siderite with irregularly distributed inclusions.

Determination of Co, Cr, Cu, Fe, Ga, Ge, Ni, P, and S in a siderite.

A single sample of the meteorite will serve for the determination of these nine elements; the size of sample required depends on the class of siderite under investigation: for hexahedrites, ataxites, and finest octahedrites a 1-g. sample may be assumed to be representative; but with a very coarse octahedrite it will be obvious that a sample approximately 5 mm. cube may fail to include the true proportion of taenite.

A rough calculation of the minimum size of sample was made, assuming that the taenite lamellae are uniformly t mm. apart and contain 30% Ni: for a sample weighing $2t^3$ g., the standard deviation from the true mean nickel content, due to an excess or deficit of taenite in the sample, will be approximately $\frac{1}{3}$% of the amount present, or 0·02 to 0·03% Ni; thus for such a sample we can be reasonably certain that the sampling error of the nickel content will not exceed 0·1% Ni and will be less than the probable analytical errors. For the less abundan elements, the relative precision of the analytical methods is not so good, and a rather smaller sample, say of t^3 g., will be acceptable.

In the detailed procedure set out below three separate portions of 1 g. of meteorite serve for the determination of Ge, S, and P, and the residues from the distillations for the Ge and S are combined to give a solution derived from 2 g. of meteorite, which serves for the determination of the remaining elements, while aliquot parts from the solution used for P serve for check determinations. Thus there should be no appreciable error due to excess or deficit of taenite in the sample, unless the meteorite is an octahedrite with band width exceeding 1·0 mm.; for octahedrites coarser than this the size of sample must be increased and the scale of operation adjusted accordingly: each of the three portions should weigh at least t^3 g. Similar calculations apply to siderites bearing regularly distributed inclusions of small or moderate dimensions, t then being the spacing of these inclusions (in mm.).

It will in general be advantageous for the sample to be tabular in shape, provided the thickness is not less than about $2t$ mm.; for in a tabular sample macroscopic inclusions are less likely to be obscured. It will also be useful (though not essential) to polish, etch, and examine both faces of the tablet, to make sure that the structure and microscopic inclusions are representative of the main mass.

Preparation of the working meteorite solutions.

Assuming that we are dealing with an ataxite, hexahedrite, or octahedrite of band width less than 1 mm., a 3-g. sample, free from macroscopic inclusions, will have been obtained and will be sawn into three approximately equal pieces, *X*, *Y*, and *Z*. One of these, *X*, is used for the determination of phosphorus, and it has been found that in order to recover all the phosphorus this sample must be dissolved under oxidizing conditions; simple attack with 1:1 hydrochloric acid[1] is unlikely to dissolve all the schreibersite, and furthermore some of the phosphorus will be lost. This portion is therefore dissolved in aqua regia, evaporated to dryness, 5 ml. conc. HCl added and the solution again evaporated to dryness to destroy nitrates, and this second residue dissolved in 5 ml. conc. HCl and a little water, and diluted to 100 ml. in a volumetric flask;[2] this constitutes solution *A*. Reagent blanks must be prepared for solution *A*, and for solutions *B*1, *B*2, *C*, and *D* described

[1] That is, a mixture of equal parts conc. HCl, sp. gr. 1·18, and water.

[2] If larger samples than 1 g. are necessary, the amount of acid and final bulk of solution *A* should be increased proportionally. Similarly the scale of operation on the other two samples, and the bulk of solutions *B* and *C*, must be increased proportionally. But the size of the aliquots for the several determinations need not be increased.

below; these may be labelled solutions *a*, *b*1, *b*2, *c*, and *d*. The preparation and utilization of these working solutions is outlined diagrammatically in table I.

TABLE I. Schematic course of analysis for iron meteorites (larger samples are needed for coarsest, coarse, and some medium octahedrites).

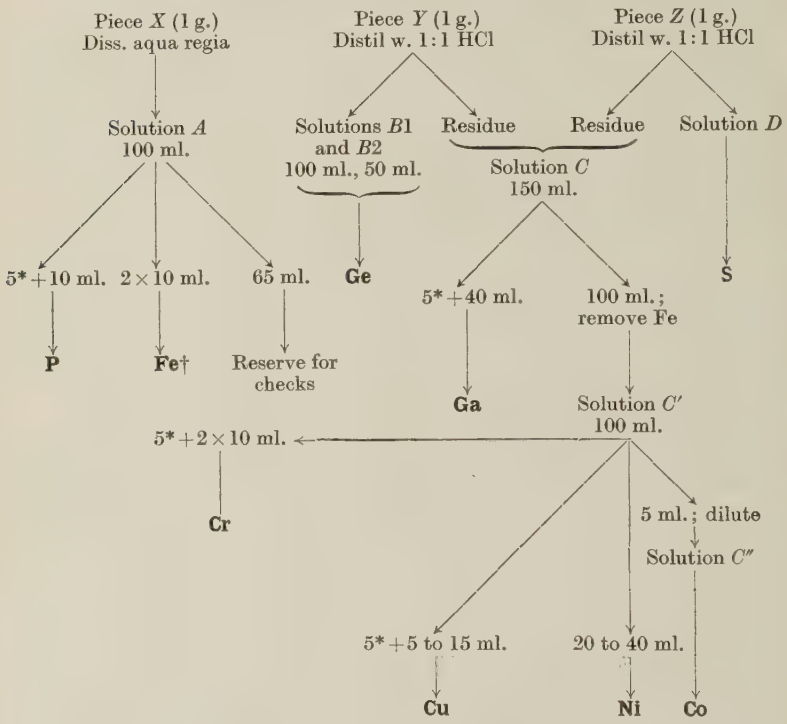

* Portion for preliminary rough determination.
† Iron will usually be determined by difference.

A second piece, *Y*, of the meteorite is placed in a flask fitted with a tap funnel, still head, and condenser, and a 50-ml. cylinder is placed under the end of the condenser. Fifty ml. of 1:1 HCl are run into the flask, which is gently heated until the meteorite has dissolved; the heat is then increased and 20 ml. of acid are distilled over into the cylinder, 10 ml. 1:1 HCl run into the flask and a further 20 ml. of acid distilled over, making 40 ml. in all. Distillation is stopped and the distillate transferred to a 100-ml. volumetric flask and made to volume with water (solution *B*1). The cylinder is replaced, 15 ml. 1:1 HCl run into the flask,

and a further 20 ml. of distillate collected, transferred to a 50-ml. volumetric flask, and made up with water (solution *B*2). The residue in the flask is transferred to a 150-ml. volumetric flask and reserved without dilution to volume (part of solution *C*).

The third piece, *Z*, of meteorite is placed in a 50-ml. flask fitted with a reflux condenser and a dropping funnel the stem of which reaches to the bottom of the flask. The upper end of the reflux condenser is connected by glass tubing to two bubblers in series, both containing absorbing solution (1 g. $ZnSO_4.7H_2O$ and 50 ml. ammonia sp. gr. 0·880, diluted to 1 litre); arrangements are made to lead a current of nitrogen[1] through the apparatus, via the dropping funnel, during the determination. The first bubbler should be a 250-ml. flask; it is charged with 100 ml. of absorbing solution and the second with 25 ml.; 20 ml. of 1:1 HCl are run into the 50-ml. flask, a slow nitrogen current started, and the flask heated gently until the meteorite has dissolved and then boiled gently for about 15 min. The residual solution in the flask is united with solution *C*, the residue from the other distillation (for Ge), and the combined solutions diluted to volume (150 ml.).

The contents of the second bubbler are added to the first (no rinsing is necessary), and the inlet tube of the first bubbler is rinsed; the combined solutions (solution *D*) are titrated for sulphide as described below.

Sulphide.

To solution *D* add 10 ml. of an iodate–iodide solution (130 mg. KIO_3 and 550 mg. KI in 200 ml. water) and, after mixing, 10 ml. conc. HCl; mix and cool by standing the flask in cold water and titrate with standard N/50 sodium thiosulphate, using starch as indicator. A reagent blank, solution *d*, is treated similarly, and the difference between the two titrations gives the sulphide sulphur in piece *Z* of the meteorite; $H_2S+I_2 \rightarrow S+2H^++2I^-$.

Germanium.[2]

A stock standard germanium solution is prepared by dissolving 72 mg. of GeO_2 in 10 to 15 ml. 0·4% NaOH and diluting to 50 ml. with water. This solution contains 1 mg. Ge per ml.; working standards (1 μg. Ge per ml.) are prepared by dilution as required.

A phenylfluorone reagent is prepared by dissolving 30 mg. of 9-phenyl-2:3:7-trihydroxy-6-fluorone in a mixture of 85 ml. ethyl alcohol and 5 ml. dilute sulphuric acid (1:6 by volume) and making up to

[1] If nitrogen is not available carbon dioxide may be used.

[2] After H. J. Cluley, Analyst, 1951, vol. 76, p. 523.

100 ml. with alcohol. The approximate germanium content of solution *B*1 is first ascertained by a trial[1] on a 10-ml. aliquot, and then for the determination proper an aliquot containing between 5 and 30 μg. Ge is run into a 50-ml. volumetric flask, together with 5 ml. 0·5% gum arabic solution. The HCl content of the aliquot used is calculated, on the assumption that the 100 ml. of solution *B*1 contain 20 ml. conc. HCl (sp. gr. 1·18), and sufficient conc. HCl is added to make the total 5 ml., together with enough water to bring the total volume to about 30 ml. The solution is cooled below 20° C., if necessary, 15 ml. of phenylfluorone reagent run in from a pipette, and the flask filled to the mark; after standing for 30 min. the optical density is compared with a reagent blank made up from solution *b*1, at a wave-length[2] of 510 mμ, and with that of solutions of known germanium content made up in the same manner from the diluted standard solution.

The germanium content of 25 ml. of solution *B*2 is determined in the same way, and the total germanium content of the meteorite in parts per million can then be calculated; 100 ml. of solution *B*1 and 50 ml. of solution *B*2 were obtained from piece *Y* of the meteorite.

Phosphorus.

Standard phosphate and reagent solutions are prepared as follows—Phosphate: about 900 mg. KH_2PO_4 are weighed out accurately and dissolved in 200 ml. H_2O for a stock solution, which is diluted 1/100 for use, and will then contain approximately 10 μg. P per ml. Reagent: 2·0 g. ammonium molybdate are dissolved in 40 ml. water and mixed with 60 ml. of 1:1 (by volume) sulphuric acid to form a stock solution; immediately before use, 50 ml. of this stock molybdate solution are diluted to about 160 ml., 20 ml. of 0·15% aqueous hydrazine sulphate added, and the volume made up to approximately 200 ml.

Ten ml. of solution *A*, representing a tenth of piece *X* of the meteorite, are run in a 100-ml. beaker, and 10 ml. of the blank solution *a* in a second beaker. Ten ml. of 10% aqueous $Na_2SO_3.5H_2O$ are added to each of these beakers and the solutions boiled gently for 5 min. A third beaker receives 20 ml. water, and a fourth receives an amount of standard phosphate solution containing about as much phosphorus as 10 ml. of

[1] It is usually convenient to make the preliminary estimates by reference to a standard curve, but the actual determination should be made against standard solutions prepared at the same time as the unknown. The same applies in the other colorimetric procedures described below.

[2] A spectrophotometer is the most suitable instrument for this and the other determinations described below, but a filter-type absorptiometer may be used.

solution *A* (as determined by a trial run on 5 ml. of solution *A*), together with enough water to make up 20 ml.

Twenty-five ml. of freshly prepared molybdate–hydrazine reagent are run into each of the four beakers, which are covered and placed on a boiling-water bath for 40 min., then removed and allowed to cool to room temperature, after which they are made up to 100 ml. or 50 ml. in volumetric flasks according to the intensity of the colour. The optical density of each solution is measured against the appropriate blank at a wave-length of 650 mμ.

Gallium.

The method is based on the extraction of gallium from hydrochloric acid solution by *iso*-propyl ether, extraction of iron being prevented by reduction to the ferrous state; the extracted gallium is complexed with Rhodamine B, and the lake extracted by a mixture of monochlorbenzene and carbon tetrachloride.[1] The extraction of the Rhodamine B lake is not complete, and for accurate results it is essential that the conditions should be closely adhered to, especially the strengths of acid. Accordingly, the concentration of the 7N hydrochloric acid and of the 6N hydrochloric acid + $TiCl_3$ prescribed below must be checked by titration and adjusted if necessary.

The stock standard gallium solution is prepared by dissolving 27 mg. pure Ga_2O_3 in 6N HCl and making up to 200 ml. with 6N HCl; this solution contains about 100 μg. Ga per ml., and should be diluted with 6N HCl to prepare working standards.

The approximate gallium content of solution *C*, the 150 ml. of which were obtained by combining pieces *Y* and *Z* of the meteorite, is first ascertained by a trial on a 5-ml. aliquot, and for the determination proper an aliquot not exceeding 40 ml. and containing, if possible, between 5 and 20 μg. Ga is run into a 100-ml. beaker and evaporated to dryness on the water bath. An equal volume of solution *c* is evaporated in a second beaker to serve as a blank. An appropriate amount of gallium standard is evaporated in a third beaker, and an equal amount of 6N hydrochloric acid in a fourth. The residue in each of the four beakers is dissolved in 5 ml. of 7N hydrochloric acid and transferred to a 100-ml. separating funnel, using a further 10 ml. of acid for washing out the beaker.

About 2 ml. 15% w/v titanous chloride are added to reduce the iron, followed by 15 ml. of *iso*-propyl ether, and the separator is gently shaken

[1] F. Culkin and J. P. Riley, Analyst, 1958, vol. 83, p. 208.

for 1 min. The aqueous phase is run into a second separator, shaken for 1 min. with 10 ml. of *iso*-propyl ether, and the aqueous phase discarded. The combined ether extracts are washed by shaking for 10 sec. with 3 ml. of 7N hydrochloric acid and a drop of titanous chloride, then run into a 100-ml. beaker, covered and placed on a hot water bath until all the ether has evaporated. To each of the evaporated gallium extracts is added 5 ml. of 6N hydrochloric acid containing about 1% titanous chloride; the covered beaker is allowed to stand on the water bath for 10 min., cooled, and the solution transferred to a 10-ml. volumetric flask and made up to volume with 6N hydrochloric acid + titanous chloride. Five ml. of this solution are transferred to a 50-ml. separating funnel, 0·5 ml. of a 0·5% solution[1] of Rhodamine B in 6N hydrochloric acid are added, and the gallium lake extracted with 10 ml. of a mixture of 50 ml. carbon tetrachloride and 150 ml. chlorbenzene by shaking for 5 min. on a mechanical shaker. After standing for 10 min. a few drops of liquid are run out of the funnel, the stem is dried out with filter paper, and some of the extract run into a 1-cm. photometer cell and its optical density measured against the CCl_4–C_6H_5Cl solvent at a wave-length of 562 mμ. The appropriate blank should be run through at the same time so that all readings are comparable, since the optical densities of both sample and blank alter with time.

Iron.

It is usually adequate to obtain the iron content of a siderite by difference, but if for any reason a direct determination is desired, two 10-ml. portions of solution *A*, each representing a tenth of piece *X* of the meteorite, may be reduced and titrated.

Removal of iron from the working solutions.

The determinations of Co, Cr, Cu, and Ni are best made on iron-free solutions, and accordingly a large aliquot of solution *C* is taken and the iron removed by extraction with *iso*-propyl ether from 8N hydrochloric acid solution.[2]

[1] The proportion of dyestuff in the Rhodamine B bought from different suppliers of chemicals varies, and in order to obtain the maximum extraction of the complex it may be necessary to double or even quadruple the concentration prescribed below; preliminary experiments with 0·5%, 1%, and 2% solutions and standard gallium solution should be made with each new batch of dyestuff to ascertain the appropriate strength.

[2] E. H. Swift, Journ. Amer. Chem. Soc., 1936, vol. 58, p. 2573.

A hundred ml. of solution *C* are evaporated to dryness on the water bath, dissolved in 8N hydrochloric acid, and transferred to a 100-ml. separating funnel, using about 20 ml. acid in all. Twenty ml. *iso*-propyl ether are added and the funnel shaken for about 1 min., then the aqueous layer is run into a second funnel, rinsing the stopper and delivery tube of the first funnel with small amounts of 8N hydrochloric acid; the ethereal layer is washed with 10 ml. of 8N acid, shaking for about 20 sec. and the aqueous layer combined with that from the first extraction. The combined aqueous solutions are extracted with a further 20 ml. of ether and the ethereal layer washed with acid as before. The second ether extract should be nearly colourless, and the aqueous layer a clear green; if this is not the case, a third ether extraction will be needed. The final aqueous layer is run into a 150-ml. beaker, evaporated to dryness, dissolved in 1 ml. hydrochloric acid and a little water and made up to 100 ml. in a volumetric flask to form solution *C'*, derived from two-thirds of the combined pieces *Y* and *Z* of meteorite. A reagent blank, solution *c'*, is prepared similarly from 100 ml. of solution *c*.

The final ether layers are accumulated in a residue bottle, washed with water to remove ferric chloride, and the ether recovered by distillation after destroying any peroxides by shaking with a little ferrous sulphate solution.

Nickel.

The approximate nickel content of the meteorite will be known unless it is a nickel-rich ataxite. An aliquot of solution *C'* containing not more than 30 mg. Ni is run into a 250-ml. beaker, 1 g. ammonium chloride and 0·5 g. tartaric acid added, and the solution diluted to 200 ml.; 5 ml. of a 1% alcoholic solution of dimethyl glyoxime are added for every 10 mg. of nickel present, the solution heated to boiling-point and ammonia added until it is alkaline. The beaker is covered and left 2 hrs. on the water bath, filtered on a porosity grade 3 silica or glass filter crucible, washed with hot water, dried at 110 to 120° C., and weighed.

Cobalt.

Five ml. of solution *C'* are diluted to 100 ml. in a volumetric flask to give a dilute working solution *C''*, 10 ml. of which represent 1/300 of the two pieces *Y* and *Z* of meteorite. A preliminary estimation on 10 ml. of solution *C''* is made to ascertain the approximate cobalt content, and an aliquot containing 20 to 40 μg. is run into a 15-ml. beaker and evaporated to dryness on the water bath. In a second beaker 5 or 10 ml. of diluted

standard cobalt solution (about 4 μg. per ml., prepared by dilution of a stock solution containing about 1 mg. Co per ml.) are evaporated, while a third beaker will receive the reagent blank diluted from solution *c'*. A buffer solution is prepared, containing 0·62 g. boric acid, 7·2 g. $Na_2HPO_4.12H_2O$, and 2·0 g. NaOH in 100 ml., and to each beaker is added 1·5 ml. 4·2% citric acid, 1·8 ml. buffer solution, and then 4·0 ml. of 0·2% nitroso-R-salt solution. The beakers are covered and replaced on the boiling water bath and left there for 10 to 15 min., then 1·5 ml. of nitric acid, sp. gr. 1·42, are run into each beaker, and the beakers are left on the water bath for a further 10 to 15 min., placed in the dark till cool, transferred to 15-ml. volumetric flasks, and made to volume. The optical densities of the standard and meteorite solutions are measured against the reagent blank at wave-length 550 mμ.

Copper.

After a trial run on 5 ml. of solution *C'* to ascertain the approximate copper content, an aliquot containing not more than 40 μg. Cu (usually 5 to 15 ml.) is run into a separating funnel; 1 ml. of 10% hydroxylamine hydrochloride and 1 ml. of 10% tartaric acid are added, and the solution diluted to about 35 ml. and mixed well. The pH is adjusted to 5·5 with 1:1 ammonia, using narrow-range indicator papers, and diluted to 40 ml.: 5 ml. of an 0·05% solution of 2:2'-diquinolyl in *iso*-amyl alcohol are added and the funnel shaken for 2 min. (preferably mechanically). After standing for 4 min. the aqueous layer and a few drops of the alcohol are drained off and discarded, the stem of the funnel is dried with filter paper and a 1-cm. spectrophotometer cell filled with the alcoholic layer.

The same aliquot of the blank solution *c'* and a suitable amount of a standard copper solution are treated in the same way (the stock copper standard may conveniently contain 1 mg. Cu per ml. and be diluted to 5 μg. Cu per ml. for the working standard).

The optical densities of the meteorite solution, standard, and blank are measured against 2:2'-diquinolyl reagent at wave-length 545 mμ.

Chromium.

Direct photometric comparison of the diphenyl carbazide colour from a meteorite solution with a standard does not give satisfactory results, but the following technique proved reliable.

A trial run is made on a 5-ml. aliquot of solution *C'* (representing 1/30 of pieces *Y* and *Z* of the meteorite), comparing directly against the standard chromium solution (a stock solution is prepared by reducing a

sulphuric acid solution of potassium dichromate with sulphur dioxide, boiling off the sulphur dioxide, and diluting to about 4 mg. Cr per ml. with dilute sulphuric acid; this is diluted to 4 μg. Cr per ml. for a working standard).

Two 10-ml. aliquots of solution *C′* are run into two beakers, and to one is added an amount of standard chromium solution containing about as much chromium as is already present in the 10-ml. aliquot; 10 ml. of the blank solution *c′* are run into a third beaker. To each beaker 1·7 ml. of 6N H_2SO_4 is added, and the solutions evaporated as far as possible on the water bath, the sides of the beakers rinsed and the solutions re-evaporated to expel chlorides thoroughly. Twenty ml. of water, 5 drops of 1·7% silver nitrate solution, and about 0·5 g. ammonium persulphate are added to each beaker and the liquid level marked; the beakers are then covered and boiled gently for 10 min., adding water occasionally to maintain the original level of liquid. The sides of the beakers are then rinsed and the boiling repeated. The solutions are cooled, transferred to 50-ml. volumetric flasks, and diluted to about 45 ml.; 1 ml. of a 0·25% solution of diphenyl carbazide in acetone is added and the solutions made up to volume and well mixed. The optical densities of the meteorite solution and of the meteorite solution plus added chromium are measured against the blank prepared from solution *c′* in 1-cm. cells, at wave-length 540 mμ; the measurements should be made as quickly as possible as the colour fades. If *N* μg. of chromium were added, and if the optical densities of the meteorite aliquot and of the meteorite aliquot with added chromium are *P* and *Q* respectively, the chromium content of the meteorite aliquot (1/15 of pieces *Y* and *Z* of meteorite) is $NP/(Q-P)$ μg.

Check determinations.

Sixty-five ml. of solution *A* have been held in reserve; this can be used for check determinations of Ni, Co, Cu, or Cr, and for the determination of certain other elements when suitable techniques have been devised.

THE ACTION OF DRY CHLORINE AT 250 TO 350° C. ON METEORITES.

In 1932 one of the authors[1] showed that pure dry chlorine at 250 to 300° C. attacks the metal, sulphide, and phosphide phases of a stony meteorite completely but does not affect the olivine or pyroxene. With

[1] M. H. Hey, Min. Mag., 1932, vol. 23, p. 48; cf. idem, ibid., p. 12; J. Kokta, Coll. Czech. Chem. Comm., 1937, vol. 9, p. 471 [M.A. 7–173].

siderites having up to at least 18% Ni the attack is equally successful, and the specimen may be in the form of lumps or tablets up to at least 5 mm. thick; but a siderite having 34% Ni was not attacked by chlorine. Iron, sulphur, phosphorus, and germanium distil quantitatively and although no direct experiments have yet been made, other evidence[1] suggests that gallium too will be found in the distillate. Nickel, cobalt, chromium, and copper are known to remain as chlorides.

Recent work has confirmed and extended these results: feldspars, apatite, magnetite, and chromite are not attacked provided the chlorine is dry and free from HCl. Traces of HCl give rise to an attack on the oxides, on olivine, and to a lesser extent on pyroxene; contrary to expectation, the attack on olivine resulting when the chlorine contains a trace of HCl does not lead to sublimation of ferric chloride, the only cation released being magnesium, which appears as chloride.[2]

The chlorine attack is particularly valuable in the study of stony meteorites, where it permits of a much cleaner removal of metal than is possible by magnetic separation[3] or the mercuric ammonium chloride method;[4] it is hoped to discuss its use in this connexion in a future paper. As applied to siderites, its principal value lies in the fact that there is no attack on acid-soluble silicates or oxides, enabling inclusions of these materials to be isolated conveniently.

The apparatus used for the treatment with chlorine is shown in figs. 1 and 2. The chlorine is well washed with water and thoroughly dried in a series of bubblers and then passed in a fairly rapid stream over the meteorite. The reaction tube, which is heated in a small electric furnace, consists of two parts connected by a ground joint. The chlorine enters through the side-tube of part *A*, the straight inner tube being a thermocouple well;[5] to the right of the ground joint, as shown in the figures, part *A* is a fairly close fit in the outer part *B*, the annular space between the two being no more than $\frac{1}{2}$ to 1 mm.; thus the chlorine, leaving part *A* by four holes near its right-hand end, passes through the last $\frac{1}{2}$ inch of the annular space in a rapid stream, to prevent back-diffusion of

[1] L. M. Dennis and J. A. Bridgeman, Journ. Amer. Chem. Soc., 1918, vol. 40, p. 1534.

[2] 0·7 g. of olivine heated to 310° C. for 40 hrs. in a current of chlorine containing a little HCl gained 2 mg. in weight and was then very hygroscopic. There was no sublimate of $FeCl_3$; leaching of the residue with water gave a solution containing Mg together with chlorine corresponding to 1·5 mg. $MgCl_2$, but no iron.

[3] G. T. Prior, Min. Mag., 1913, vol. 17, p. 24.

[4] L. Fletcher, ibid., 1894, vol. 10, p. 287.

[5] This well is placed eccentrically, near the top of part *A*, rather than centrally as drawn, so that a larger boat can be accommodated.

$FeCl_3$, which can be troublesome. The horizontal part of the outer tube, *B*, is 1 inch in internal diameter and 11 inches long; it turns sharply down, the vertical part being $\frac{1}{2}$ inch in internal diameter and 9 inches long overall, the last $4\frac{1}{2}$ inches projecting into a 250-ml. conical flask, to which section *B* is connected by a ground joint. Most of the ferric

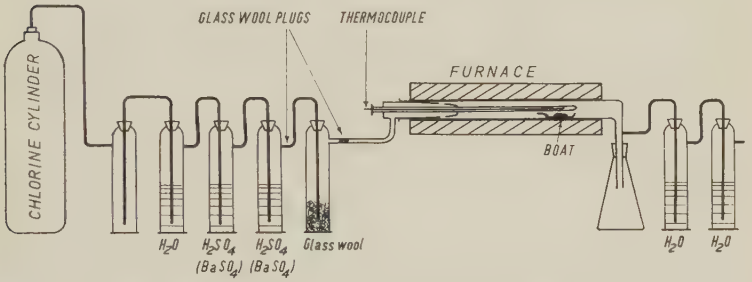

FIG. 1. Apparatus for the chlorine attack on meteorites. The sulphuric acid in the wash-bottles is saturated with barium sulphate; the appearance of a deposit or cloudiness indicates that the acid is becoming diluted and inefficient as a drying agent.

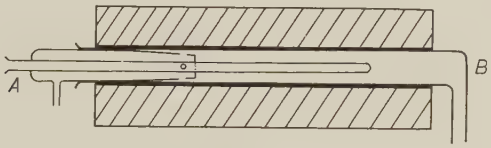

FIG. 2. Detail of the chlorination tube.

chloride collects in the conical flask and the vertical part of section *B*, the rest, together with the more volatile halides, being collected in a couple of water-charged bubblers.

The weighed piece of meteorite, carefully cleaned from rust and grease, is placed in a porcelain boat in the reaction tube. A stony meteorite must be crushed fairly fine, but a siderite can be successfully attacked in the lump. A rapid current of chlorine is passed through the apparatus until the air has been displaced, then the reaction tube is heated gradually until reaction begins and ferric chloride starts to sublime. The heat is increased when the reaction slows down, and is raised finally to about 350° C. and maintained there for at least an hour (a large lump of a siderite, a coarsely crushed stone, or a stone in which silicate and metal or sulphide are intimately intergrown, may take up to 2 hours for the

whole reaction). The reaction tube is allowed to cool below 100° C. with a slow current of chlorine still passing. The boat is withdrawn, cooled in a desiccator, and weighed.

The residue in the boat is now leached with water; if there is a large bulk of insoluble materials, as with a stony meteorite, the insolubles can be filtered off on a glass filter-crucible, porosity grade 4, washed, dried, and weighed; but if there is very little insoluble material, as with most siderites, it should be separated by centrifuging, withdrawing the bulk of the solution with a narrow-bore siphon (turned up at the intake end to avoid disturbing the solids), and washing by dilution and centrifuging, then washed out into a small weighed dish, evaporated, dried, and weighed.

With most siderites, the insoluble residue is very small in amount but sufficient for X-ray and optical study. The aqueous solution obtained by leaching the residue in the boat contains all the Ni, Co, Cu, and Cr, with at most traces of Fe. It can be used for the determination of all these elements by the methods described in the first part of this paper, using suitably sized aliquots.

Work on the best utilization of the distillate is still proceeding. Preliminary tests suggest that phosphorus may be determined on a suitable aliquot by the method described above, but it is not yet certain whether the receiver and traps collect germanium quantitatively, and the fate of any silicide or carbide present is still under investigation. Graphite remains unattacked and is collected with the insoluble matter.

The use of Buerger's algorithm in crystallographic calculations.

By R. J. Davis, M.A., D.Phil.

Dept. of Mineralogy, British Museum (Natural History), London S.W. 7.

[Taken as read 23 March 1961.]

Summary. Buerger (Zeits. Krist., 1957, vol. 109, p. 42) describes an algorithm for deriving data for the reduced unit cell from those obtained for an arbitrary crystal setting. It is shown that indices can be added to the algorithm so that one also derives the transformation matrix for the change of setting. Conversely, a known transformation matrix forms a set of instructions for using the algorithm to transform unit cell data, whether X-ray or morphological, from the initial to the final setting. One can thus use the algorithm to calculate the lengths of any unit cell vectors and the angles between them, and, using reciprocal cell data, to obtain any interfacial angles. Worked examples of these applications show that the proposed calculation method is shorter and simpler than those at present accepted.

IN the triclinic crystal system, the choice of axes is arbitrary and it is frequently necessary to change from one choice to another. The preferred choice is usually the axes of the reduced cell, at angles as near right as possible. The transformation matrix for the required change may or may not be known; it is usually known for the recalculation of goniometric results to a new setting, and the normal spherical trigonometrical methods of doing this are described in standard textbooks; it is usually unknown for the reduction of X-ray measurements to the reduced cell, when two procedures are possible. The standard procedure is based on Delaunay's representation of the unit cell and is fully described, e.g. by Ito (1950) and Henry and Lonsdale (1952); it yields only cells having all angles obtuse. Buerger (1957) has introduced a second method of cell-reduction that is simpler than the Delaunay procedure and has the great virtue that it yields the reduced cell with angles as near right as possible, regardless of whether all are obtuse or one is acute. With minor modifications, Buerger's method can be applied to a variety of crystallographic calculations to give simplified procedures and it is the purpose of this paper to describe these applications.

In Buerger's method the cell is represented by a^2, b^2, c^2, $bc\cos\alpha$, $ca\cos\beta$, $ab\cos\gamma$, and they are written in the triangular array below:

$$\begin{array}{ccc} & [001] & \\ & c^2 & \\ & ca\cos\beta \quad bc\cos\alpha & \\ [100]\ a^2 & ab\cos\gamma \quad\quad b^2\ [010] & \end{array} \quad = \quad \begin{array}{ccccc} & & [001] & & \\ & & s_{33} & & \\ & s_{31} & & s_{23} & \\ [100]\ s_{11} & & s_{12} & & s_{22}\ [010] \end{array}$$

The meaning of the symbols s_{11}, &c., as used by Buerger, will be clear from the above. It is convenient to add the indices at the corners of the array as shown.

Buerger obtains the reduced cell by using the following transformation or algorithm:

$$\begin{array}{ccccc} & & [001] & & \\ & & s_{33} & & \\ & s_{31} & & s_{23} & \\ [100]\ s_{11} & & s_{12} & & s_{22}\ [010] \end{array} \longrightarrow \begin{array}{ccccc} & & [001] & & \\ & & s_{33} & & \\ [100] & s_{11} & & s_{31} & (s_{23}+ms_{31}) \\ & & (s_{12}+ms_{11}) & & (s_{22}+2ms_{12}+m^2s_{11}) \quad [m10] \\ & & \xrightarrow[m]{} & & \end{array}$$

This transformation can clearly be applied in six possible directions in the array, two opposite directions parallel to each of the three sides, and m can be any positive or negative integer. The new indices are those of the new axes in terms of the original choice of axes; thus the new b-axis above is the $[m10]$ vector of the old cell; so that, written in columns, the new indices form the zone-symbol transformation matrix from the new to the original setting, Z_{21}; here $Z_{21} = [1m0/010/001]$. It follows that, written in rows, the indices form the face-index transformation matrix, F_{12}, from the original to the new axes; here $F_{12} = [100/m10/001]$.

The aim of a cell-reduction is to apply the above transformation as many times and in as many directions as necessary, until the terms in the middle of the sides of the triangle are brought as near zero as possible, that is so that each is less than half either of its neighbouring corner terms. Furthermore, any two midpoint terms can be changed in sign, with corresponding sign changes in the indices at the corner between them, and this is finally applied so as to make the midpoint terms adjacent to the new c-axis negative. The new axes are, of course, selected so as to make $c^2 < a^2 < b^2$.

Experience has shown that cell-reduction can equally well be carried out in reciprocal space,[1] when the cell is represented by:

[1] It seems possible that for a triclinic reduced cell with one angle very near 60° or 120°, or rather with a midpoint term very nearly one-half of an adjacent corner term, the reduced reciprocal cell may differ from the reduced real cell. In such cases one would wish to check the reduced reciprocal cell elements by converting to real cell elements and thence to s_{11}, &c., for possible further reduction in real space.

$$\begin{array}{ccc} & (001) & \\ & c^{*2} & \\ & c^*a^*\ \cos\beta^*\ \ b^*c^*\cos\alpha^* & \\ (100)\ a^{*2} & a^*b^*\cos\gamma^* & b^{*2}\ (010) \end{array} = \begin{array}{ccc} & (001) & \\ & s^*_{33} & \\ s^*_{31} & & s^*_{23} \\ (100)\ s^*_{11} & s^*_{12} & s^*_{22}\ (010) \end{array}$$

The transformation is carried out as above, and the indices now yield F_{21} when written in columns and Z_{12}, the zone-symbol transformation matrix, when written in rows. The new axes are selected to make $c^{*2}>a^{*2}>b^{*2}$, and the midpoint terms adjacent to the new c^*-axis are made positive.

Example 1. A crystal of cobaltomenite, adjusted to an arbitrary axis, yielded zero and first layer Weissenberg photographs from which one could find:

$$\begin{array}{ccc} & (001) & \\ & c^{*2} & \\ & c^*a^*\cos\beta^*\ \ b^*c^*\cos\alpha^* & \\ (100)\ a^{*2} & a^*b^*\cos\gamma^* & b^{*2}\ (010) \end{array} = \begin{array}{ccc} & (001) & \\ & 0{\cdot}0323 & \\ -0{\cdot}0316 & & -0{\cdot}0001_5 \\ (100)\ 0{\cdot}0884_5 & -0{\cdot}0511 & 0{\cdot}0857_5\ (010) \end{array}$$

One then has, tackling first the most glaring midpoint anomaly (italicized):

$$\begin{array}{ccc} & (001) & \\ & 0{\cdot}0323 & \\ -0{\cdot}0316 & & -0{\cdot}0001_5 \\ (100)\ 0{\cdot}0884_5 & -0{\cdot}0511 & 0{\cdot}0857_5\ (010) \end{array} \longrightarrow \begin{array}{ccc} & (001) & \\ & 0{\cdot}0323 & \\ 1\swarrow & & \\ 0{\cdot}0007 & & -0{\cdot}0001_5 \\ (101)\ 0{\cdot}0575_5 & -0{\cdot}0512_5 & 0{\cdot}0857_5\ (010) \end{array}$$

and by repeating the procedure along the base of the triangle:

$$\begin{array}{ccc} & (001) & \\ & 0{\cdot}0323 & \\ 0{\cdot}0007 & & -0{\cdot}0001_5 \\ (101)\ 0{\cdot}0575_5 & -0{\cdot}0512_5 & 0{\cdot}0857_5\ (010) \end{array} \longrightarrow \begin{array}{ccc} & (001) & \\ & 0{\cdot}0323 & \\ 0{\cdot}0007 & & 0{\cdot}0005_5 \\ (101)\ 0{\cdot}0575_5 & 0{\cdot}0063 & 0{\cdot}0408\ (111) \\ & \xrightarrow[1]{} & \end{array}$$

yielding a reduced reciprocal cell with its angles already appropriately all acute (midpoint terms all positive). The reciprocal cell elements can readily be derived from the above: $a^* = 0{\cdot}202$ Å.$^{-1}$, $b^* = 0{\cdot}180$ Å.$^{-1}$, $c^* = 0{\cdot}240$ Å.$^{-1}$, $\alpha^* = 89{\cdot}1°$, $\beta^* = 82{\cdot}5°$, $\gamma^* = 89{\cdot}1°$, and from the indices $Z_{12} = [111/001/101]$, i.e. the initial choice of c-axis, the rotation axis of the Weissenberg photographs, is the [111] vector of the reduced cell. It is clear, even from the final triangular array, that since the two midpoint terms adjacent to the new b-axis are nearly zero within the probable measurement error, the reduced cell is dimensionally nearly primitive monoclinic about b. From the information yielded by Z_{12} it was easy to reset the crystal to the b-axis and confirm the monoclinic symmetry.

It may be noted that symmetry in the reduced cell introduces special relations between various of the s_{11}, &c., or certain terms take special values. A list of the standard forms for s_{11}, &c., is given by Buerger (1957), who also lists the appropriate transformation matrices F_{12} for transforming the reduced to the conventional cell (the two may differ, e.g. when the latter is centred).

Unlike cell-reduction, for some crystallographic calculations the face-index matrix is already known or easily determined, and it is required to recalculate cell elements to a new setting. The normal methods are often laborious. The recalculation can be done as if it were a cell-reduction, by the method outlined above, but using now the face-index matrix as a set of instructions for carrying it out (or the zone-symbol matrix when one is dealing with the reciprocal cell). For this purpose one may note two other transformations of the triangular array.

Firstly, if one is only interested in cell angles or axial ratios, the six numbers may *all* be multiplied by a given factor without altering the cell or the corner indices. Thus the array may be divided by b^2 to give a representation of the cell in terms of the morphological elements:

$$\begin{array}{ccc} & [001] & \\ & (c/b)^2 & \\ & (c/b)(a/b)\cos\beta \quad (c/b)\cos\alpha & \\ [100]\ (a/b)^2 & (a/b)\cos\gamma & 1\ [010] \end{array}$$

Secondly, *one* axis may be multiplied by an appropriate integer, m,[1] with a corresponding change in the corner indices and adjacent midpoint terms:

$$\begin{array}{ccc} [001] & & [001] \\ s_{33} & & s_{33} \\ s_{31}\quad s_{23} & \longrightarrow & s_{31}\quad ms_{23} \\ [100]\ s_{11}\quad s_{12}\quad s_{22}\ [010] & & [100]\ s_{11}\ ms_{12}\quad m^2s_{22}\quad [0m0]\times m \end{array}$$

Example 2. In reviewing the crystallographic data for anapäite, it became clear that Popoff (1902) had miscalculated his cell elements from his original measurements. These were recalculated in the usual way to yield:

$$a:b:c = 1{\cdot}4233:1:1{\cdot}1213,$$
$$\alpha = 97^\circ\,12\tfrac{1}{2}',\ \beta = 95^\circ\,16\tfrac{1}{2}',\ \gamma = 70^\circ\,10\tfrac{1}{2}'.$$

Palache (1933) gave further measurements and cell elements in a new setting, together with the face-index transformation matrix Popoff→

[1] In some cases, when transforming reciprocal cell data using a zone-symbol transformation matrix, m may be a simple positive or negative fraction, both in this transformation and in that first described.

Palache $F_{12} = [101/020/\bar{1}01]$. From the data above, calculation proceeded:

```
                [001]                                          [1̄01]
                1·2571                                  1̄ ↗    3·5762
        −0·1467   −0·1407          ⟶                          −2·1724   −0·6239
[100] 2·0257   0·4832   1·0000 [010]          [100] 2·0257   0·4832   1·0000 [010]

                [1̄01]                                          [1̄01]
                3·5762                                  1 ↙    3·5762
   ⟶        −4·3448   −1·2478          ⟶                          −0·7686   −1·2478
  [200] 8·1028   1·9328   4·0000 [020]          [101] 2·9894   0·6850   4·0000 [020]
    ×2                        ×2
                [1̄01]
                0·8941
  ×1/4
  ⟶        −0·1922   −0·3145
[101] 0·7474   0·1713   1·0000 [020]
```

from which the axial ratios and interaxial angles are readily extracted to give $a:b:c = \sqrt{0{\cdot}7474}:1:\sqrt{0{\cdot}8941} = 0{\cdot}8645:1:0{\cdot}9456$, $\alpha = \cos^{-1}(-0{\cdot}3145/\sqrt{0{\cdot}8941 \times 1}) = 109° 15\frac{1}{2}'$, $\beta = 103° 36'$, $\gamma = 78° 34\frac{1}{2}'$. These results are now in good agreement with Palache's, and were actually confirmed by the much more laborious calculation using spherical trigonometry.

One can clearly use the same method, applying the transformation matrices listed by Buerger, to convert reduced to conventional cells after cell reduction. Moreover, the method can also obviously be applied to determine the lengths of cell vectors or the angles between them, e.g. the inter-edge angles of crystal faces, using data for the real cell, or else to determine interfacial angles using data for the reciprocal cell.

Example 3. Small prisms of synthetic cobaltomenite were available, with striated faces too small for goniometry. X-ray and optical examination showed that the prism faces were $(hk0)$ and the terminal face $(h0\bar{l})$. From measurement of inter-edge angles on the various faces under the microscope, the diagonal $[l0h]$ of the terminal face was inclined at $61\frac{3}{4}° \pm 2°$ to the prism axis $[00l]$. The X-ray measurements yielded elements $a:b:c = 0{\cdot}8592:1:0{\cdot}7352$, $\beta = 98° 58\frac{1}{2}'$, from back reflection oscillation photographs. One may calculate various angles $[l0h]:[001]$ using one side only of the triangular array:

```
[100] s11  s31  s33 [001] = [100] 0·7382   −0·0985   0·5405 [001]
                          → [101] 1·0817    0·4420   0·5405 [001]
                                  ←————————————————
                                          1
```

whence $[101]:[001] = \cos^{-1}(0{\cdot}4420/\sqrt{(1{\cdot}0817 \times 0{\cdot}5405)}) = 54° 40'$. $[101]$ is thus about 7° off the terminal face diagonal, a discrepancy confirmed

almost exactly by an oscillation photograph taken with the X-ray beam perpendicular to the terminal face. The above calculation can readily be extended to other indices, to match by trial and error the observed angle. Thus, omitting abortive trials, the calculation might proceed:

[101] 1·0817 0·4420 0·5405 [001] → [505] 27·0425 2·2100 0·5405 [001]
×5
→ [504] 23·1630 1·6695 0·5405 [001]
←————————
−1

whence [504]:[001] = 61° 51′, in best agreement with the observed angle. The terminal face, therefore, has diagonals [010] and [504] and is thus $(40\bar{5})$.

The application of this calculating method to other cases will be obvious from the above. Clearly the full triangular array is required when dealing with [*hkl*] vectors or (*hkl*) faces.

Acknowledgements. I am grateful to Dr. M. H. Hey and Mr. P. G. Embrey for their encouragement, for reading the manuscript, and for several clarifications.

References.

Buerger (M. J.), 1957. Zeits. Krist., vol. 109, p. 42.
Henry (N. F. M.) and Lonsdale (K.), 1952. International Tables for X-ray Crystallography. Kynoch Press, Birmingham, vol. 1, p. 530.
Ito (T.), 1950. X-ray Studies on Polymorphism. Maruzen Co. Ltd., Tokyo, p. 189.
Palache (C.), 1933. Zeits. Krist., vol. 86, p. 280.
Popoff (S. P.), 1902. Zeits. Kryst. Min., vol. 37, p. 267.

SHORT COMMUNICATIONS

X-ray powder data for holmquistite from Rhodesia.

The following table was accidentally omitted from the paper by O. von Knorring and G. Hornung, Min. Mag., 1961, vol. 32, p. 733.

Table II. X-ray powder data for holmquistite from Benson mine, Southern Rhodesia. Fe-$K\alpha$ radiation, camera diameter 9 cm.

d, Å.	*I.*	*d*, Å.	*I.*	*d*, Å.	*I.*
8·1	vs	2·12	m	1·460	w
5·0	vw	2·11	w	1·435	w
4·80	vw	2·08	w	1·415	w
4·38	s	2·04	w	1·385	m
3·80	vw	2·02	w	1·345	w
3·58	m	1·945	w	1·329	w
3·27	w	1·920	w	1·303	m
3·19	w	1·840	w	1·275	w
3·15	w	1·800	w	1·265	w
2·98	vs	1·790	w	1·251	w
2·77	s	1·755	w	1·230	w
2·68	m	1·730	w	1·190	vw
2·62	m	1·700	w	1·170	w
2·52	s	1·675	w	1·157	w
2·45	w	1.620	vw	1·130	w
2·39	w	1·580	w	1.100	w
2·27	w	1·560	m	1·081	w
2·24	w	1·515	vw	1·062	w
2·22	w	1·495	w	1·052	w
2·19	w	1·479	m		

The Editor

Structural relationships within pseudomorphs after olivine.

Current investigations by optical and single-crystal X-ray diffraction have shown that iddingsite—the name applied to deep reddish-brown alteration products of olivine—is a polycrystalline aggregate that frequently contains more than one mineral species. The constituents vary considerably in different occurrences. For instance, Brown and Stephen[1] described iddingsite from New South Wales, Australia, containing goethite and a layer-lattice silicate, while Smith[2] described one from Markle basalt, Edinburgh, containing hematite, chlorite, and quartz.

Yet another mineral assemblage, saponite, goethite, and hematite, has been found in pseudomorphs after olivine in weathered Dunsapie basalt, Edinburgh.

The orientational relationship of these minerals has been studied and compared with the data obtained by previous investigators.[1, 2, 3] Since the Dunsapie basalt pseudomorphs contain no remnant olivine, the author has been able to relate the orientation of the alteration products only indirectly to the structure of the original olivine.

The goethite crystals are apparently all oriented with their three orthorhombic axes perpendicular to the three cleavage planes of the iddingsite. In the iddingsite containing goethite examined by Brown and Stephen,[1] the normals to these planes were shown to be parallel to the orthorhombic axes of olivine, and since the a_G axis (the subscripts G, F, H, L, and S in the text represent goethite, forsterite, hematite, layer lattice silicate, and saponite respectively) is normal to the principal cleavage plane of the Dunsapie iddingsite, the orientation of the goethite with respect to the original olivine is probably the same as that observed for 80% of the goethite in the New South Wales sample, with $[100]_G \| [100]_F$; $[010]_G \| [010]_F$; and $[001]_G \| [001]_F$. Brown and Stephen suggested that the three possible directions of orientation for goethite, based on sheets of oxygen atoms in hexagonal close-packing, are not exactly equivalent and that the cation configuration in the olivine influences the orientation to a considerable extent and accounts for the marked preference for one orientation.

The saponite crystals are aligned with respect to the goethite crystals so that $[100]_S \| [010]_G$; $[010]_S \| [001]_G$; and $(001)_S \perp [100]_G$—an arrangement comparable to the orientational relationship in the New South Wales sample where $a_L \| b_F \| b_G$ and $c_L \| a_F \| a_G$. However, oscillation photographs have shown that the saponite crystals give, in aggregate, a symmetry that is effectively hexagonal, and thus $[100]_S$ may also be parallel to the equivalent directions $[0\bar{1}6]_G$ and $[0\bar{1}\bar{6}]_G$ at 120° to each other.

The orientation of the hematite crystals with respect to goethite is similar to that obtained by Goldsztaub[3] and by Francombe and Rooksby[4] on dehydrating a single crystal of goethite: $[10\bar{1}0]_H \| [010]_G$ and $[0001]_H \| [100]_G$. The $[10\bar{1}0]_H$ axis in the Dunsapie sample may be parallel to any one of three equivalent directions. Similarly, Goldsztaub[3] found that, on dehydration, goethite does not give a single crystal of hematite but an assemblage of small crystals in two orientations rotated 180° from each other in the plane normal to their trigonal axes.

The hematite crystals in the Dunsapie pseudomorphs are oriented with respect to the saponite crystals so that $[100]_S \| [10\bar{1}0]_H$, and $(001)_S \perp [0001]_H$, which is as one would expect because of the similar orientational relationship between chlorite and hematite in the pseudomorphs after olivine in Markle basalt.[2]

Summarizing the above results, the three alteration products in the pseudomorphs after olivine in Dunsapie basalt may be arranged so that $[100]_S \| [010]_G$, $[0\bar{1}6]_G$, $[016]_G$, $[10\bar{1}0]_H$; and $(001)_S \perp [100]_G \| [0001]_H$. The structural unit dimensions corresponding to these directional relations are as follows: $2a_S \simeq b_G \simeq 2a_H$ and $c_S \simeq 3a_G \simeq c_H$.

Macaulay Institute for Soil Research, WILMA W. SMITH
Craigiebuckler,
Aberdeen.

[1] G. Brown and I. Stephen, Amer. Min., 1959, vol. 44, p. 251.
[2] W. W. Smith, Min. Mag., 1959, vol. 32, p. 324.
[3] S. Goldsztaub, Compt. Rend. Acad. Sci. Paris, 1931, vol. 193, p. 533.
[4] M. H. Francombe and H. P. Rooksby, Clay Min. Bull., 1959, vol. 4, p. 1.

Some observations concerning viscosity and anionic groups in silicate melts.

THE study of the viscosity of silicate melts has steadily increased in importance in petrology and industry. The slope of the viscosity curve has industrial significance wherever process automation of melts is present. Most theoretical considerations of viscosity reveal a relationship of this quantity to the geometry and internal and external anionic forces of the unit of flow.

The purpose of this study was to discover whether any data existed that on re-analysis would yield supporting or conflicting data on the theory of anionic groups as described in a previous publication (de Wys, 1960). It was felt that if various anionic groups had an effect on viscosity characteristics this would most likely be obvious in the slope of the viscosity curves, which is an indication of the activation energy for viscous flow.

According to Eyring's 'hole' theory it would appear reasonable to assume that the fluidity of a liquid will be related to the number of holes. Since the number of holes in a solid is related to its temperature elevation, $\triangle T$, above its most dense state it would appear reasonable, in view of modern solid–liquid transition theory, that the increase in the

number of holes in a liquid above those present in its most ordered state might also be related to the $\triangle T$ above the melting point or liquidus.

Therefore in replotting iso-viscosity curves on a phase equilibrium diagram it was felt that this should be done at a constant $\triangle T$ above the liquidus, rather than at a constant T, a technique that, although generally practised and of industrial concern, tends to ignore the morphological realities of the phase diagram to which the iso-viscosity curves pertain.

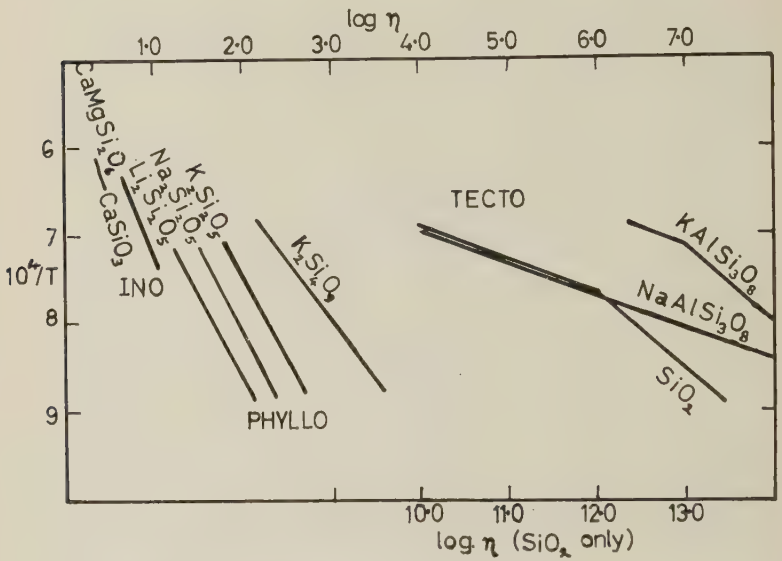

FIG. 1. Log viscosity plotted against $1/T$ (°C.), to show similarity of slopes of those liquids originating from compounds with similar crystal structures. Tecto slopes from data of N. L. Bowen; phyllo slopes from Shartsis, Spinner, and Capps; ino slopes determined by the author.

Fig. 1 shows plots of log viscosity of various congruent melting compounds against the inverse of absolute temperature. The similarity of the slopes of those liquids believed to have similar liquid structures is clear. It is of some interest to note that the $K_2Si_4O_9$ liquid, originating from a compound with a probable structure somewhat more complex than the phyllo but less than a tecto silicate, has a slope indicating an activation energy for viscous flow somewhat in between these two types.

It was of some interest to know whether the slope of the viscosity curve would change on crossing boundary curves in a ternary system since

those curves separate regions in which certain anionic groups predominate. Fig. 2, which was derived by replotting the data from Machin and Yee (1948), indicates that the structural response of viscosity to a change in the predominance of a liquid structure is significant.

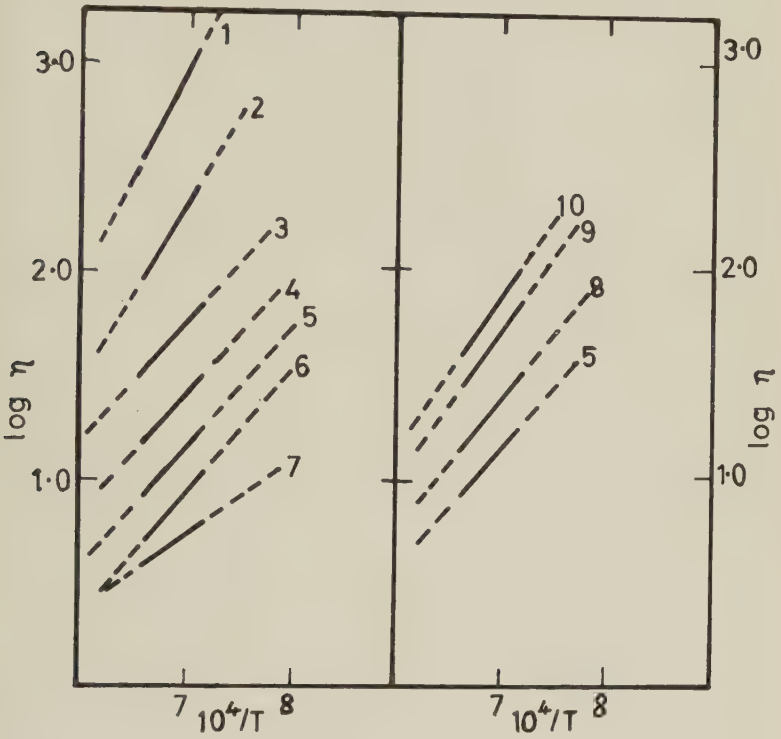

FIG. 2. Log viscosity plotted against $1/T$ (°C.) for a series of melts in the system CaO–Al_2O_3–SiO_2; for lines 1 to 7, Al_2O_3 is 10 mol. %, while CaO is 20, 25, 30, 35, 40, 45, and 50 wt. % respectively; for lines 5, 8, 9, and 10, SiO_2 is 50 wt. %, and CaO 40, 35, 30, and 25 wt. % respectively. The compositions for lines 1 and 2 fall within the SiO_2 field of the system; for lines 3, 4, 5, 6, and 8 within the $CaSiO_3$ field; for line 7 within the Ca_2SiO_4 field; and for lines 9 and 10 within the $CaAl_2Si_2O_8$ field.

The viscosity data presented by the above authors were also replotted at a constant $\triangle T$ above the liquidus surface, fig. 3. The iso-viscosity lines change directions when crossing into different primary fields where different liquid structures predominate.

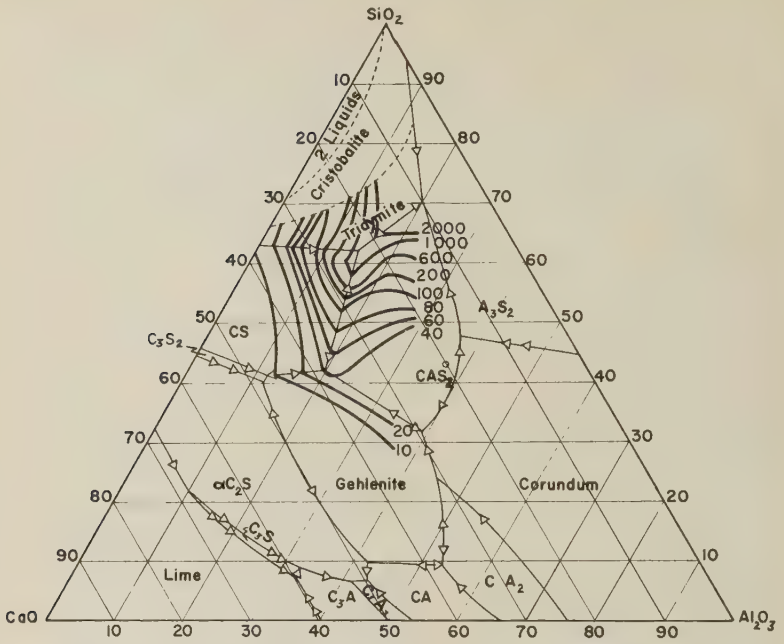

FIG. 3. Iso-viscosity curves in the system CaO–Al_2O_3–SiO_2, plotted for a temperature 50° C. above the liquidus.

Conclusion. It appears to the author that the above data tend to support the structure concept that various silicate anionic groups are present in silicate melts of different composition. It would seem by the viscosity response that the slope of the viscosity : temperature relation is strongly influenced by the dominant anionic group present in the mixture of anionic groups. From a practical point of view it would appear that by careful selection of anionic group mixtures the slope of the viscosity curve may be controlled.

International Business Machines Corp.
San Jose,
California, U.S.A.

E. CHRISTIAAN DE WYS

References.

DE WYS (E. C.), 1960. Min. Mag., vol. 32, p. 640.

BOWEN (N.), 1934. Trans. Amer. Geophys. Union, pt. 1, p. 249.

SHARTSIS (L.), SPINNER (S.), and CAPPS (W.), 1957. Journ. Amer. Ceram. Soc., vol. 35, p. 155.

MACHIN (J. S.) and YEE (T. B.), 1948. Ibid., vol. 31, p. 200.

Weathering of sulphide minerals in coal: production of ferrous sulphate heptahydrate.

Microscopic examination of subsection B in a pillar sample of Greta seam coal revealed greenish-white fibres up to $\frac{1}{2}$ in. long, which tended to occur radially in small spherical nests and appeared to be produced by weathering of sulphide minerals. The fibrous mineral was readily soluble in water and ferrous iron was the major cation present. The upper inch of the subsection was composed of felted crystals of the greenish-white, fibrous mineral with a ground mass of clay, coal, and pyrite nodules. From its optical properties the greenish-white fibrous mineral appeared to be melanterite ($FeSO_4.7H_2O$), and examination with a polarizing microscope showed that the samples were probably monoclinic.

To settle doubts as to the constitution of the samples their X-ray diffraction patterns were taken and proved to resemble that of melanterite on the A.S.T.M. card; but agreement was not complete. In an attempt to resolve the difficulty an investigation of pure ferrous sulphate was carried out. Three samples were examined: blue-green crystals and white powder separated from a sample of ferrous sulphate that had become partially dehydrated, and freshly recrystallized ferrous sulphate.

	$Fe^{\cdot\cdot}$.	SO_4''.	H_2O.
Blue-green crystals . .	20·1%	34·3%	45·6%
White powder . . .	24·6	44·6	30·8
Recrystallized $FeSO_4.7H_2O$.	19·8	35·0	45·2

Chemical analyses indicate that the white powder is the tetrahydrate, the other two samples being the heptahydrate. Metals other than iron were present only in small quantities; a spectrochemical analysis shows about 0·1% Mg, between 0·01 and 0·1% Al and Mn, about 0·01% Si, and traces of Cu, Ni, Co, Ga, Ti, and Y.

The X-ray diffraction patterns of the two hydrates were determined (table I) and found to differ from those listed in the relevant A.S.T.M. cards (0560/d/1–0253). These determinations were made under standard conditions (Co-$K\alpha$, 42 kV, 15 mA, Fe filter) and the diffraction photographs were photometered with an automatic double-beam microdensitometer. The samples were prepared by grinding the repeatedly recrystallized heptahydrate and the tetrahydrate to pass a 200 British Standard mesh screen and subjecting them to gentle extrusion.[1]

The X-ray diffraction pattern given by the sample of greenish-white

TABLE I. X-ray diffraction data recorded by the authors.

Ferrous sulphate heptahydrate				Ferrous sulphate tetrahydrate			
d, Å.	*I.*	*d*, Å.	*I.*	*d*, Å.	*I.*	*d*, Å.	*I.*
6·60	4	1·95	27	6·60	19	1·64	13
5·92	7	1·90	10	5·72	6	1·62	17
5·26	42	1·86	22	5·31	67	1·59	9
4·69	100	1·84	28	4·73	43	1·56	11
4·42	19	1·74	9	4·37	100	1·48	13
3·95	29	1·68	10	3·90	52	1·43	33
3·70	54	1·65	5	3·35	56	1·38	20
3·53	2	1·61	9	3·20	45	1·30	29
3·35	13	1·59	3	2·93	72	1·26	9
3·20	42	1·54	11	2·71	30	1·24	9
3·06	23	1·52	11	2·56	48	1·16	11
2·95	14	1·49	12	2·40	39	1·13	11
2·71	46	1·45	6	2·34	48	1·23	9
2·61	45	1·39	7	2·24	44	1·22	7
2·45	20	1·35	9	2·10	15	1·09	7
2·40	18	1·32	5	1·95	39		
2·29	13	1·30	5	1·88	35		
2·25	7	1·24	6	1·78	22		
2·18	5	1·21	4	1·74	17		
2·06	12	1·19	5	1·71	15		
2·00	24	1·17	6	1·66	13		

fibres was the same as that given by the ferrous sulphate heptahydrate. This confirms the identity of the sample as melanterite.

Acknowledgements. The authors are indebted to Miss M. C. Clark for spectrochemical analyses and to R. J. Cosstick for chemical analyses.

Division of Coal Research,
Commonwealth Sci. Indust. Research Organization,
P.O. Box 175, Chatswood,
New South Wales.

M. KOSSENBERG
A. C. COOK

[1] M. Kossenberg, Journ. Sci. Instr., 1955, vol. 32, p. 117.

BOOK REVIEWS

BRUHNS (W.) and RAMDOHR (P.) *Petrographie.* Sammlung Göschen, vol. 173. Berlin, 1960. 141 pp., 21 figs. 3.60 DM.

This small book gives a condensed and well-rounded survey of the whole field of petrology and is extremely good value. The descriptive aspects predominate and make it especially valuable for those geologists

who have to deal with macroscopic and microscopic aspects of rocks without going deeper into the mineralogical and physico-chemical details of petrology.

The first, general, part (40 pp.) contains chapters on petrographic methods, on the main rock-forming minerals, and on formation and subdivision of rocks. In the second, special, part the authors devote 60 pages to the igneous, 20 to the sedimentary, and 30 to the metamorphic rocks. Texture and geologic appearance of igneous rocks as well as their subdivision according to Tröger are briefly mentioned. For the most important rock types at least two chemical analyses are given. The authors emphasize the importance of certain rocks for the formation of economic mineral deposits.

For sedimentary rocks, the usual subdivision into clastic, chemical, and biochemical ones (including phosphorites, ironstones, and coppershales) is applied.

In spite of limited space, facies concept and the application of petrofabrics are mentioned, followed by the discussion of a few selected examples of metamorphic rocks.

E. F. Stumpfl

Krinov (E. L.). *Principles of Meteoritics.* Translated from the Russian by Irene Vidziunas. Translation edited by Harrison Brown. (International Series of Monographs on Earth Sciences, vol. 7.) London and New York (Pergamon Press), 1960. xi + 535 pp., 154 text-figs., 7 plates. 70s. net.

In 1955 a book by E. L. Krinov entitled 'Основы метеоритики' was published in Moscow. This book dealt with all aspects of meteoritics largely from a Russian point of view although references were given to German and English literature. The book under review is a translation with some additions (but little revision) to bring the book up to date.

It cannot be said that the translation does justice to the original. Apart from the reproduction, which is 'by non-letterpress setting and photo-lithography', for which the publishers excuse themselves on the grounds of speed and cost, there are too many errors and examples of poor arrangement of tables and figures to make the book acceptable as it stands. There are several numerical errors in the text references to the list of literature at the end of the volume, five occurring between pages 162 and 176, and the setting of eighteen of the fifty-two tables sideways (instead of upright as in the Russian edition) makes reading tedious; in tables 4 and 19 it is necessary to turn the book upside down to read the

column headings. Similarly with the illustrations; even when the figure is printed upright, the caption often runs vertically, and in the case of fig. 152, which incidentally appears to have been printed upside down, the position of the caption makes the illustration incomprehensible. The literature references are not free from errors and in addition suffer from the defect that in many instances only the date and volume of the journal are quoted. The standard of English also is not what one has the right to expect.

One of the most interesting figures in the Russian edition is fig. 52 which shows on a map of Russia the place of fall and the nature (iron, stony iron, stone) of every meteorite known to have fallen in the U.S.S.R. This map is referred to in the text and Appendix I gives the necessary details of each meteorite. Whereas in the Russian edition no fault can be found with this map, the map in the English edition looks as if it has been started and then abandoned. In any event it is useless.

The book consists of eight chapters and three appendices, the headings of which are: I, Meteoritics as a branch of science; II, Motion and fall of Meteorites; III, Morphology of Meteorites; IV, Chemistry of Meteorites; V, Mineralogy and petrography of Meteorites; VI, Physical property of Meteorites; VII, Tektites and Silica Glass; VIII, The origin of Meteorites; Appendix I, Catalogue of Meteorites of the U.S.S.R.; Appendix II, Meteorites of rare type; Appendix III, Classification of the surface structure of the fusion crust of Meteorites (illustrated by the 7 plates). There are also the usual literature references and indexes. In Chapter VI the author describes mainly the work that has been done on the spectral reflectivity of stony meteorites, on the results of which he bases a classification of stony meteorites.

In addition to the avoidable shortcomings already mentioned, no attempt appears to have been made to revise the accounts of earlier results, shown by later work to be wrong or doubtful. Finally it must be said that whereas the Russian edition appears to have been a reasonably sound textbook, the English edition has suffered from indifferent editing.

A. A. M.